OFFICE OF CIVILIAN RADIOACTIVE WASTE MANAGEMENT

CALCULATION COVER SHEET

1. QA: QA
Page: 1 Of: 79

2. Calculation Title

Precipitates/Salts Model Calculations for Various Drift Temperature Environments

3. Document Identifier (including Revision Number)

CAL-EBS-PA-000012 REV 00

4. Total Attachments	5. Attachment Numbers – Number of pages in each
0	N/A

	Print Name	Signature	Date
6. Originator	Paul Mariner	SIGNATURE ON FILE	20 Dec 01
7. Checker	Richard Metcalf	SIGNATURE ON FILE	20 Dec 01
8. Lead	James Nowak	SIGNATURE ON FILE	20 Dec 01

9. Remarks

This calculation uses the Precipitates/Salts model developed in *In-Drift Precipitates/Salts Analysis* (ANL-EBS-MD-000045 Rev. 00 ICN 03) to predict evaporative evolution of a wide range of waters predicted to seep into the repository drift or observed in ground water samples collected from Yucca Mountain.

Revision History

10. Revision No.	11. Description of Revision
00	Initial issue.

CONTENTS

Page

FIGURES

Page

TABLES

Page

ACRONYMS AND ABBREVIATIONS

ACC	accession number
AMR	Analysis/Model Report
BSC	Bechtel SAIC Company
C/C_o	concentration factor
CRWMS M&O	Civilian Radioactive Waste Management Services Management and Operations
DIRS	Data Input Reference System
DTN	Data Tracking Number
EBS	Engineered Barrier System
HRH	high relative humidity
IS	ionic strength
ISa	ionic strength approximation (Equation 1)
LRH	Low Relative Humidity
PT4	data0.pt4, a thermodynamic database developed in this AMR for EQ3/6
PT5v1	data0.pt5, a revision of PT4, version 1
PT5v2	data0.pt5, a revision of PT4, version 2
Q^e	evaporation rate
Q^s	incoming seepage rate
QA	Quality Assurance
R^{es}	relative evaporation rate (Q^e/Q^s)
RH	relative humidity
SSPA	Supplemental Science and Performance Analyses
THC	thermohydrological-chemical
TIC	Technical Information Center number
Tptpll	lower lithophysal zone of the crystal-poor member of the Topopah Spring tuff
Tptpmn	middle nonlithophysal zone of the crystal-poor member of the Topopah Spring tuff
TSPA	Total System Performance Assessment
TSw	Topopah Spring welded hydrogeologic unit
TWP	Technical Work Plan

1. PURPOSE

The objective and scope of this calculation is to assist Performance Assessment Operations and the Engineered Barrier System (EBS) Department in modeling the geochemical effects of evaporation within a repository drift. This work is developed and documented using procedure AP-3.12Q, *Calculations*, in support of *Technical Work Plan For Engineered Barrier System Department Modeling and Testing FY 02 Work Activities* (BSC 2001a).

The primary objective of this calculation is to predict the effects of evaporation on the abstracted water compositions established in *EBS Incoming Water and Gas Composition Abstraction Calculations for Different Drift Temperature Environments* (BSC 2001c). A secondary objective is to predict evaporation effects on observed Yucca Mountain waters for subsequent cement interaction calculations (BSC 2001d). The Precipitates/Salts model is documented in an Analysis/Model Report (AMR), *In-Drift Precipitates/Salts Analysis* (BSC 2001b).

2. METHOD

The Precipitates/Salts model was used to perform the calculations in this document. This model, explained in detail in *In-Drift Precipitates/Salts Analysis* (BSC 2001b, Section 6.4), is summarized in Section 4, as are the methods of calculation. Any deviations from these methods are explained in detail in Sections 3 and 5. The control of electronic management of data was accomplished in accordance with methods specified in the Technical Work Plan (TWP) (BSC 2001a).

3. ASSUMPTIONS

The model assumptions for this calculation are identical to assumptions described in Section 5 of *In-Drift Precipitates/Salts Analysis* (BSC 2001b) and Section 3 of *Precipitates/Salts Model Results for THC Abstraction* (CRWMS M&O 2001). All model assumptions are used in Sections 5 and 6.

Assumptions were also made for the input data sets listed in Table 1 and Table 2. These input assumptions are described in detail in the following subsections.

3.1 NITRATE CONCENTRATIONS

Nitrate was added to the waters listed in Table 1. These waters have no reported nitrate concentrations. The concentration of nitrate added was determined based on an assumed nitrate to chloride molar ratio.

Assumption 3.1.1. The molar ratio of nitrate to chloride for the first twelve waters listed in Table 1 is assumed to be 0.1.

Rationale: This molar ratio is justified based on a rounded average of the molar ratios in the four Topopah Spring welded hydrogeologic unit (TSw) pore water samples listed in Table 6 of

CRWMS M&O (2000, pp. I-17 and I-19). No further confirmation is required for this assumption.

Assumption 3.1.2. The molar ratio of nitrate to chloride for the last four waters listed in Table 1 is assumed to be 1.0.

Rationale: This molar ratio is justified based on a rounded average of the molar ratios in the seven UZ-14 perched water samples having measurements for both nitrate and chloride in Table 8 of CRWMS M&O (2000, pp. I-22). No further confirmation is required for this assumption.

3.2 CARBON DIOXIDE FUGACITY

The carbon dioxide fugacity was fixed in each simulation for the inputs in Table 1. For the crown seepage waters, the fugacity was fixed at the value provided by DTN: MO0110SPAEBS13.038. However, for some of the invert waters simulated for the Supplemental Science and Performance Analyses (SSPA) (BSC 2001e, Section 6.3.3), the carbon dioxide fugacities of the corresponding crown seepage waters were assumed. This was done to prepare the outputs for the mixing model presented in the SSPA (BSC 2001e, Section 6.3.3).

Assumption 3.2.1. Several of the invert waters (specifically, cases HLi, HHi, LLi, and LHi in Table 1) were assumed to have the carbon dioxide fugacities of the corresponding crown seepage waters (i.e., cases HLc, HHc, LLc, and LHc, respectively).

Rationale: This assumption is justified because the corresponding carbon dioxide fugacities are always within a factor of three and nearly always within a factor of two (DTN: MO0110SPAEBS13.038). These differences are within the range of uncertainty of the THC model predictions. No further confirmation is required for this assumption.

3.3 MINERAL SUPPRESSIONS

Mineral suppressions are addressed in Section 5.4 of *In-Drift Precipitates/Salts Analysis* (BSC 2001b). For a subset of the simulations presented below, several of the minerals were not suppressed because they were performed for SSPA prior to ICN 03 of *In-Drift Precipitates/Salts Analysis* (BSC 2001b). Instead of rerunning these files with the new suppressions, an assumption was made that these additional suppressions do not considerably affect the qualified outputs of the model. This approach also allows for qualified documentation of the model predictions previously performed for the SSPA.

Assumption 3.3.1. Excluding talc, chrysotile, and magnesite from the list of suppressed minerals does not considerably affect the qualified outputs (i.e., pH, chloride concentration, and ionic strength) for those simulations in which these minerals were not suppressed (specifically, cases HLi, HHi, LLi, LHi, HLc, HHc, LLc, and LHc in Table 1).

Rationale: This assumption is justified by the results. Of these three minerals, only talc precipitated. Section 6.6 presents the results of rerunning case HHi with talc, chrysotile, and magnesite suppressed. The results show that qualified model outputs (i.e., pH, chloride

concentration, and ionic strength) are not considerably affected, and the differences are within the range of model uncertainty. No further confirmation is required for this assumption.

3.4 LOW RELATIVE HUMIDITY SALTS MODEL

The low relative humidity (LRH) salts model was used to predict ionic strength and chloride concentration below a relative humidity of 85 percent for the HHi and LHi cases of the sensitivity THC model abstraction (Table 1). An assumption was made to extend these calculations to other THC model sensitivity abstractions.

Assumption 3.4.1. The LRH salts model results for the HHi and LHi cases in Table 1 are assumed to adequately approximate the results for the HLi, HHc, HLc, LLi, LHc, and LLc cases. Specifically, the HHi case results are applied to the HLi, HHc, and HLc cases, and the LHi case results are applied to the LLi, LHc, and LLc cases.

Rationale: This assumption is justified by: 1) the similarity of the results of the HHi and LHi cases (Section 6.2.1); 2) the small effects of CO_2 fugacity (Section 6.2.1); 3) the small differences in results between seepage wicking into the invert and seepage at the crown of the drift (Section 6.1); and 4) the level of uncertainty (factor of ten) in the accuracy of the LRH model (BSC 2001b, Section 6.5.2). No further confirmation is required for this assumption.

3.5 PERCHED WATER COMPOSITION

Assumption 3.5.1. Because perched water is a subset of ambient fluids that could contact cementitious materials located in and around a potential repository drift, a potential fluid composition representing perched water has been selected for Precipitates/Salts model evaporation calculations that feed sensitivity calculations performed in *Seepage Grout Interactions Model Calculations* (BSC 2001d, Table 6-1.7). The assumed representative perched water composition is identical to a perched water sample collected on 8/3/1993 from borehole USW UZ-14 within the Topopah Spring welded unit. This composition is documented in Table 8 of CRWMS M&O (2000, p. I-22). This assumption is used in Section 6.7.

Rationale: The assumed representative perched water composition is corroborated by other perched water sample measurements listed in Table 8 of CRWMS M&O (2000, p. I-22). This composition has been used in previous sensitivity studies using previous versions of the Precipitates/Salts model (Mariner 2001). The use of this assumed input allows for direct comparison to previous sensitivity calculations. Because results for sensitivity studies are not generally used as direct input into TSPA models, this composition is sufficient to evaluate the representative potential effects. Therefore, this assumption is justified and requires no further confirmation.

3.6 DRIFT-SCALE HEATER TEST WATER COMPOSITION

Assumption 3.6.1. Because Drift-Scale Heater Test waters are a potential subset of thermally perturbed waters that could contact cementitious materials located in and around a potential repository drift, a potential fluid composition representing Drift-Scale Heater Test water has been selected for Precipitates/Salts model evaporation calculations that feed sensitivity

calculations performed in *Seepage Grout Interactions Model Calculations* (BSC 2001d, Table 6-1.8). The assumed representative composition of Drift-Scale Heater Test water is a Drift-Scale Heater Test water sample collected on 1/26/1999 from borehole 60-3. This composition is documented in DTN: LL990702804244.100. This assumption is used in Section 6.7.

Rationale: This water composition is corroborated by other Drift-Scale Heater Test water compositions reported in DTN: LL990702804244.100 and has been used in previous sensitivity studies using previous versions of the Precipitates/Salts model (Mariner 2001). The use of this assumed input allows for direct comparison to previous sensitivity calculations. Because results for sensitivity studies are not generally used as direct input into TSPA models, this composition is sufficient to evaluate the representative potential effects. Therefore, this assumption is justified and requires no further confirmation.

4. USE OF COMPUTER SOFTWARE AND MODELS

All computer calculations were performed on a Hewlett Packard Pavilion 7410P, an IBM-compatible personal computer, serial number US72352516. This computer uses a Microsoft Windows 95 operating system and is located in Colorado Springs, Colorado.

4.1 MODELS

The Precipitates/Salts model, developed and validated in *In-Drift Precipitates/Salts Analysis* (BSC 2001b), was used to perform the calculations in this document. The model incorporates two submodels, the Low Relative Humidity (LRH) model and the High Relative Humidity (HRH) model. Use of the Precipitates/Salts model in this calculation is justified because the model was specifically designed to perform these calculations (BSC 2001b).

4.2 SOFTWARE

The HRH salts model calculations were performed using the code EQ3/6 v7.2b [CSCI: URCL-MA-110662, Wolery 1992a and 1992b, Wolery and Daveler 1992, CRWMS M&O 1998a] with the solid-centered flow-through addendum [EQ6 V7.2bLV, STN: 10075-7.2bLV-00, CRWMS M&O 1999a and 1999b]. These software were obtained from Configuration Management and installed on the IBM-compatible computer identified at the beginning of Section 4. They were appropriate for the application and were used only within the range of validation in accordance with AP-SI.1Q *Software Management* and the Precipitates/Salts AMR (BSC 2001b). The Precipitates/Salts AMR restricts the use of these codes to a water activity of about 0.85 and higher.

MathSoft Mathcad7 Professional, a commercially-available software package for technical calculations, was used to perform and display the routine algebraic calculations of the LRH salts model. Every equation and calculation is displayed in the referenced Mathcad7 worksheets. Calculated values are represented graphically in the worksheets and have been hand-checked using a calculator to verify the software provided correct results. Because the software requires every equation to be displayed sequentially and in detail, a qualified individual can reproduce these calculations from worksheet displays without recourse to the originator. No macros or

software routines were developed for, or used by, this software, and consequently it is an exempt software application in accordance with Section 2.1 of AP-SI.1Q.

Microsoft Excel 97 SR-2, a commercially-available spreadsheet software package, was used to chart data and to calculate the ionic strength approximation (*ISa*) and concentration factor (C/C_o). Spreadsheet calculations were validated by hand calculations using the equations presented in Section 5.2, and charts were validated by visual inspection. These actions confirm that the spreadsheet application provided correct results. No macros or software routines were developed for, or used by, this software, and consequently it is an exempt software application in accordance with Section 2.1 of AP-SI.1Q.

5. CALCULATION

Section 5.1 describes the input to the calculations while Section 5.2 describes the calculations performed.

5.1 INPUT

The calculations required the following types of input: 1) thermodynamic constants for potentially important ground-water constituents, and 2) values for model input variables.

5.1.1 Thermodynamic Database

Two thermodynamic databases were used in the evaporation calculations. The PT5v1 Pitzer thermodynamic database (DTN: MO0110SPAPT545.016) was used for cases HLi, HHi, LLi, LHi, HLc, HHc, LLc, and LHc in Table 1. These calculations were originally performed prior to the development of the PT5v2 database. The PT5v2 database (DTN: MO0110SPAPT245.017) was used in the rest of the simulations. The only difference between the two databases is that nesquehonite is not included in the PT5v1 database. These databases are developed and discussed in the Precipitates/Salts AMR (BSC 2001b).

5.1.2 Input Variables

The input variables for the simulations include temperature, pH, fugacity of CO_2, redox potential, and initial concentrations of the aqueous components. Table 1 and Table 2 list the sources of the acquired input data used in the EQ3/6 input files in this calculation.

Not all waters identified in Table 1 and Table 2 have a complete set of values for input variables. Values were entered for redox potential, but they did not affect the results because no redox reactions were simulated. Waters in Table 2 were evaporated at 96°C and were evaporated at three different values for CO_2 fugacity: 10^{-1}, 10^{-3}, and 10^{-6}. Nitrate was added to the waters in Table 1 as described in Section 3.1, and CO_2 fugacity was modified for four of the Table 1 waters as described in Section 3.2. Minerals were suppressed for each water as explained in Section 3.3.

Table 1. References for REV 01 THC Model Abstraction Data Used in EQ3/6 Input Files

Case Description	Case Abbreviation	Reference
Base Case THC Model Abstraction for Seepage at the Crown of the Drift in the Tptpmn Lithology	Bmc	BSC 2001c, Table 4
Base Case THC Model Abstraction for Seepage Wicking into the Invert in the Tptpmn Lithology	Bmi	BSC 2001c, Table 5
Base Case THC Model Abstraction for Seepage at the Crown of the Drift in the Tptpll Lithology	Blc	BSC 2001c, Table 6
Base Case THC Model Abstraction for Seepage Wicking into the Invert in the Tptpll Lithology	Bli	BSC 2001c, Table 7
High Temperature and Low Carbon Dioxide Partial Pressure Case for Seepage at the Crown of the Drift in the Tptpll Lithology	HLc	BSC 2001c, Table 8
High Temperature and High Carbon Dioxide Partial Pressure Case for Seepage at the Crown of the Drift in the Tptpll Lithology	HHc	BSC 2001c, Table 9
Low Temperature and Low Carbon Dioxide Partial Pressure Case for Seepage at the Crown of the Drift in the Tptpll Lithology	LLc	BSC 2001c, Table 10
Low Temperature and High Carbon Dioxide Partial Pressure Case for Seepage at the Crown of the Drift in the Tptpll Lithology	LHc	BSC 2001c, Table 11
High Temperature and Low Carbon Dioxide Partial Pressure Case for Matrix Imbibition into the Invert in the Tptpll Lithology	HLi	BSC 2001c, Table 12
High Temperature and High Carbon Dioxide Partial Pressure Case for Matrix Imbibition into the Invert in the Tptpll Lithology	HHi	BSC 2001c, Table 13
Low Temperature and Low Carbon Dioxide Partial Pressure Case for Matrix Imbibition into the Invert in the Tptpll Lithology	LLi	BSC 2001c, Table 14
Low Temperature and High Carbon Dioxide Partial Pressure Case for Matrix Imbibition into the Invert in the Tptpll Lithology	LHi	BSC 2001c, Table 15
High Temperature and High Carbon Dioxide Partial Pressure Case for Seepage at the Crown of the Drift in the Tptpll Lithology, Initialized Using Water Composition of UZ-14 Perched Water	HHcp	BSC 2001c, Table 16
High Temperature and High Carbon Dioxide Partial Pressure Case for Matrix Imbibition into the Invert in the Tptpll Lithology, Initialized Using Water Composition of UZ-14 Perched Water	HHip	BSC 2001c, Table 17
Low Temperature and High Carbon Dioxide Partial Pressure Case for Seepage at the Crown of the Drift in the Tptpll Lithology, Initialized Using Water Composition of UZ-14 Perched Water	LHcp	BSC 2001c, Table 18
Low Temperature and High Carbon Dioxide Partial Pressure Case for Matrix Imbibition into the Invert in the Tptpll Lithology, Initialized Using Water Composition of UZ-14 Perched Water	LHip	BSC 2001c, Table 19

DTN: MO0110SPAEBS13.038

Table 2. References for Additional EQ3/6 Input Files

Case Description	Reference
Chemical composition of perched water sample collected from borehole USW UZ-14 within the Topopah Spring welded unit on 8/3/1993	Assumption 3.5.1
Chemical analysis of Drift-Scale Heater Test water sample from borehole 60-3 on 1/26/1999	Assumption 3.6.1

5.2 CALCULATIONS

The calculations involved both submodels of the Precipitates/Salts model, the high relative humidity (HRH) salts model and the low relative humidity (LRH) salts model.

5.2.1 High Relative Humidity (HRH) Salts Model

Each HRH salts model evaporation calculation was performed using EQ3/6 according to the procedures described in Section 6.4.2.1 of the Precipitates/Salts AMR (BSC 2001b). Water was evaporated by declaring it a "special reactant" with a rate constant of -1.0. The maximum reaction progress was iteratively adjusted to achieve a final water activity of 0.85. Before each evaporation simulation, the water composition was electrically balanced by allowing EQ3/6 to adjust the Na, Cl, or other major ion concentration, depending on which ion's concentration would be changed the least to achieve electrical balance.

Model predictions were exported to text files using the EQ3/6 postprocessor (PP.EXE) included in the EQ6 software package. These text files were imported into Excel worksheets where the ionic strength approximation (*ISa*) and concentration factor (C/C_o) could be calculated and the results plotted. C/C_o was calculated by dividing the total nitrate concentration by the initial nitrate concentration. Nitrate does not precipitate in the high relative humidity range modeled by the HRH salts model.

The ionic strength approximation (*ISa*) parameter of the Precipitates/Salts model is not the true ionic strength. Instead, it is an approximation of the true ionic strength (*I*) according to the following equation:

$$ISa = C_{Na} + C_K + 4(C_{Ca} + C_{Mg}) \quad \text{(Eq. 1)}$$

where C_i is the molality of component *i*, and *i* represents sodium (Na), potassium (K), calcium (Ca), or magnesium (Mg). This approximation is included in the results because it is identical to the approximation used by the colloids model (CRWMS M&O 1998b, Section 4.4.3.3.1) and Precipitates/Salts model (BSC 2001b, Section 6.3.2).

5.2.2 Low Relative Humidity (LRH) Salts Model

The LRH salts model was used to predict ionic strength and chloride concentration below a relative humidity of 85 percent for the HHi and LHi cases of the sensitivity THC model abstraction (Table 1). These results were extended to the HLi, HHc, HLc, LLi, LHc, and LLc cases as described in Assumption 3.4.1 (Section 3.4).

LRH salts model calculations were performed as described in Section 6.4.1 of the Precipitates/Salts AMR (BSC 2001b). Additional assumptions relevant to the LRH calculations are documented in Section 3 of the REV 00 THC model abstraction evaporation calculation (CRWMS M&O 2001). The effective solubility of the non-nitrate salts was adjusted between 3.3 and 4.2 molal to provide a smooth transition between the LRH and HRH model results.

This submodel was designed for waters that evaporatively evolve into a sodium nitrate brine. Section 6.8 describes the uncertainties and limitations of results of this submodel.

6. RESULTS

In this section, the results of the calculations are presented. Section 6.1 presents the HRH model results for the base case REV 01 THC model abstraction, and Section 6.2 presents the HRH model results for the sensitivity cases of the REV 01 THC model abstractions. Section 6.3 compares and summarizes the results of Sections 6.1 and 6.2. The LRH model results are presented in Section 6.4 and the lookup tables for TSPA in Section 6.5. Section 6.6 discusses the sensitivity of certain mineral suppressions. Evaporation calculations performed as input to the Seepage Grout Interactions Model are described in Section 6.7. Finally, Section 6.8 discusses important uncertainties and limitations of the calculations.

The calculations performed for this work are documented in the set of DTNs referenced in Table 3. Each case in Table 1 is divided into 5 or 6 abstraction periods. To simplify comparisons and identification of results, these periods are numbered in the document and output files as described in Table 4.

Results from selected output files are plotted in Figures 1 through 89.
Table 5 provides a cross-reference of the output files associated with each figure in this document. A complete set of output files is found in the output DTNs listed in Table 3.

Table 3. Cross-Reference of Outputs and Their DTNs

Case Abbreviation or Description	Output File DTN
Bmc, Bmi, Blc, Bli, HHcp, HHip, LHcp, LHip (Table 1)	MO0112MWDTHC12.024 (EQ3/6 input/output files)
HLc, HHc, LLc, LHc, HLi, HHi, LLi, LHi (Table 1)	MO0111MWDVAR12.021 (EQ3/6 input/output files) MO0111MWDSEE12.022 (LRH model output files) MO0111SPAPSM12.023 (Lookup tables)
Perched Water (Table 2), Drift Scale Test Water (Table 2)	MO0111MWDHRH12.019 (EQ3/6 input/output files)

Table 4. Key to Abstraction Time Periods Cited in This Report

Abstraction Time Period	Base Case [a]	High Temperature Operating Mode [b]	Low Temperature Operating Mode [c]
1	0-50 years	0-50 years	0-300 years
2	51-1,200 years	51-1,500 years	301-10,000 years
3	1,201-2,000 years	1,501-4,000 years	10,001-30,000 years
4	2,001-20,000 years	4,001-25,000 years	30,001-100,000 years
5	20,001-100,000 years	25,001-100,000 years	100,001-1,000,000 years
6	100,001-1,000,000 years	100,001-1,000,000 years	not applicable

DTN: MO0110SPAEBS13.038

NOTE: [a] Cases Bmc, Bmi, Blc, and Bli in Table 1
[b] Cases HLc, HHc, HLi, HHi, HHcp, and HHip in Table 1
[c] Cases LLc, LHc, LLi, LHi, LHcp, and LHip in Table 1

Table 5. Cross-Reference of Figures and Their Output Files

Water [a]	Figures	Output Files	Output DTN
Bmc	Figure 1 & Figure 2	MC1.6O	MO0112MWDTHC12.024
	Figure 3 & Figure 4	MC2.6O	MO0112MWDTHC12.024
	Figure 5 & Figure 6	MC3.6O	MO0112MWDTHC12.024
	Figure 7 & Figure 8	MC4.6O	MO0112MWDTHC12.024
	Figure 9 & Figure 10	MC5.6O	MO0112MWDTHC12.024
	Figure 11 & Figure 12	MC6.6O [b]	MO0112MWDTHC12.024
Bmi	Figure 13 & Figure 14	MI1.6O	MO0112MWDTHC12.024
	Figure 15 & Figure 16	MI2.6O	MO0112MWDTHC12.024
	Figure 17 & Figure 18	MI3.6O	MO0112MWDTHC12.024
	Figure 19 & Figure 20	MI4.6O	MO0112MWDTHC12.024
	Figure 21 & Figure 22	MI5.6O	MO0112MWDTHC12.024
	Figure 23 & Figure 24	MI6.6O	MO0112MWDTHC12.024
Blc	Figure 25 & Figure 26	LC1.6O	MO0112MWDTHC12.024
	Figure 27 & Figure 28	LC2.6O	MO0112MWDTHC12.024
	Figure 29 & Figure 30	LC3.6O	MO0112MWDTHC12.024
	Figure 31 & Figure 32	LC4.6O	MO0112MWDTHC12.024
	Figure 33 & Figure 34	LC5.6O	MO0112MWDTHC12.024
	Figure 35 & Figure 36	LC6.6O	MO0112MWDTHC12.024
Bli	Figure 37 & Figure 38	LI1.6O	MO0112MWDTHC12.024
	Figure 39 & Figure 40	LI2.6O	MO0112MWDTHC12.024
	Figure 41 & Figure 42	LI3.6O	MO0112MWDTHC12.024
	Figure 43 & Figure 44	LI4.6O	MO0112MWDTHC12.024
	Figure 45 & Figure 46	LI5.6O	MO0112MWDTHC12.024
	Figure 47 & Figure 48	LI6.6O	MO0112MWDTHC12.024
Hli	Figure 49 Figure 50	HLI1.6O HLI2.6O	MO0111MWDVAR12.021
	Figure 51 Figure 52	HLI3.6O HLI4.6O	MO0111MWDVAR12.021
	Figure 53 Figure 54	HLI5.6O HLI6.6O	MO0111MWDVAR12.021
HHi	Figure 55 Figure 56	HHI1.6O HHI2.6O	MO0111MWDVAR12.021
	Figure 57 Figure 58	HHI3.6O HHI4.6O	MO0111MWDVAR12.021
	Figure 59 Figure 60	HHI5.6O HHI6.6O	MO0111MWDVAR12.021
LLi	Figure 61 Figure 62	LLI1.6O LLI2.6O	MO0111MWDVAR12.021
	Figure 63 Figure 64	LLI3.6O LLI4.6O	MO0111MWDVAR12.021
	Figure 65	LLI5.6O	MO0111MWDVAR12.021
LHi	Figure 66 Figure 67	LHI1.6O LHI2.6O	MO0111MWDVAR12.021
	Figure 68 Figure 69	LHI3.6O LHI4.6O	MO0111MWDVAR12.021
	Figure 70	LHI5.6O	MO0111MWDVAR12.021
HHip	Figure 71 Figure 72	HHIP1.6O HHIP2.6O	MO0112MWDTHC12.024
	Figure 73 Figure 74	HHIP3.6O HHIP4.6O	MO0112MWDTHC12.024
	Figure 75 Figure 76	HHIP5.6O HHIP6.6O	MO0112MWDTHC12.024
LHip	Figure 77 Figure 78	LHIP1.6O LHIP2.6O	MO0112MWDTHC12.024
	Figure 79 Figure 80	LHIP3.6O LHIP4.6O	MO0112MWDTHC12.024
	Figure 81	LHIP5.6O	MO0112MWDTHC12.024
LHi1 (LRH)	Figure 82	LHI1.MCD	MO0111MWDSEE12.022
LLi1 (LRH)	Figure 83	LLI1.XLS	MO0111SPAPSM12.023
HHi (Mineral Sensitivity)	Figure 84 Figure 85	HHI1EVAP.6O HHI2EVAP.6O	MO0112MWDTHC12.024
	Figure 86 Figure 87	HHI3EVAP.6O HHI4EVAP.6O	MO0112MWDTHC12.024
	Figure 88 Figure 89	HHI5EVAP.6O HHI6EVAP.6O	MO0112MWDTHC12.024

[a] Case abbreviations are defined in Table 1. LHi1 and LLi1 refer to period 1 of the LHi and LLi cases (see Table 4).

[b] The input for this run is mistakenly from the invert instead of the crown. However, the differences in these inputs are small (BSC 2001d, Tables 4 and 5) and easily within the range of uncertainty in the derived abstracted input values (BSC 2001d, Section 6.3). The crown seepage values are within 2 percent of the invert values, except for Mg, which is nearly 10 percent higher in the invert seepage (BSC 2001d, Tables 4 and 5).

6.1 RESULTS FOR BASE CASE THC MODEL ABSTRACTION

The base case THC model abstractions include the Bmc, Bmi, Blc, and Bli cases in Table 1. The Bmc and Bmi cases are for seepage in the middle nonlithophysal zone of the crystal-poor member of the Topopah Spring tuff (i.e., Tptpmn). The Blc and Bli cases are for seepage in the lower lithophysal zone of the crystal-poor member of the Topopah Spring tuff (i.e., Tptpll). The Tptpmn and Tptpll results are presented in Sections 6.1.1 and 6.1.2, respectively. These subsections are further subdivided by seepage source, i.e., seepage from the crown of the drift or imbibed into the invert.

Figure 1 through Figure 48 present HRH salts model predictions of the evaporative evolution of these base case waters for each time period. For each case and time period, plots of the predicted aqueous and mineral evaporative evolutions are presented. The parameter *IS* represents the true ionic strength predicted by EQ3/6. As described in Section 5.2.1, *ISa* is the calculated ionic strength approximation. The concentration factor (C/C_o) on the x-axis is the total nitrate concentration divided by the nitrate concentration prior to evaporation. The plotted results span the range of concentration factors corresponding to water activities of 0.85 and higher.

The entire set of EQ3/6 input and output files for the Bmc, Bmi, Blc, and Bli cases are documented in DTN: MO0112MWDTHC12.024.

6.1.1 Tptpmn Lithology

6.1.1.1 Seepage at the Crown of the Drift (Case Bmc)

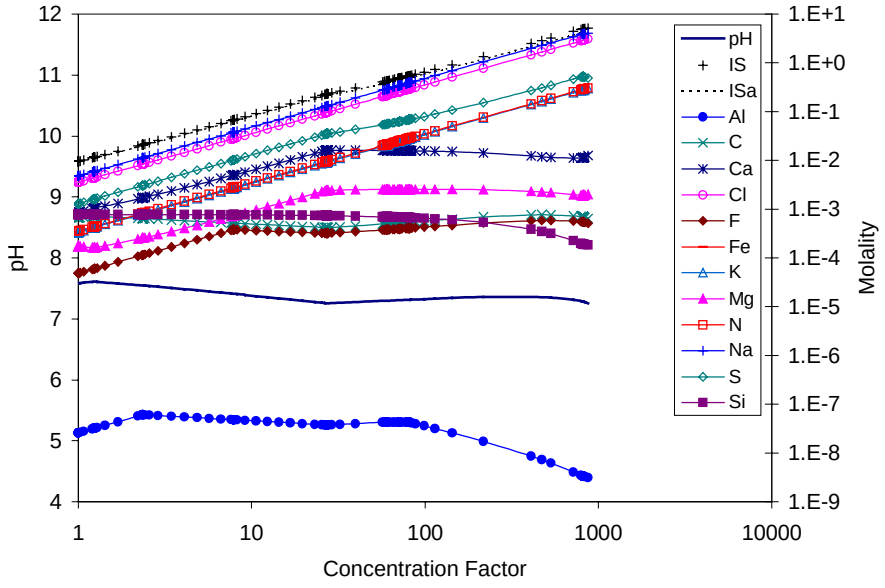

DTN: MO0112MWDTHC12.024

Figure 1. Aqueous Evaporative Evolution for the Base Case THC Model Abstraction for Seepage at the Crown of the Drift in the Tptpmn Lithology (Bmc), Period 1

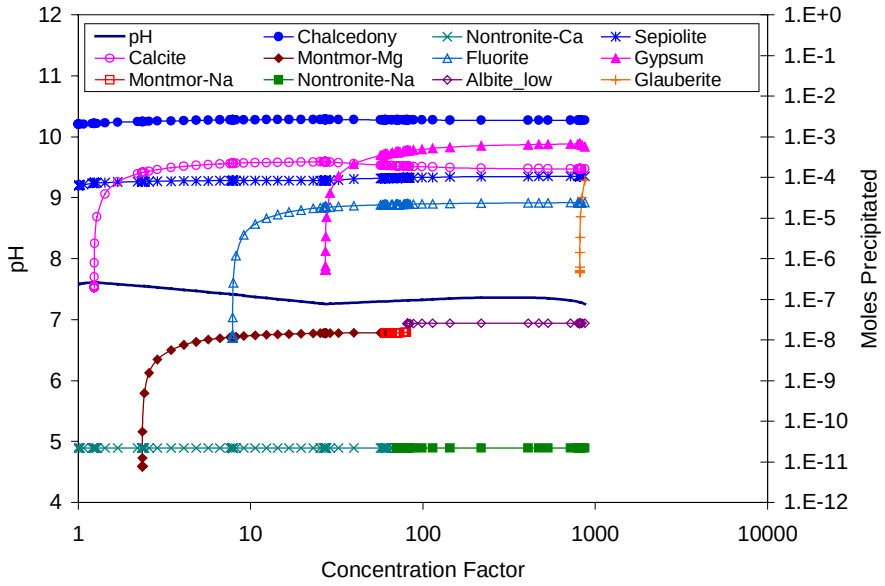

DTN: MO0112MWDTHC12.024

Figure 2. Mineral Evaporative Evolution for the Base Case THC Model Abstraction for Seepage at the Crown of the Drift in the Tptpmn Lithology (Bmc), Period 1

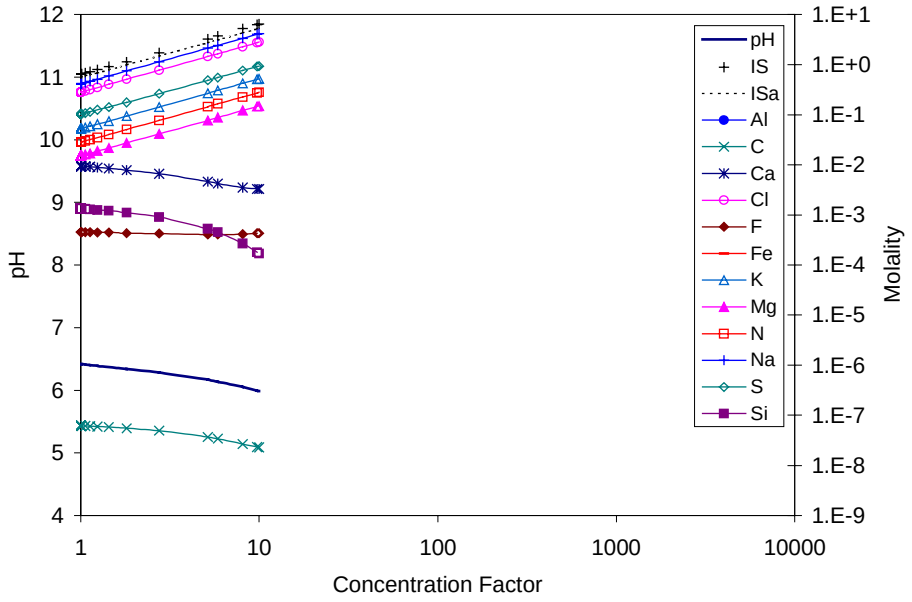

DTN: MO0112MWDTHC12.024

Figure 3. Aqueous Evaporative Evolution for the Base Case THC Model Abstraction for Seepage at the Crown of the Drift in the Tptpmn Lithology (Bmc), Period 2

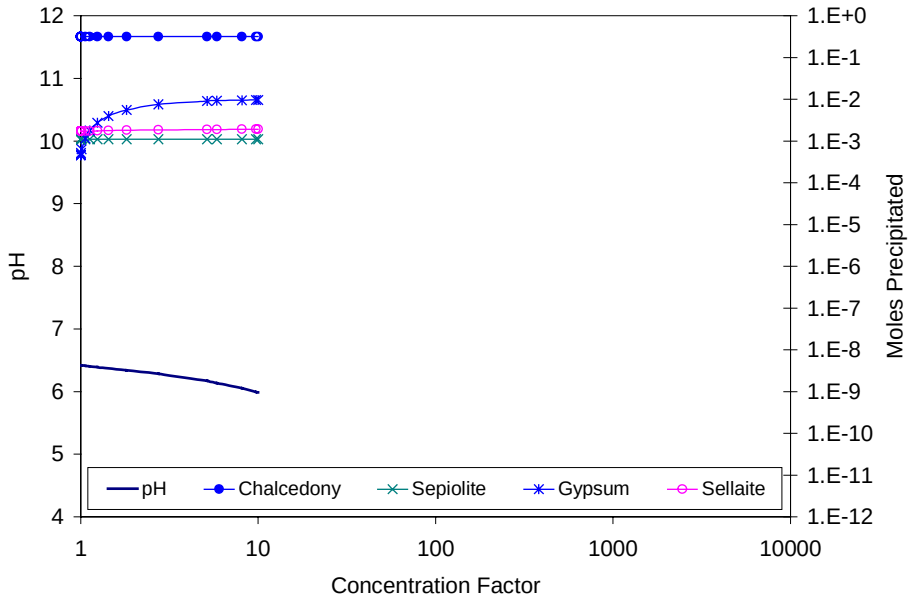

DTN: MO0112MWDTHC12.024

Figure 4. Mineral Evaporative Evolution for the Base Case THC Model Abstraction for Seepage at the Crown of the Drift in the Tptpmn Lithology (Bmc), Period 2

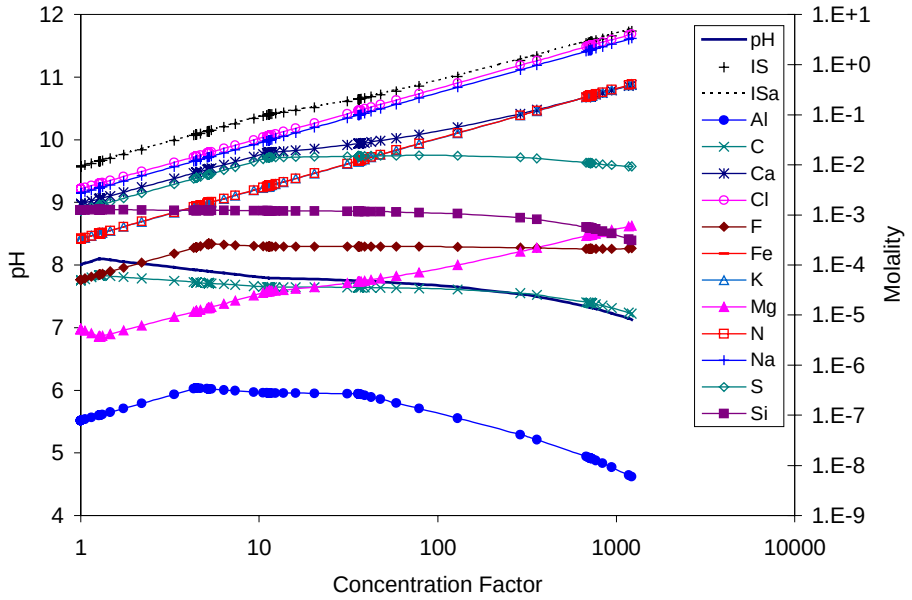

DTN: MO0112MWDTHC12.024

Figure 5. Aqueous Evaporative Evolution for the Base Case THC Model Abstraction for Seepage at the Crown of the Drift in the Tptpmn Lithology (Bmc), Period 3

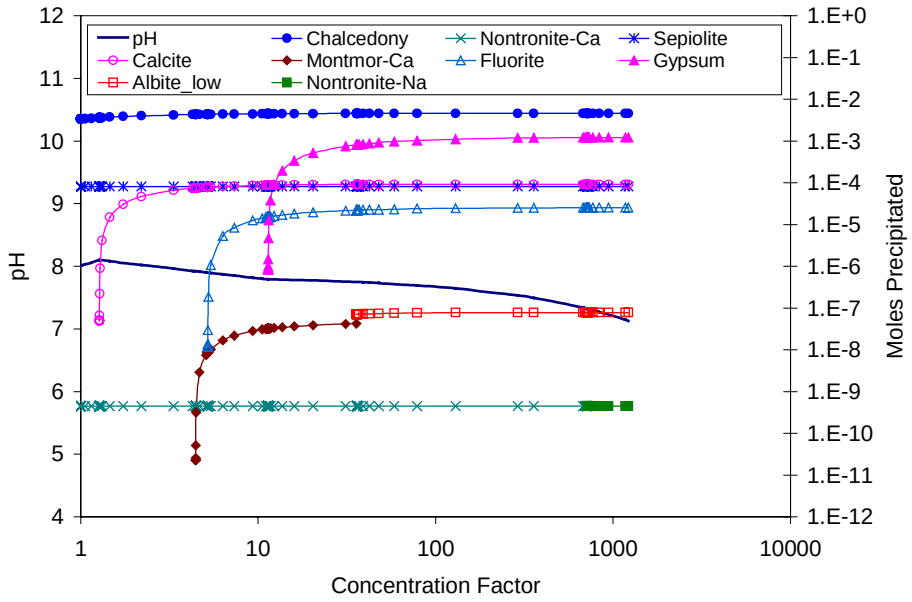

DTN: MO0112MWDTHC12.024

Figure 6. Mineral Evaporative Evolution for the Base Case THC Model Abstraction for Seepage at the Crown of the Drift in the Tptpmn Lithology (Bmc), Period 3

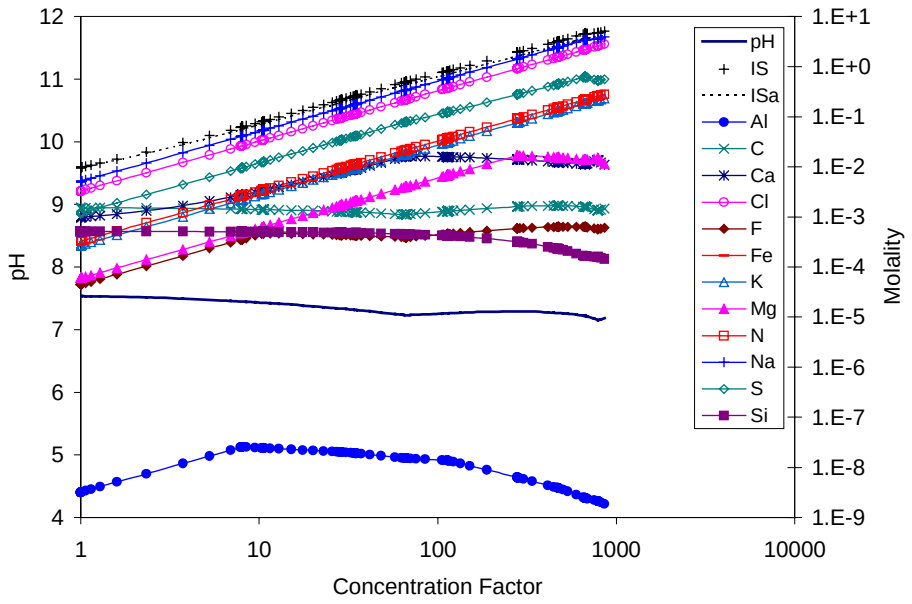

DTN: MO0112MWDTHC12.024

Figure 7. Aqueous Evaporative Evolution for the Base Case THC Model Abstraction for Seepage at the Crown of the Drift in the Tptpmn Lithology (Bmc), Period 4

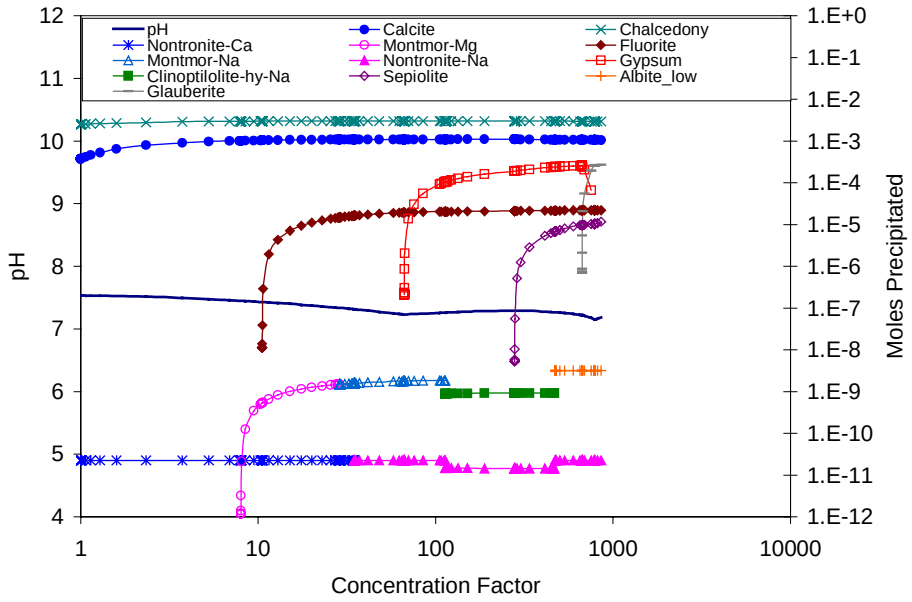

DTN: MO0112MWDTHC12.024

Figure 8. Mineral Evaporative Evolution for the Base Case THC Model Abstraction for Seepage at the Crown of the Drift in the Tptpmn Lithology (Bmc), Period 4

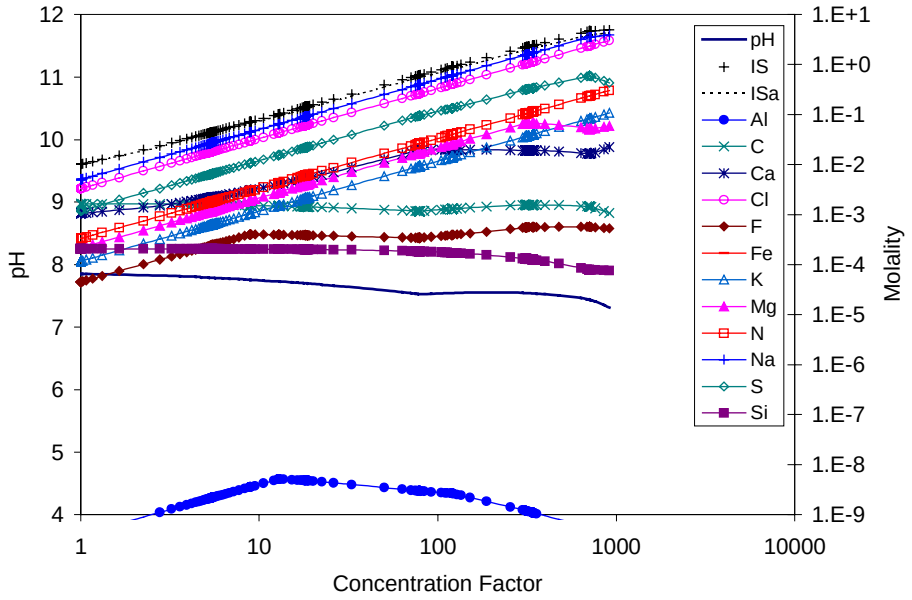

DTN: MO0112MWDTHC12.024

Figure 9. Aqueous Evaporative Evolution for the Base Case THC Model Abstraction for Seepage at the Crown of the Drift in the Tptpmn Lithology (Bmc), Period 5

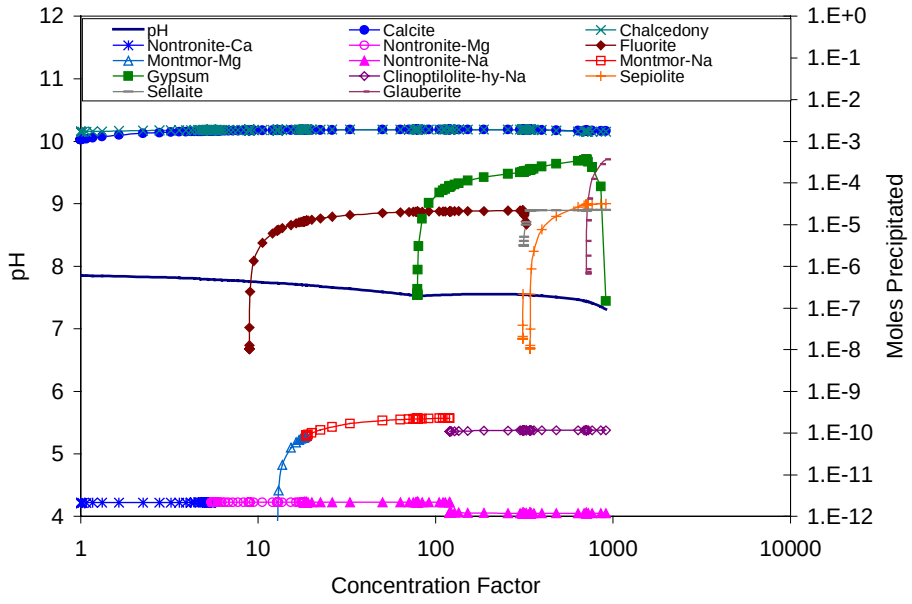

DTN: MO0112MWDTHC12.024

Figure 10. Mineral Evaporative Evolution for the Base Case THC Model Abstraction for Seepage at the Crown of the Drift in the Tptpmn Lithology (Bmc), Period 5

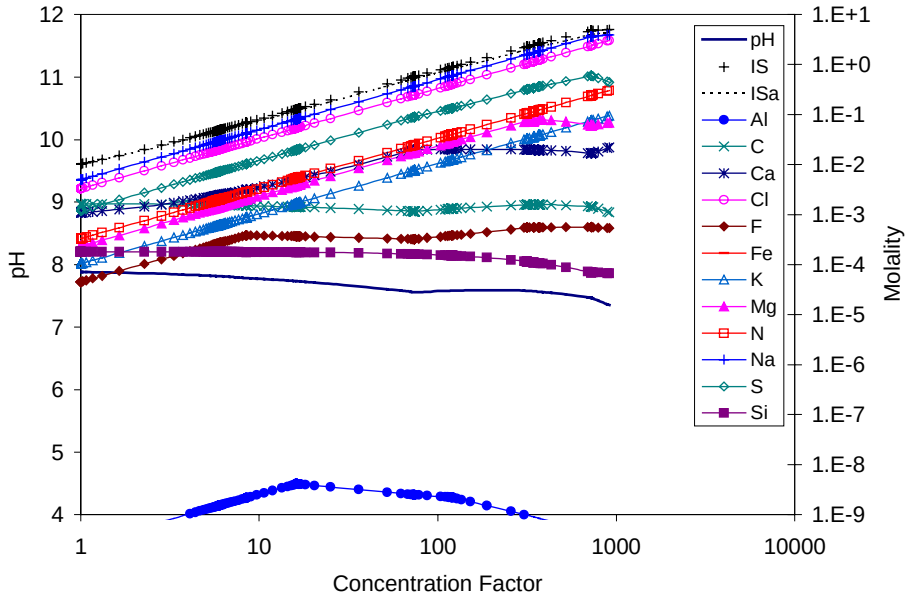

DTN: MO0112MWDTHC12.024

Figure 11. Aqueous Evaporative Evolution for the Base Case THC Model Abstraction for Seepage at the Crown of the Drift in the Tptpmn Lithology (Bmc), Period 6

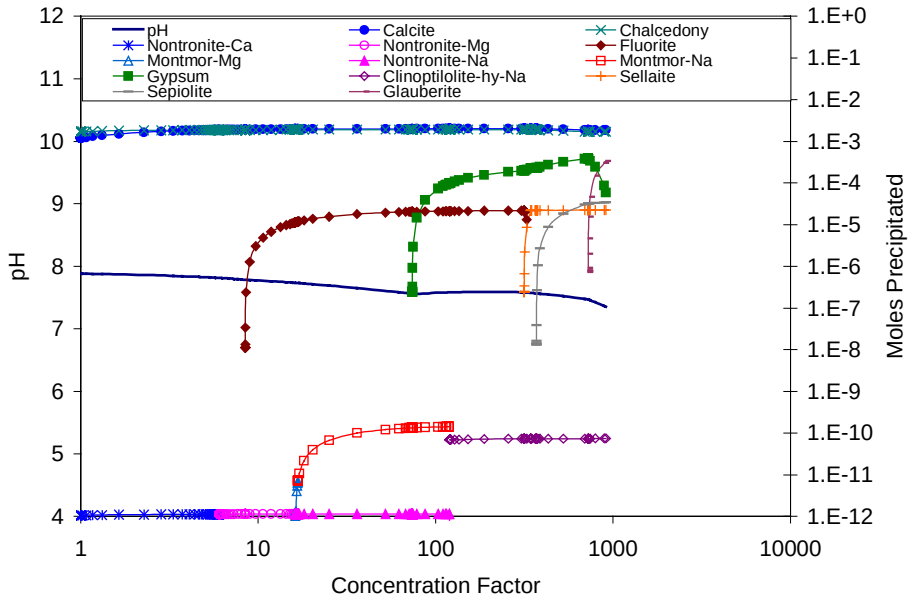

DTN: MO0112MWDTHC12.024

Figure 12. Mineral Evaporative Evolution for the Base Case THC Model Abstraction for Seepage at the Crown of the Drift in the Tptpmn Lithology (Bmc), Period 6

6.1.1.2 Water Imbibed into the Invert (Case Bmi)

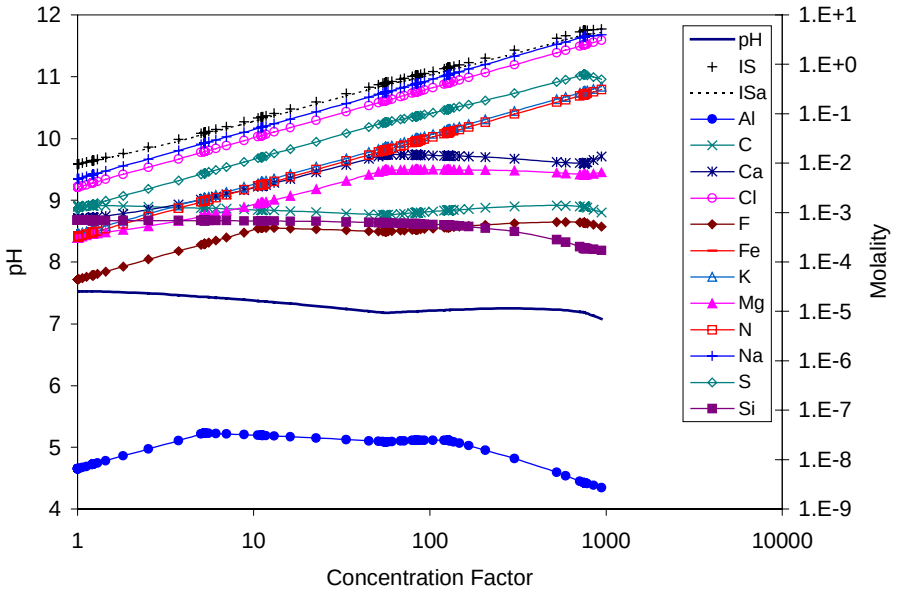

DTN: MO0112MWDTHC12.024

Figure 13. Aqueous Evaporative Evolution for the Base Case THC Model Abstraction for Seepage Wicking into the Invert in the Tptpmn Lithology (Bmi), Period 1

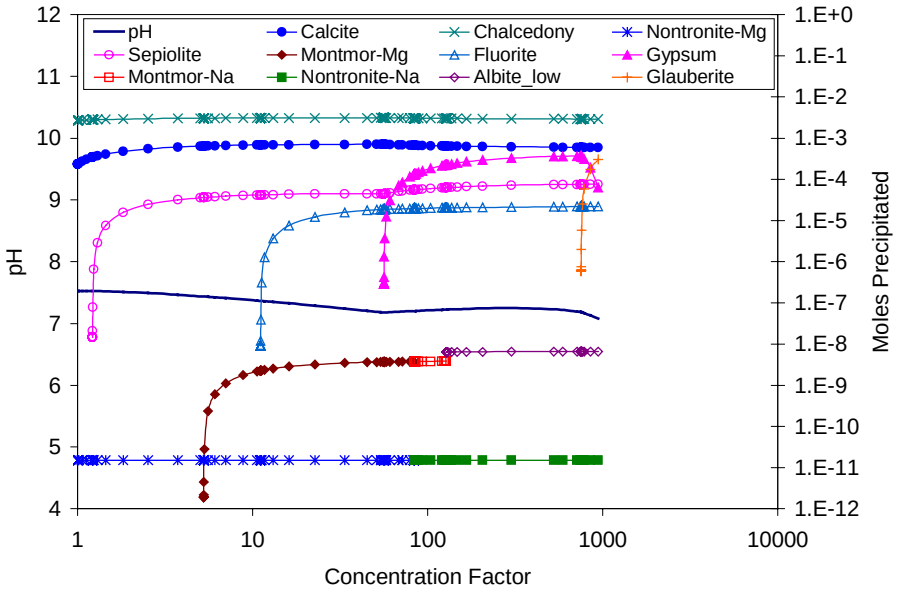

DTN: MO0112MWDTHC12.024

Figure 14. Mineral Evaporative Evolution for the Base Case THC Model Abstraction for Seepage Wicking into the Invert in the Tptpmn Lithology (Bmi), Period 1

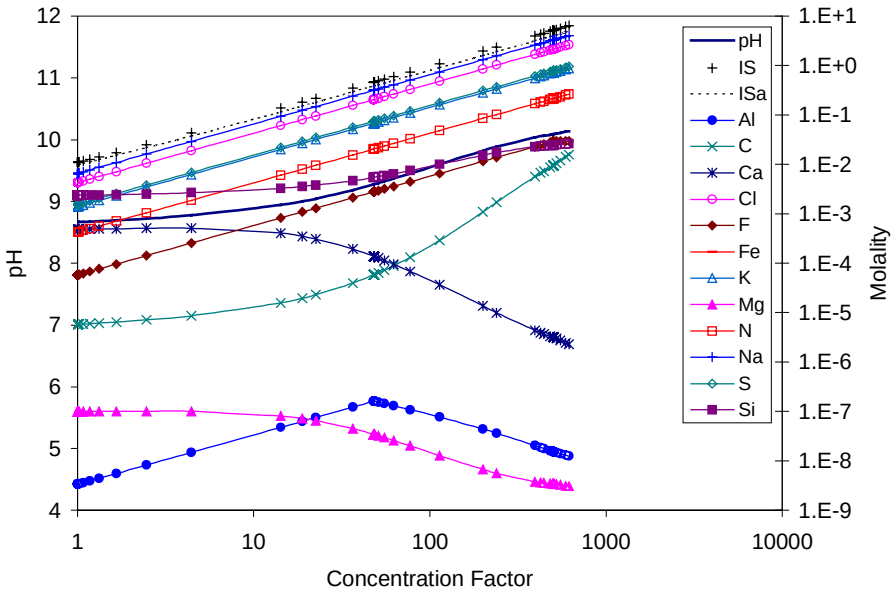

DTN: MO0112MWDTHC12.024

Figure 15. Aqueous Evaporative Evolution for the Base Case THC Model Abstraction for Seepage Wicking into the Invert in the Tptpmn Lithology (Bmi), Period 2

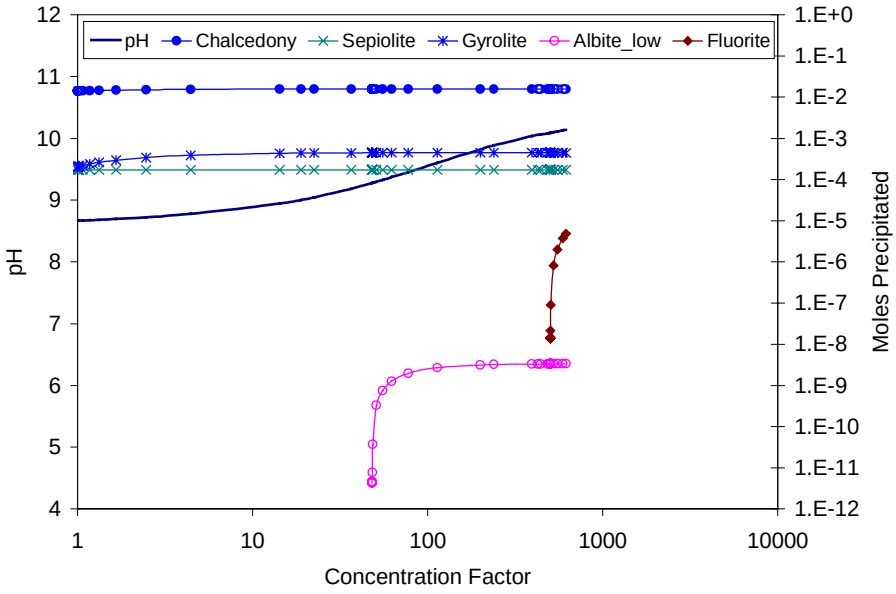

DTN: MO0112MWDTHC12.024

Figure 16. Mineral Evaporative Evolution for the Base Case THC Model Abstraction for Seepage Wicking into the Invert in the Tptpmn Lithology (Bmi), Period 2

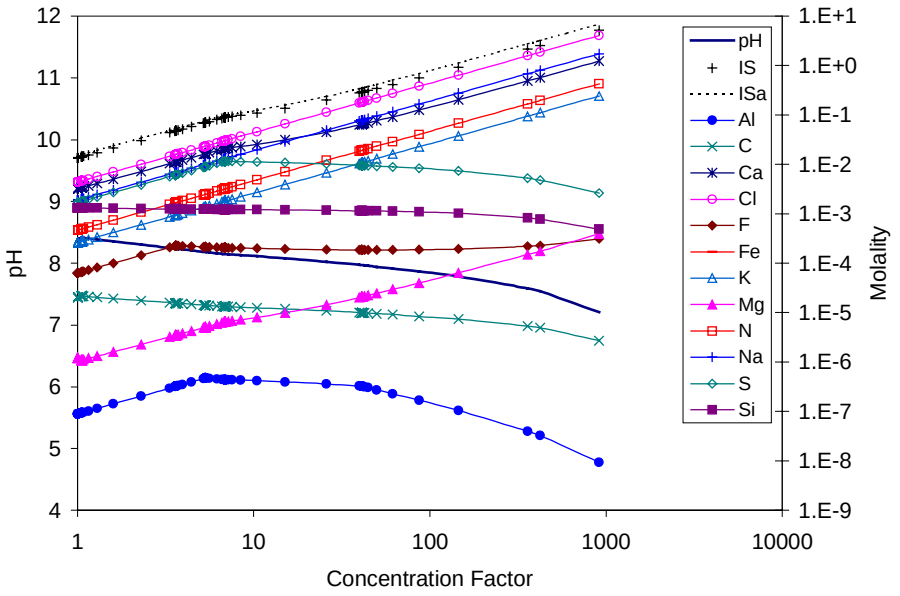

DTN: MO0112MWDTHC12.024

Figure 17. Aqueous Evaporative Evolution for the Base Case THC Model Abstraction for Seepage Wicking into the Invert in the Tptpmn Lithology (Bmi), Period 3

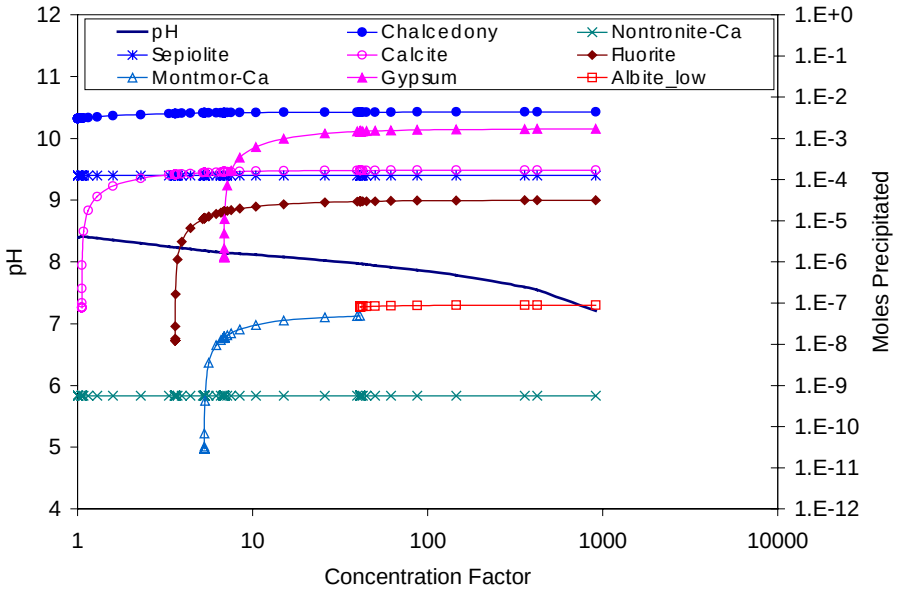

DTN: MO0112MWDTHC12.024

Figure 18. Mineral Evaporative Evolution for the Base Case THC Model Abstraction for Seepage Wicking into the Invert in the Tptpmn Lithology (Bmi), Period 3

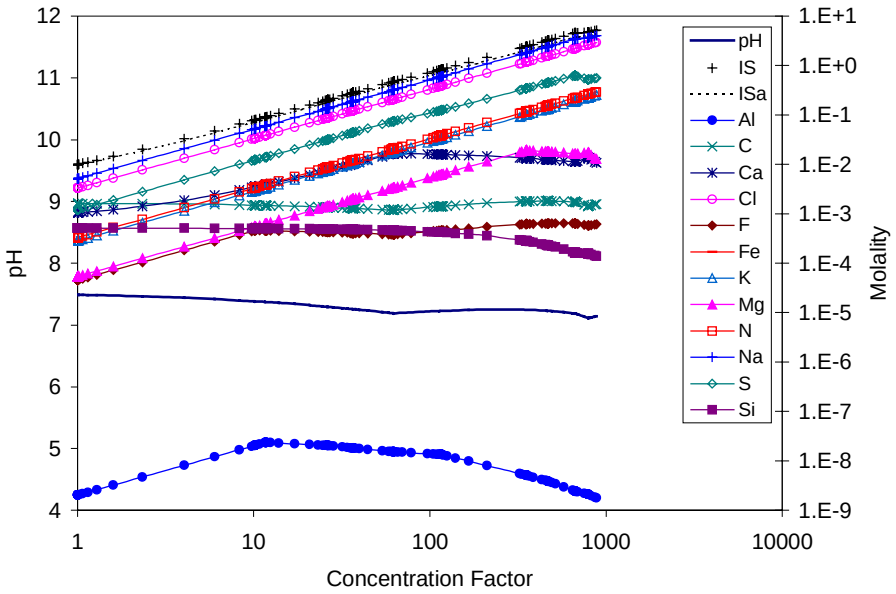

DTN: MO0112MWDTHC12.024

Figure 19. Aqueous Evaporative Evolution for the Base Case THC Model Abstraction for Seepage Wicking into the Invert in the Tptpmn Lithology (Bmi), Period 4

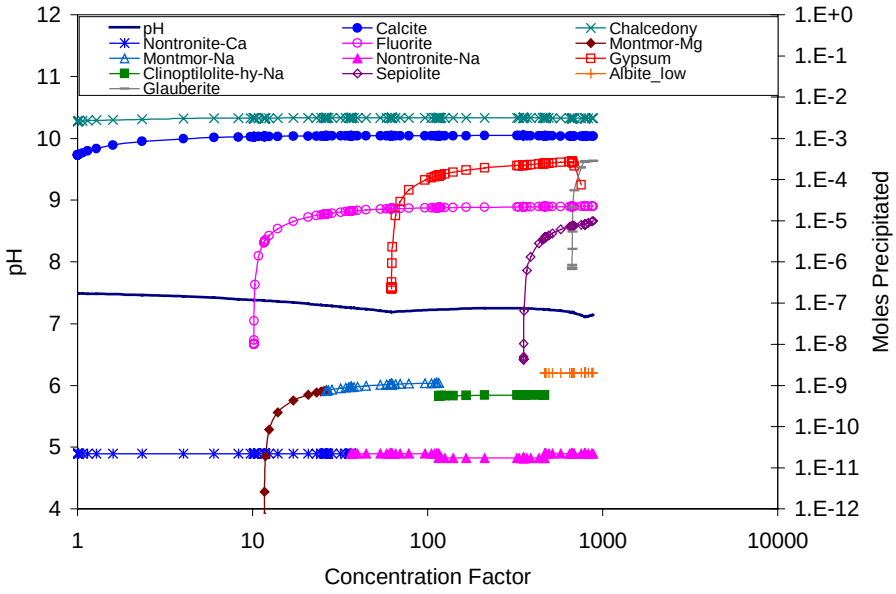

DTN: MO0112MWDTHC12.024

Figure 20. Mineral Evaporative Evolution for the Base Case THC Model Abstraction for Seepage Wicking into the Invert in the Tptpmn Lithology (Bmi), Period 4

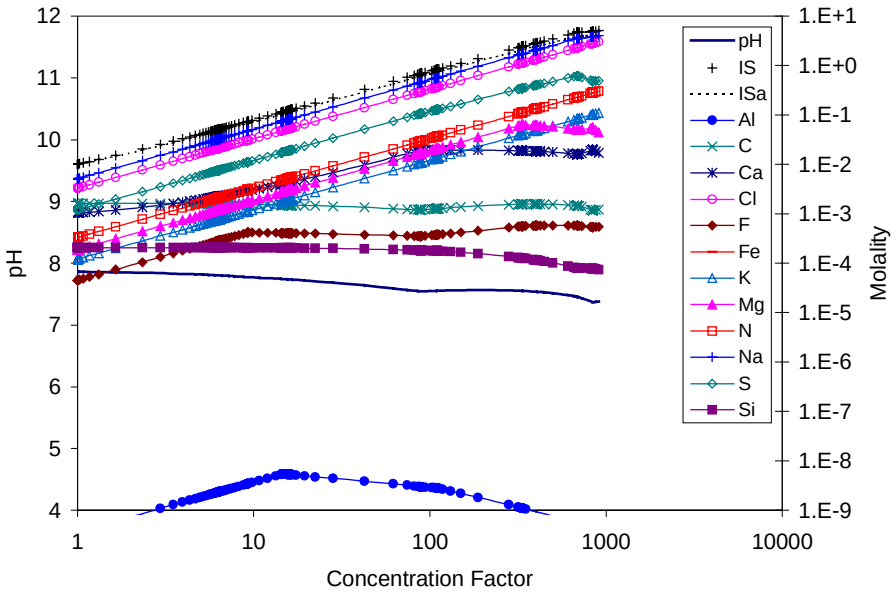

DTN: MO0112MWDTHC12.024

Figure 21. Aqueous Evaporative Evolution for the Base Case THC Model Abstraction for Seepage Wicking into the Invert in the Tptpmn Lithology (Bmi), Period 5

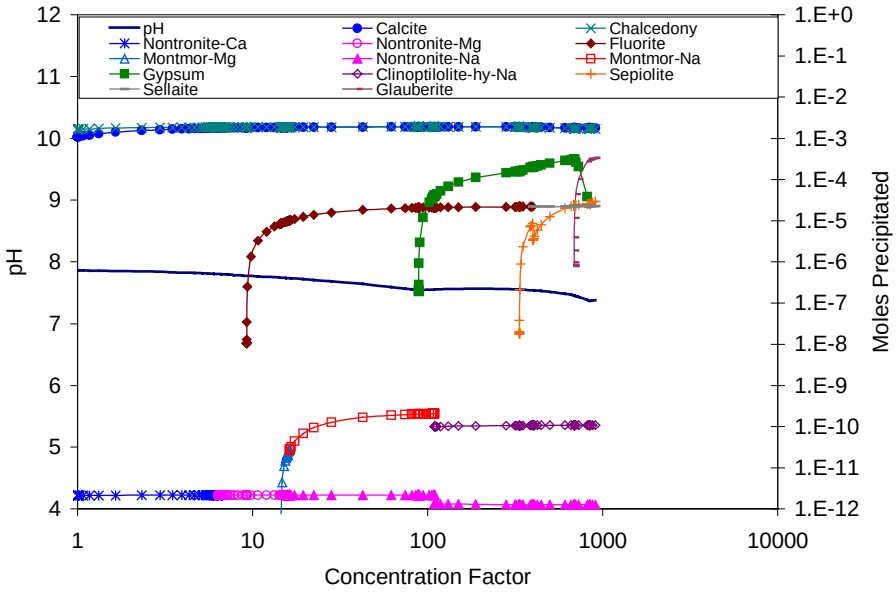

DTN: MO0112MWDTHC12.024

Figure 22. Mineral Evaporative Evolution for the Base Case THC Model Abstraction for Seepage Wicking into the Invert in the Tptpmn Lithology (Bmi), Period 5

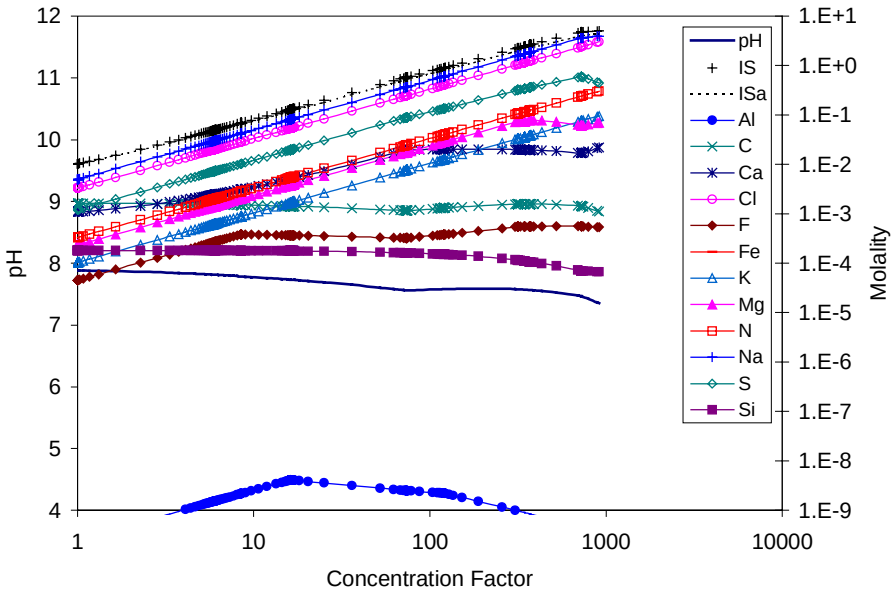

DTN: MO0112MWDTHC12.024

Figure 23. Aqueous Evaporative Evolution for the Base Case THC Model Abstraction for Seepage Wicking into the Invert in the Tptpmn Lithology (Bmi), Period 6

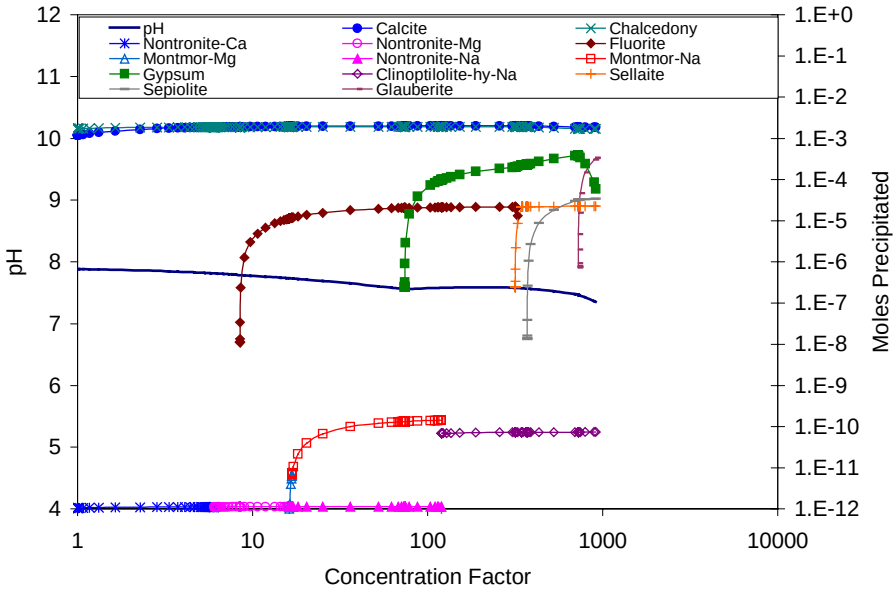

DTN: MO0112MWDTHC12.024

Figure 24. Mineral Evaporative Evolution for the Base Case THC Model Abstraction for Seepage Wicking into the Invert in the Tptpmn Lithology (Bmi), Period 6

6.1.2 Tptpll Lithology

6.1.2.1 Seepage at the Crown of the Drift (Case Blc)

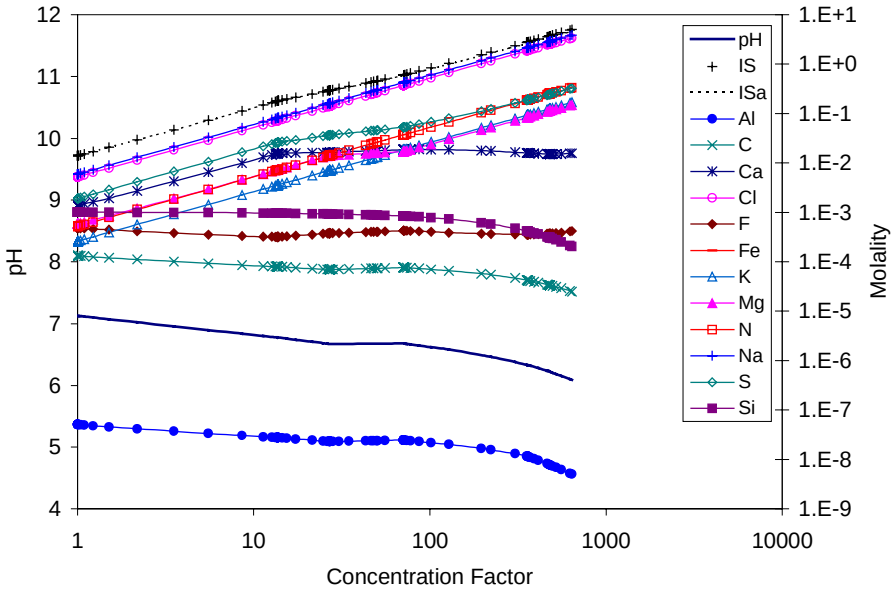

DTN: MO0112MWDTHC12.024

Figure 25. Aqueous Evaporative Evolution for the Base Case THC Model Abstraction for Seepage at the Crown of the Drift in the Tptpll Lithology (Blc), Period 1

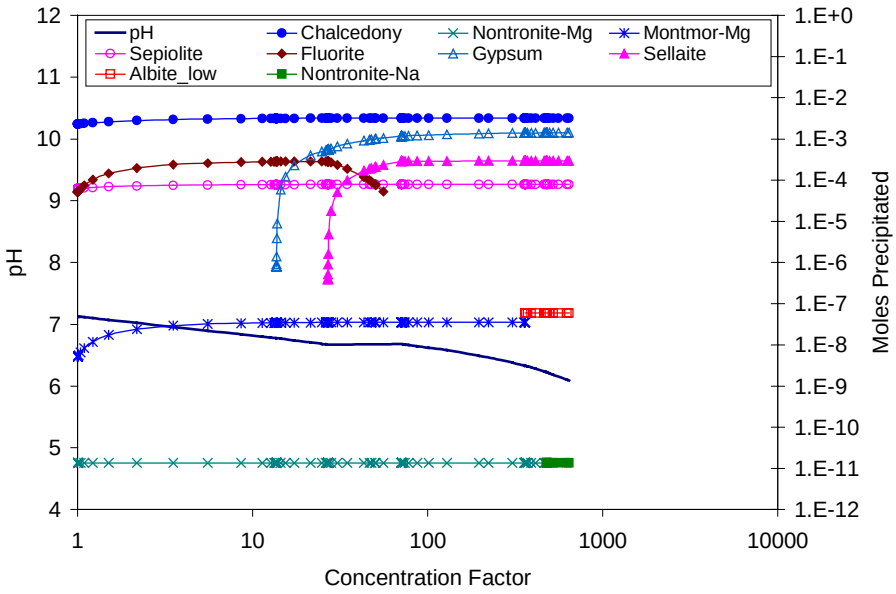

DTN: MO0112MWDTHC12.024

Figure 26. Mineral Evaporative Evolution for the Base Case THC Model Abstraction for Seepage at the Crown of the Drift in the Tptpll Lithology (Blc), Period 1

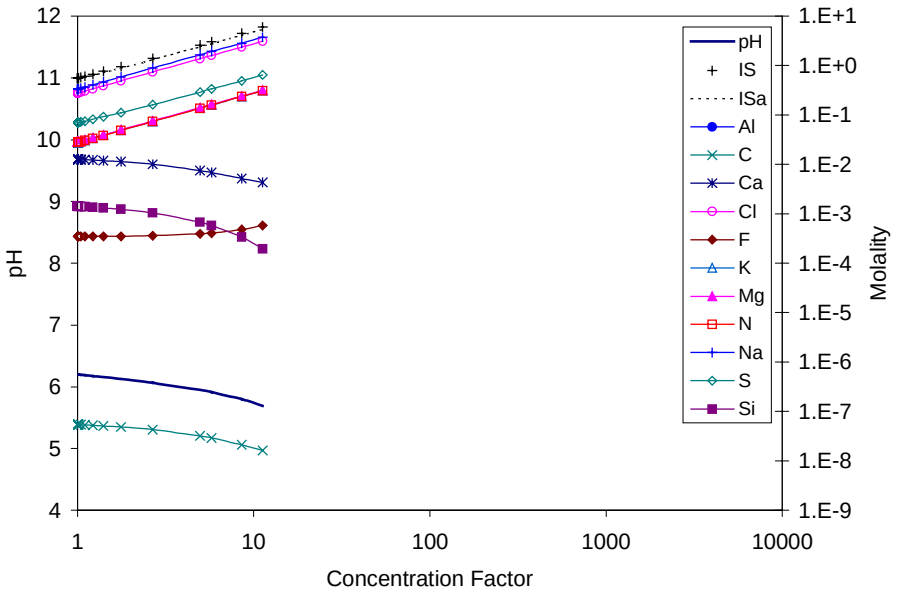

DTN: MO0112MWDTHC12.024

Figure 27. Aqueous Evaporative Evolution for the Base Case THC Model Abstraction for Seepage at the Crown of the Drift in the Tptpll Lithology (Blc), Period 2

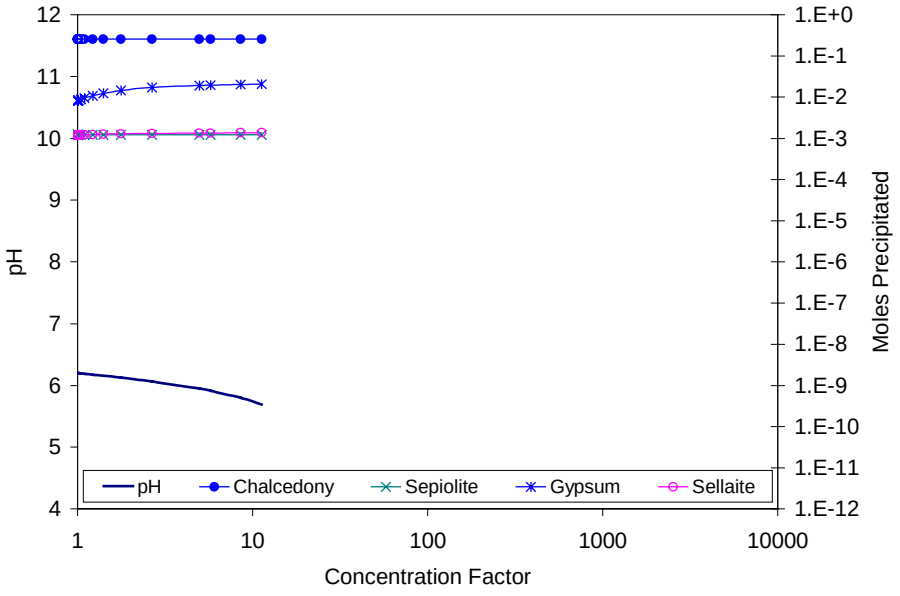

DTN: MO0112MWDTHC12.024

Figure 28. Mineral Evaporative Evolution for the Base Case THC Model Abstraction for Seepage at the Crown of the Drift in the Tptpll Lithology (Blc), Period 2

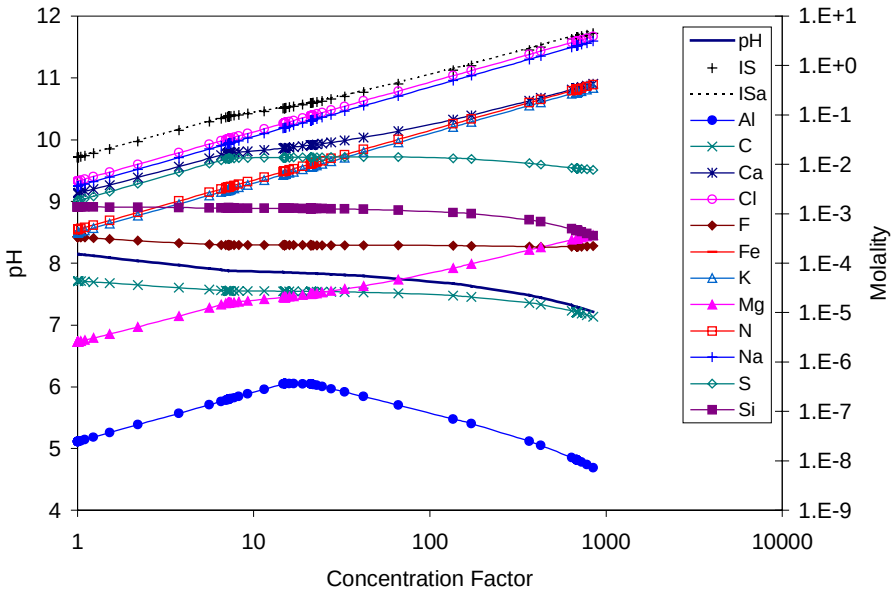

DTN: MO0112MWDTHC12.024

Figure 29. Aqueous Evaporative Evolution for the Base Case THC Model Abstraction for Seepage at the Crown of the Drift in the Tptpll Lithology (Blc), Period 3

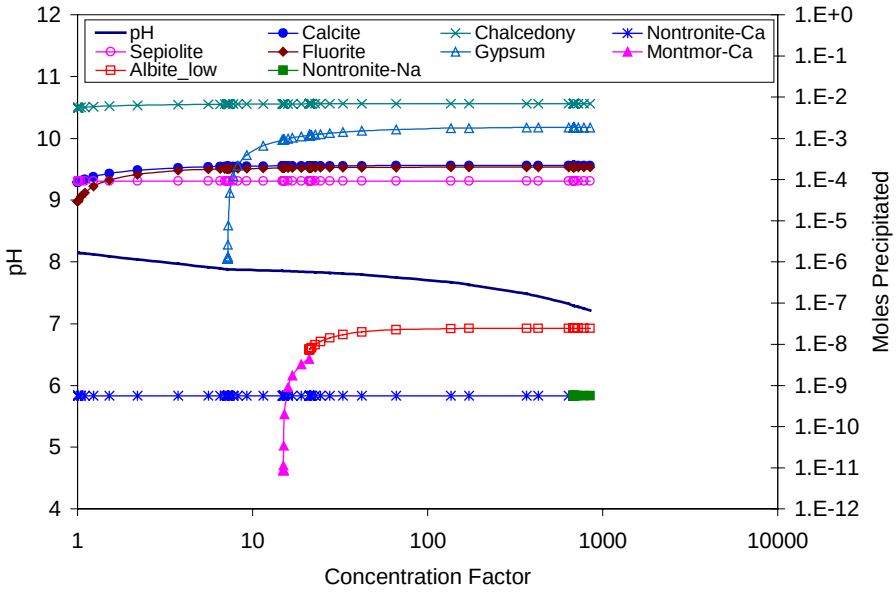

DTN: MO0112MWDTHC12.024

Figure 30. Mineral Evaporative Evolution for the Base Case THC Model Abstraction for Seepage at the Crown of the Drift in the Tptpll Lithology (Blc), Period 3

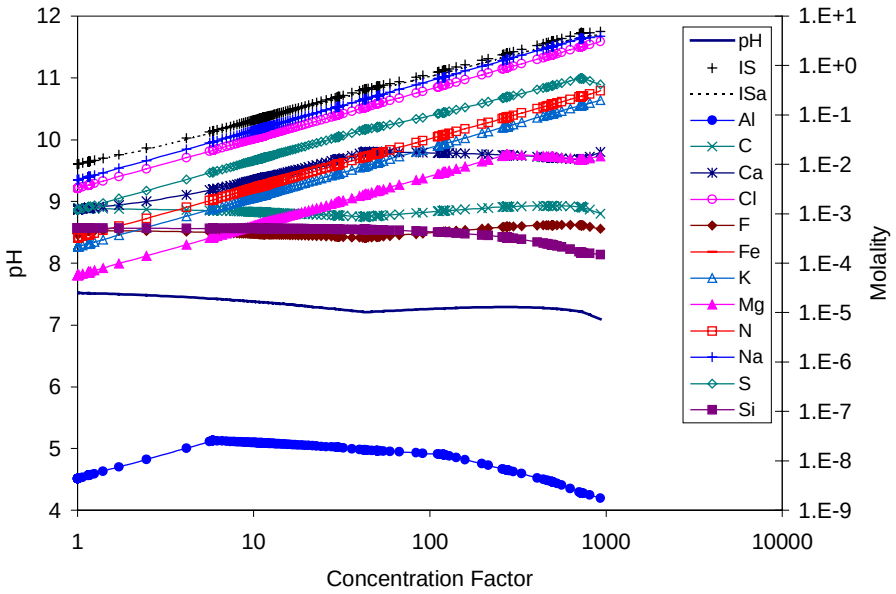

DTN: MO0112MWDTHC12.024

Figure 31. Aqueous Evaporative Evolution for the Base Case THC Model Abstraction for Seepage at the Crown of the Drift in the Tptpll Lithology (Blc), Period 4

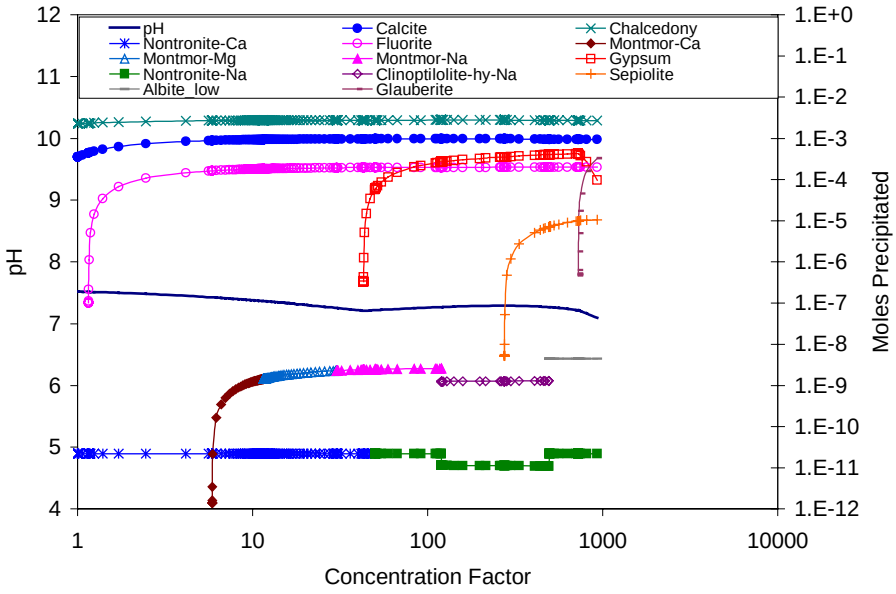

DTN: MO0112MWDTHC12.024

Figure 32. Mineral Evaporative Evolution for the Base Case THC Model Abstraction for Seepage at the Crown of the Drift in the Tptpll Lithology (Blc), Period 4

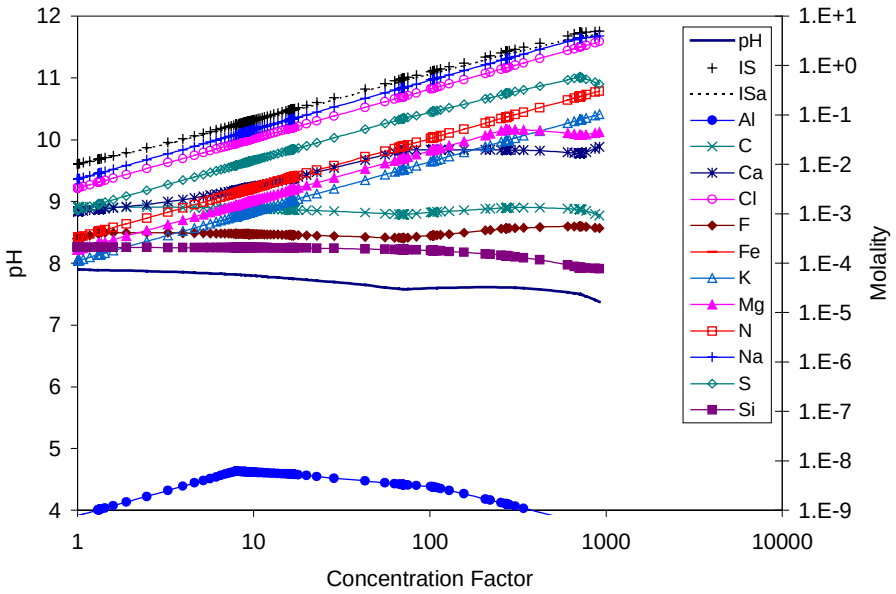

DTN: MO0112MWDTHC12.024

Figure 33. Aqueous Evaporative Evolution for the Base Case THC Model Abstraction for Seepage at the Crown of the Drift in the Tptpll Lithology (Blc), Period 5

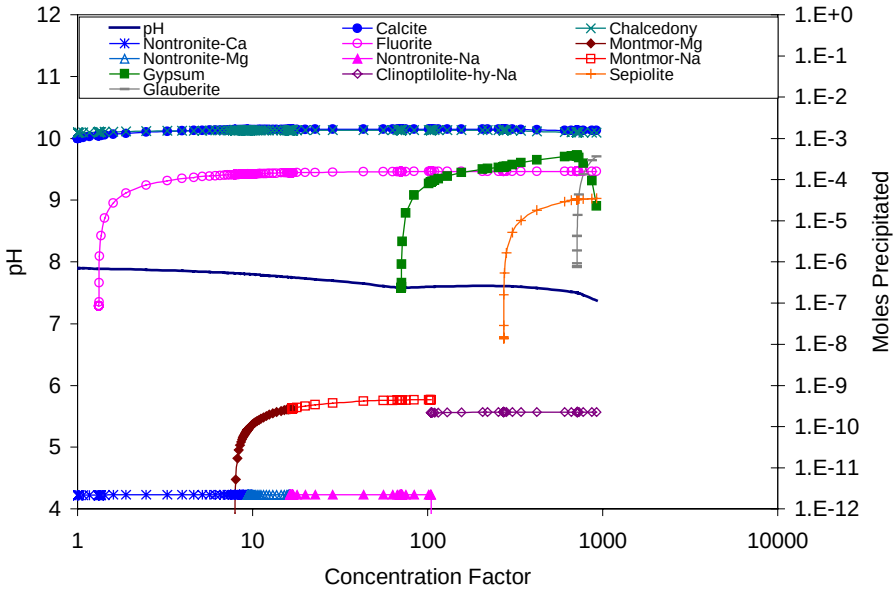

DTN: MO0112MWDTHC12.024

Figure 34. Mineral Evaporative Evolution for the Base Case THC Model Abstraction for Seepage at the Crown of the Drift in the Tptpll Lithology (Blc), Period 5

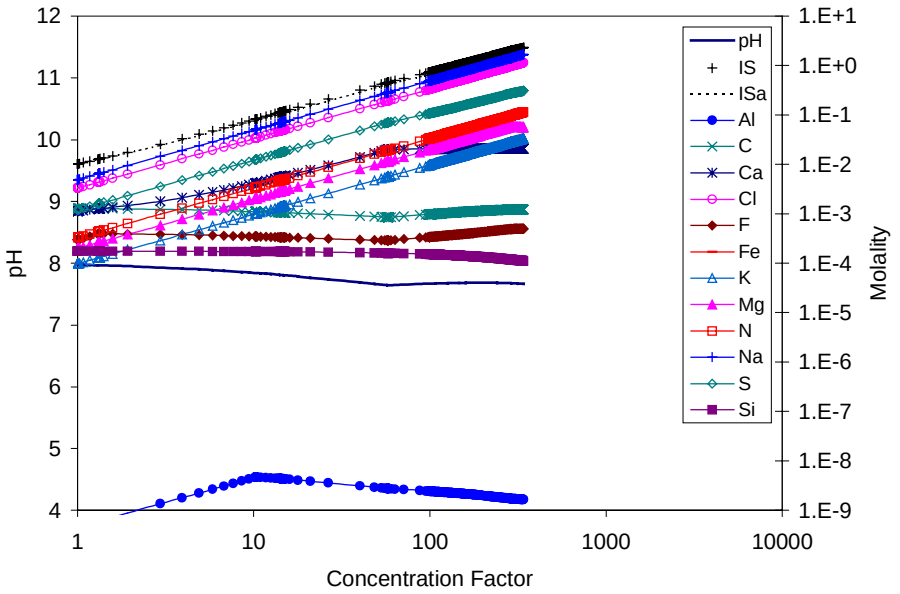

DTN: MO0112MWDTHC12.024

Figure 35. Aqueous Evaporative Evolution for the Base Case THC Model Abstraction for Seepage at the Crown of the Drift in the Tptpll Lithology (Blc), Period 6

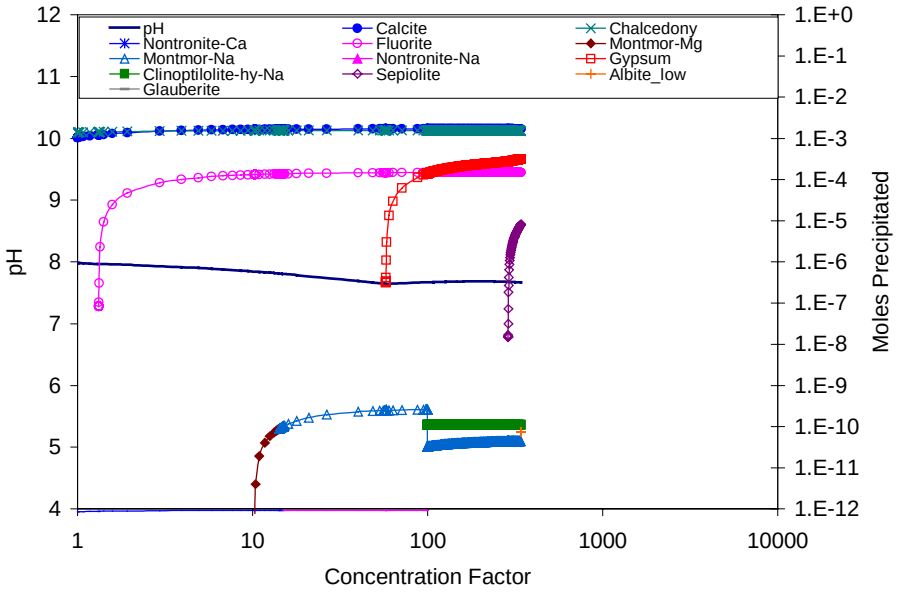

DTN: MO0112MWDTHC12.024

Figure 36. Mineral Evaporative Evolution for the Base Case THC Model Abstraction for Seepage at the Crown of the Drift in the Tptpll Lithology (Blc), Period 6

6.1.2.2 Water Imbibed into the Invert (Case Bli)

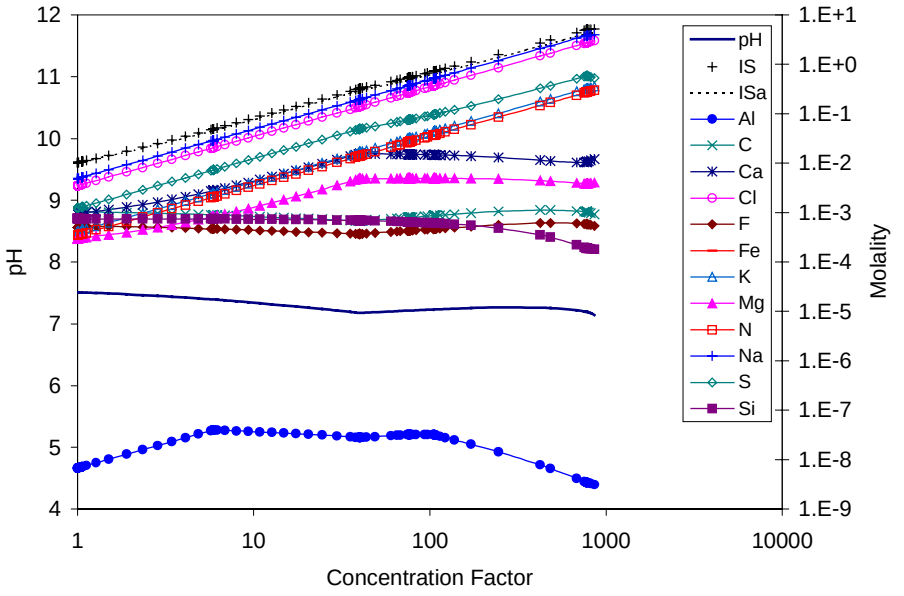

DTN: MO0112MWDTHC12.024

Figure 37. Aqueous Evaporative Evolution for the Base Case THC Model Abstraction for Seepage Wicking into the Invert in the Tptpll Lithology (Bli), Period 1

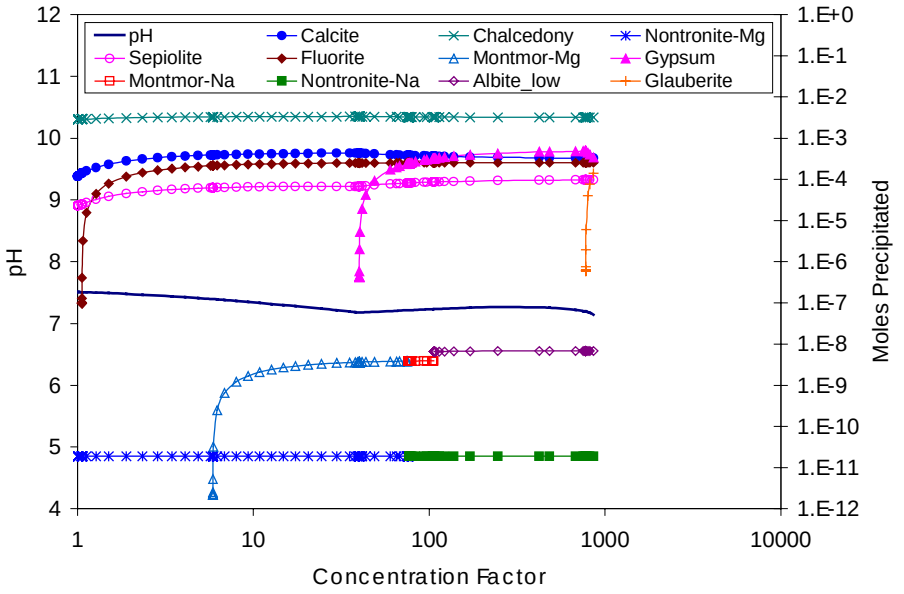

DTN: MO0112MWDTHC12.024

Figure 38. Mineral Evaporative Evolution for the Base Case THC Model Abstraction for Seepage Wicking into the Invert in the Tptpll Lithology (Bli), Period 1

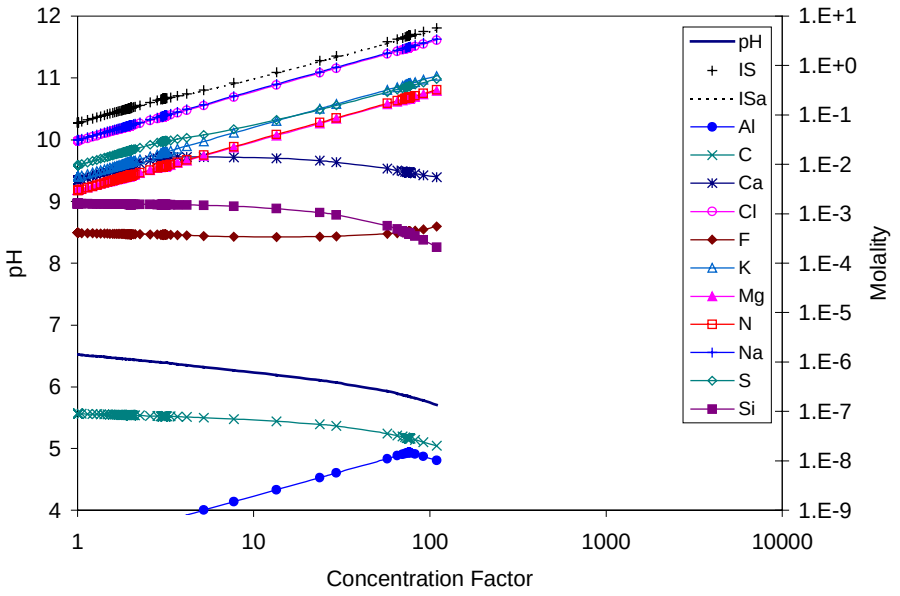

DTN: MO0112MWDTHC12.024

Figure 39. Aqueous Evaporative Evolution for the Base Case THC Model Abstraction for Seepage Wicking into the Invert in the Tptpll Lithology (Bli), Period 2

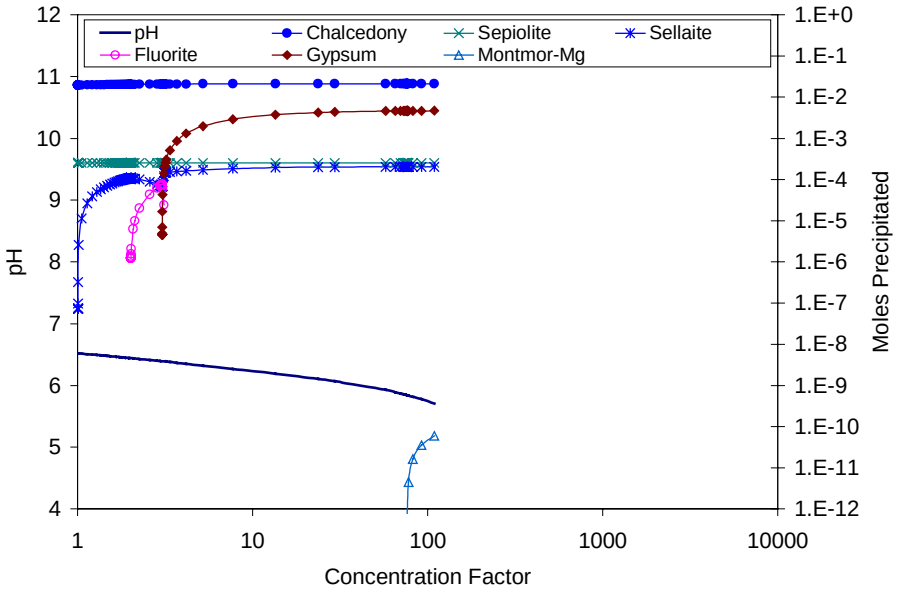

DTN: MO0112MWDTHC12.024

Figure 40. Mineral Evaporative Evolution for the Base Case THC Model Abstraction for Seepage Wicking into the Invert in the Tptpll Lithology (Bli), Period 2

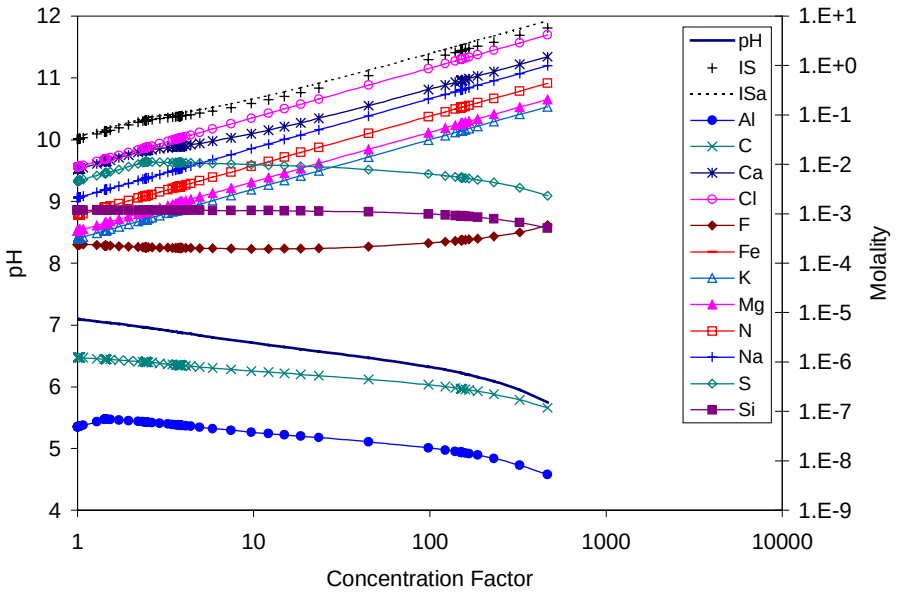

DTN: MO0112MWDTHC12.024

Figure 41. Aqueous Evaporative Evolution for the Base Case THC Model Abstraction for Seepage Wicking into the Invert in the Tptpll Lithology (Bli), Period 3

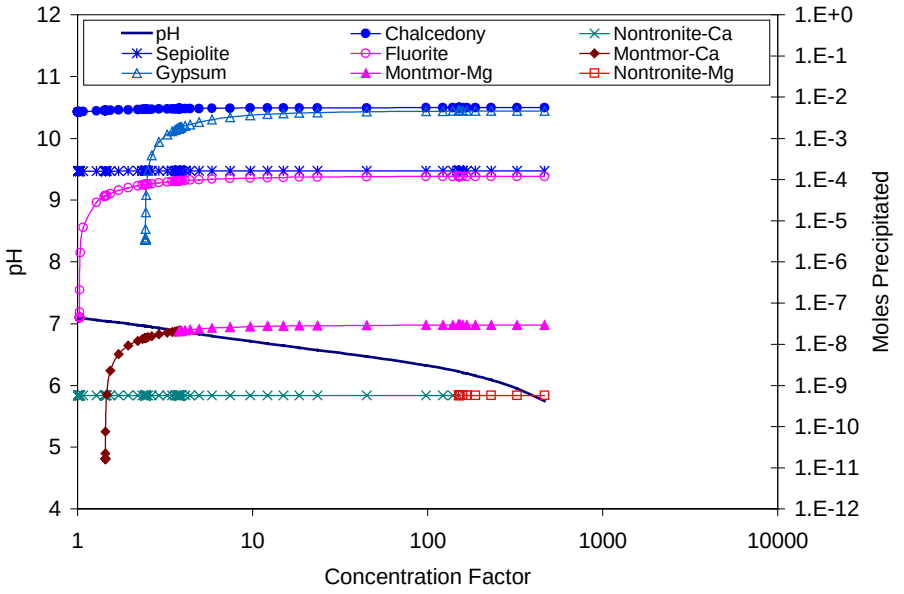

DTN: MO0112MWDTHC12.024

Figure 42. Mineral Evaporative Evolution for the Base Case THC Model Abstraction for Seepage Wicking into the Invert in the Tptpll Lithology (Bli), Period 3

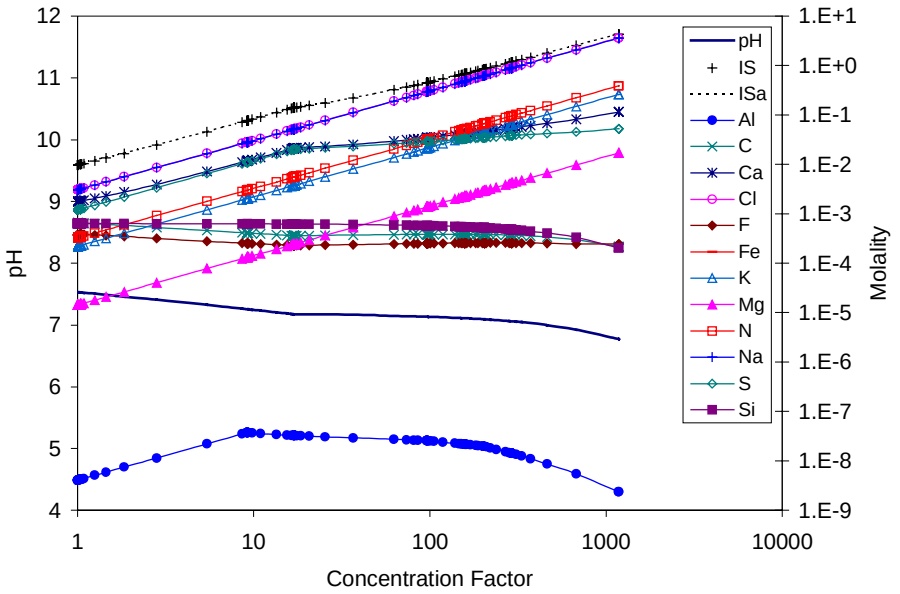

DTN: MO0112MWDTHC12.024

Figure 43. Aqueous Evaporative Evolution for the Base Case THC Model Abstraction for Seepage Wicking into the Invert in the Tptpll Lithology (Bli), Period 4

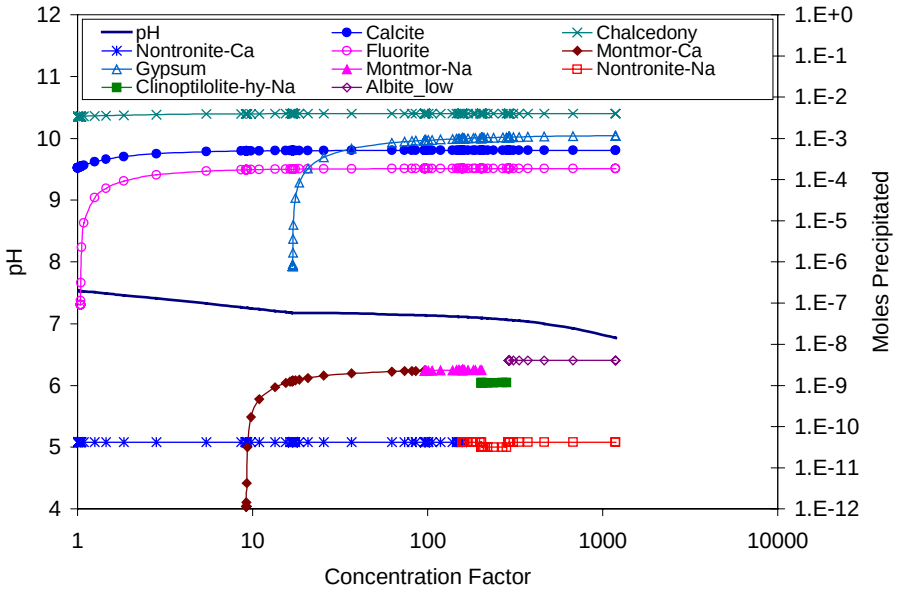

DTN: MO0112MWDTHC12.024

Figure 44. Mineral Evaporative Evolution for the Base Case THC Model Abstraction for Seepage Wicking into the Invert in the Tptpll Lithology (Bli), Period 4

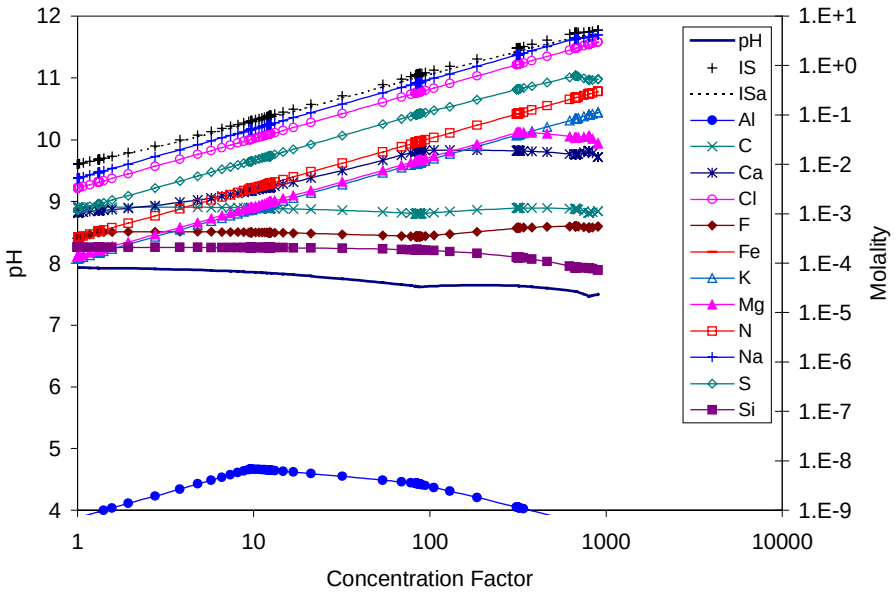

DTN: MO0112MWDTHC12.024

Figure 45. Aqueous Evaporative Evolution for the Base Case THC Model Abstraction for Seepage Wicking into the Invert in the Tptpll Lithology (Bli), Period 5

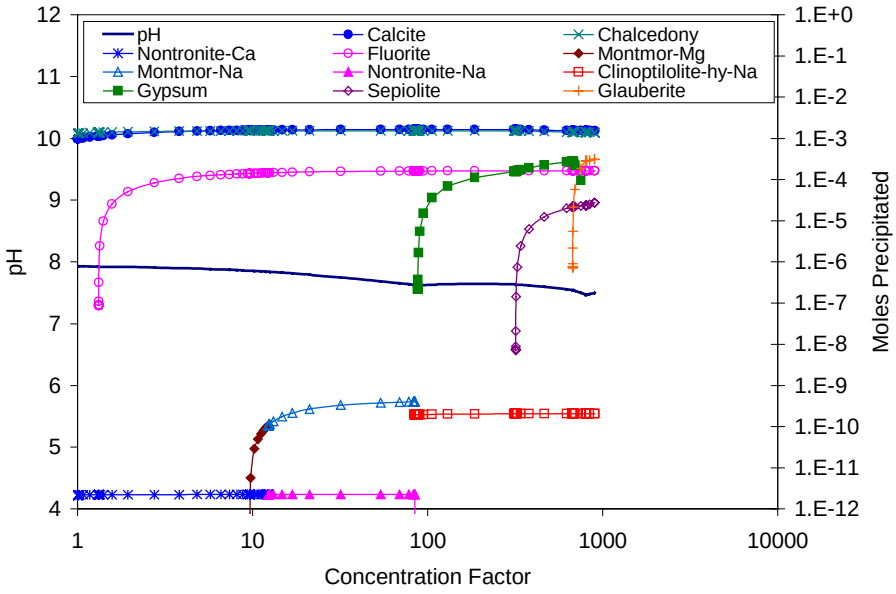

DTN: MO0112MWDTHC12.024

Figure 46. Mineral Evaporative Evolution for the Base Case THC Model Abstraction for Seepage Wicking into the Invert in the Tptpll Lithology (Bli), Period 5

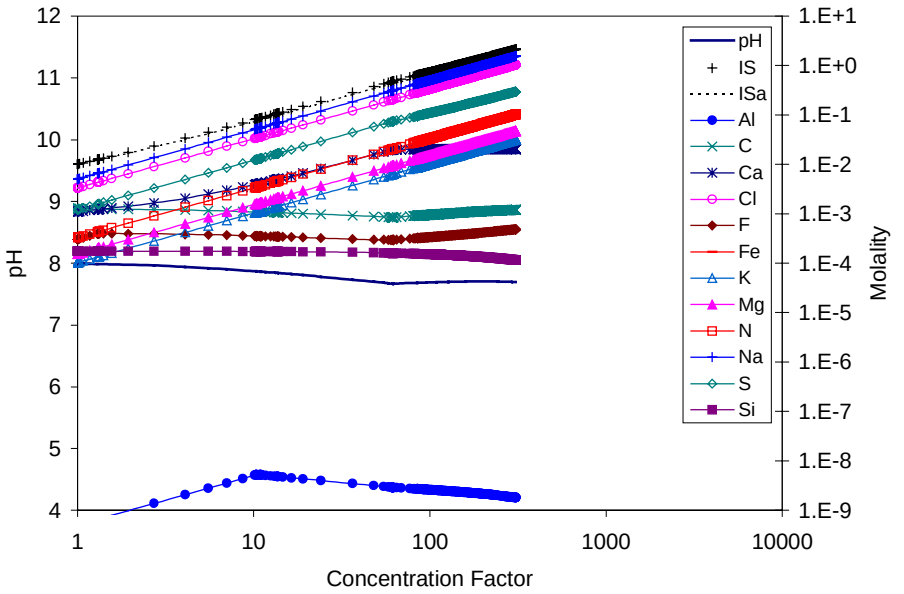

DTN: MO0112MWDTHC12.024

Figure 47. Aqueous Evaporative Evolution for the Base Case THC Model Abstraction for Seepage Wicking into the Invert in the Tptpll Lithology (Bli), Period 6

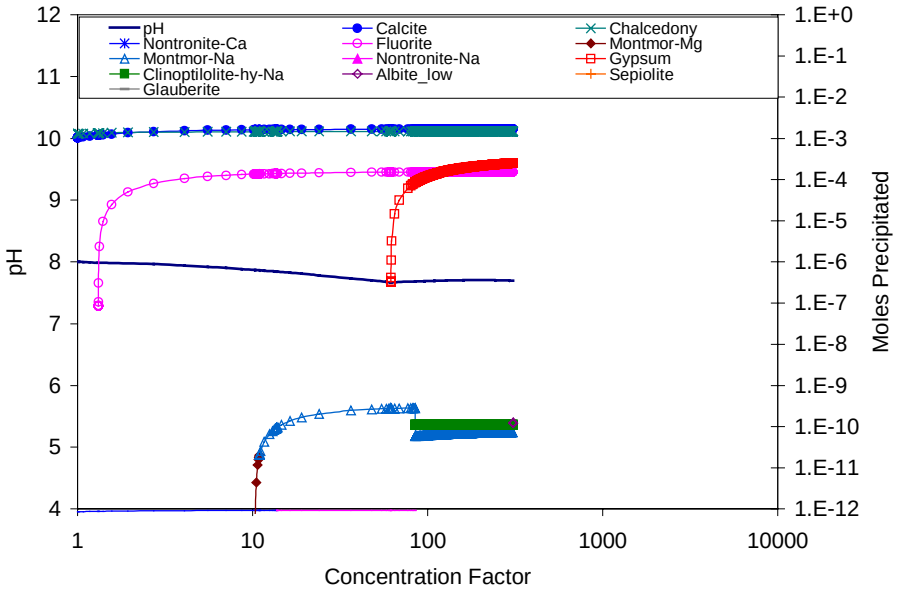

DTN: MO0112MWDTHC12.024

Figure 48. Mineral Evaporative Evolution for the Base Case THC Model Abstraction for Seepage Wicking into the Invert in the Tptpll Lithology (Bli), Period 6

6.2 RESULTS FOR SENSITIVITY THC MODEL ABSTRACTIONS

The sensitivity THC model abstractions include the HLi, HHi, LLi, LHi, HLc, HHc, LLc, LHc, HHcp, HHip, LHcp, and LHip cases in Table 1. Each of these cases is for seepage in the lower lithophysal zone of the crystal-poor member of the Topopah Spring tuff (Tptpll). The results are divided into two subsections corresponding to the composition of the water used to initialize the THC model grid blocks. Section 6.2.1 presents and/or references the results of the cases in which Topopah Spring tuff pore water was used as the initial water (i.e., cases HLi, HHi, LLi, LHi, HLc, HHc, LLc, and LHc). Section 6.2.2 presents and/or references the results of the cases in which UZ-14 perched water was used as the initial water (i.e., cases HHcp, HHip, LHcp, and LHip). Sections 6.2.1 and 6.2.2 are further subdivided by a combination of operating temperature mode (high or low) and carbon dioxide soil gas condition (high or low).

The HRH salts model predictions of the aqueous evaporative evolution of waters derived from cases HLi, HHi, LLi, and LHi are presented in Figure 49 through Figure 70. Predictions for waters derived from cases HHip and LHip are presented in Figure 71 through Figure 81. Results for seepage at the crown of the drift are not plotted. Differences in the evolution of invert and crown waters are discussed in Section 6.3.

The entire set of EQ3/6 input and output files for the HLi, HHi, LLi, LHi, HLc, HHc, LLc, and LHc cases are documented in DTN: MO0111MWDVAR12.021. The EQ3/6 input and output files for cases HHcp, HHip, LHcp, and LHip are documented in DTN: MO0112MWDTHC12.024.

6.2.1 Initial Water Composition (Pore Water)

6.2.1.1 High Temperature, Low CO_2 Partial Pressure (Case HLi)

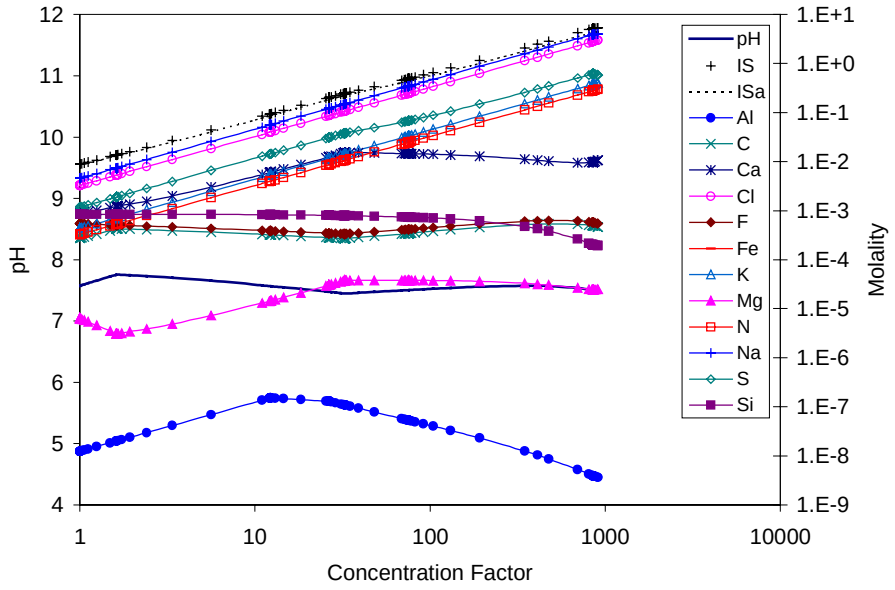

DTN: MO0111MWDVAR12.021

Figure 49. Aqueous Evaporative Evolution for the High Temperature and Low Carbon Dioxide Partial Pressure Case for Seepage Wicking into the Invert in the Tptpll Lithology (HLi), Period 1

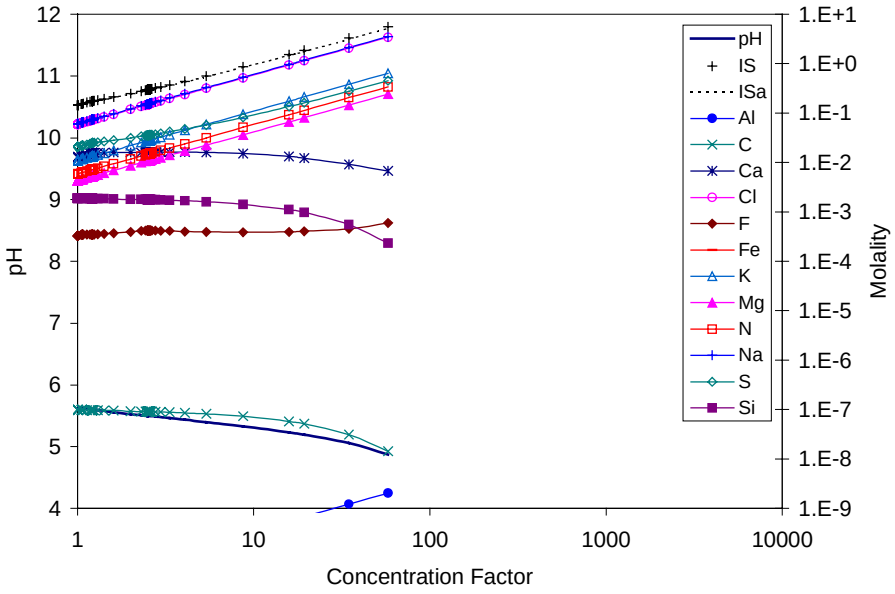

DTN: MO0111MWDVAR12.021

Figure 50. Aqueous Evaporative Evolution for the High Temperature and Low Carbon Dioxide Partial Pressure Case for Seepage Wicking into the Invert in the Tptpll Lithology (HLi), Period 2

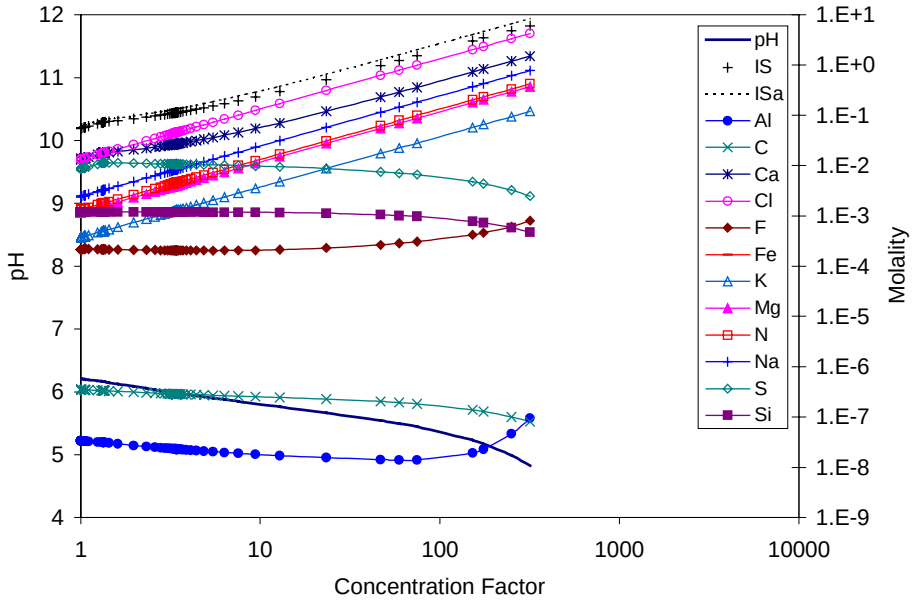

DTN: MO0111MWDVAR12.021

Figure 51. Aqueous Evaporative Evolution for the High Temperature and Low Carbon Dioxide Partial Pressure Case for Seepage Wicking into the Invert in the Tptpll Lithology (HLi), Period 3

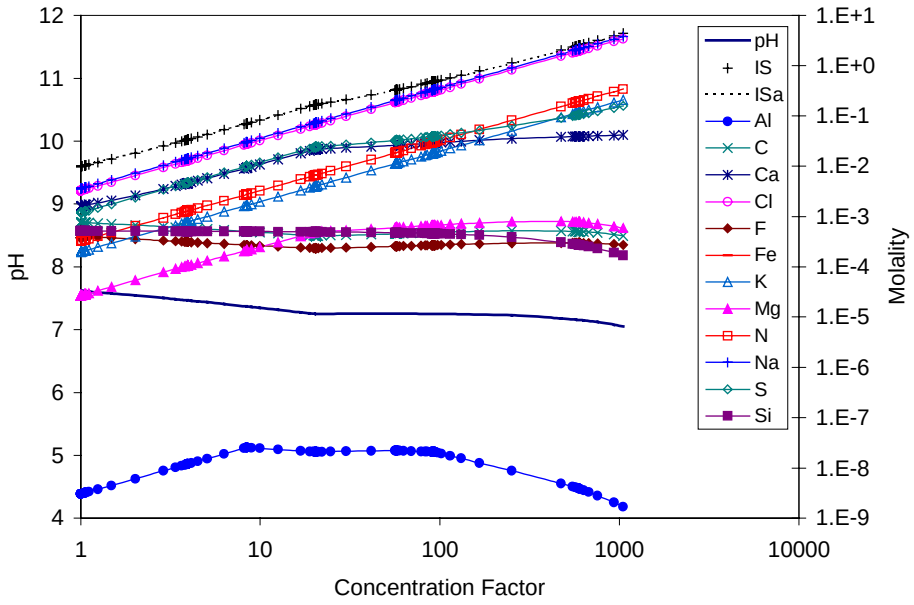

DTN: MO0111MWDVAR12.021

Figure 52. Aqueous Evaporative Evolution for the High Temperature and Low Carbon Dioxide Partial Pressure Case for Seepage Wicking into the Invert in the Tptpll Lithology (HLi), Period 4

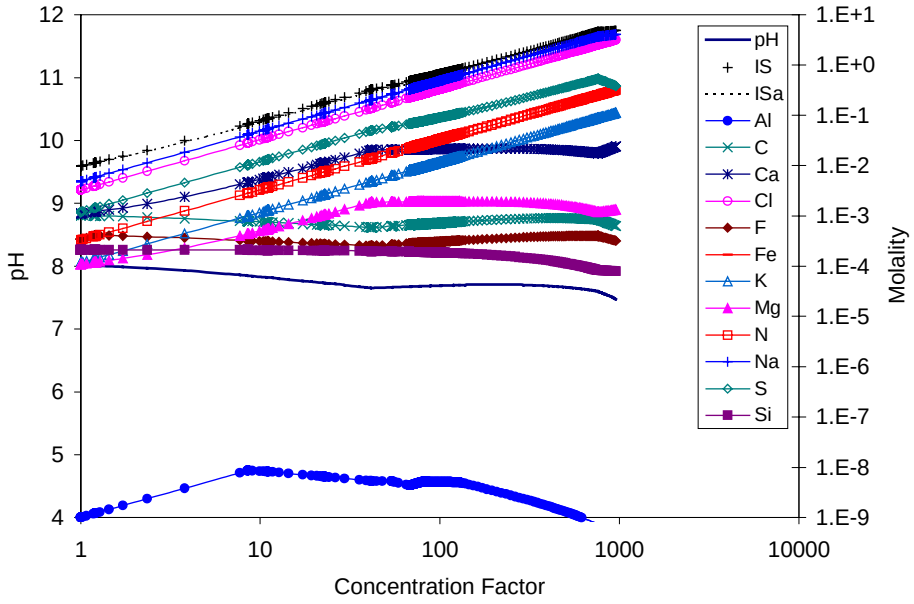

DTN: MO0111MWDVAR12.021

Figure 53. Aqueous Evaporative Evolution for the High Temperature and Low Carbon Dioxide Partial Pressure Case for Seepage Wicking into the Invert in the Tptpll Lithology (HLi), Period 5

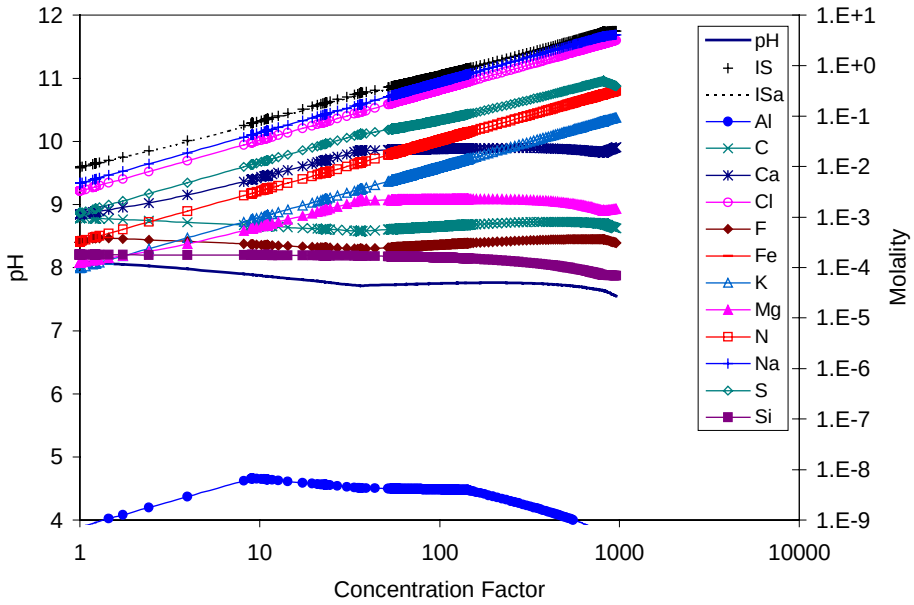

DTN: MO0111MWDVAR12.021

Figure 54. Aqueous Evaporative Evolution for the High Temperature and Low Carbon Dioxide Partial Pressure Case for Seepage Wicking into the Invert in the Tptpll Lithology (HLi), Period 6

6.2.1.2 High Temperature, High CO_2 Partial Pressure (Case HHi)

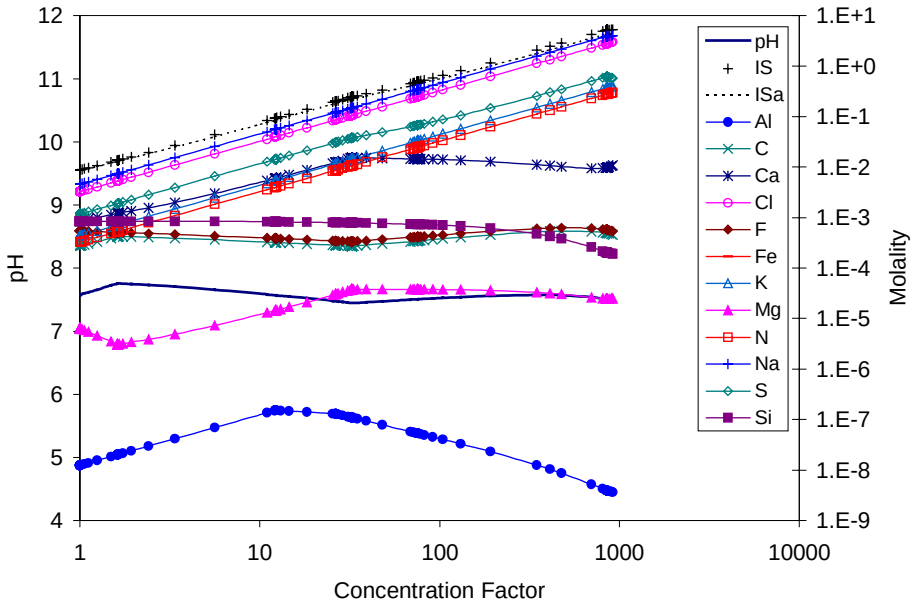

DTN: MO0111MWDVAR12.021

Figure 55. Aqueous Evaporative Evolution for the High Temperature and High Carbon Dioxide Partial Pressure Case for Seepage Wicking into the Invert in the Tptpll Lithology (HHi), Period 1

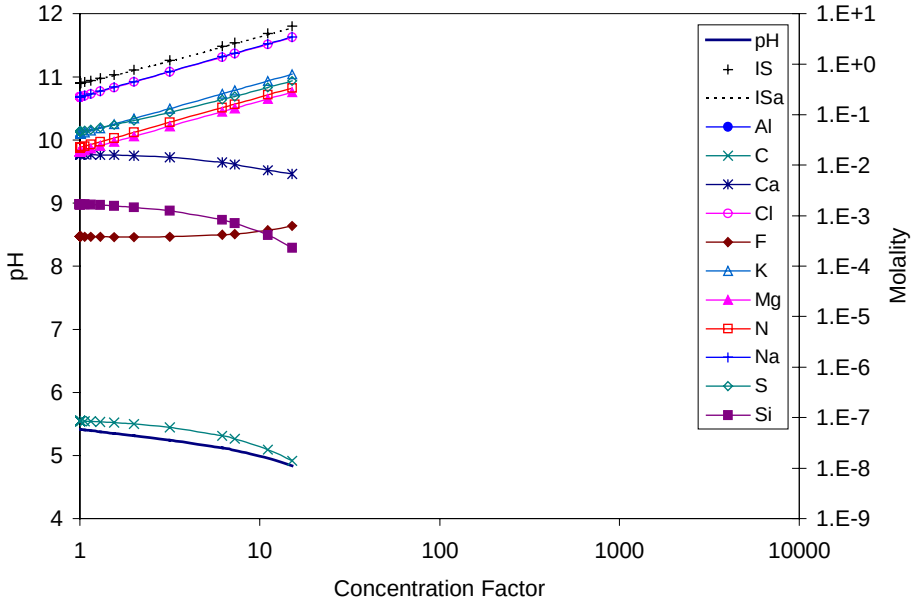

DTN: MO0111MWDVAR12.021

Figure 56. Aqueous Evaporative Evolution for the High Temperature and High Carbon Dioxide Partial Pressure Case for Seepage Wicking into the Invert in the Tptpll Lithology (HHi), Period 2

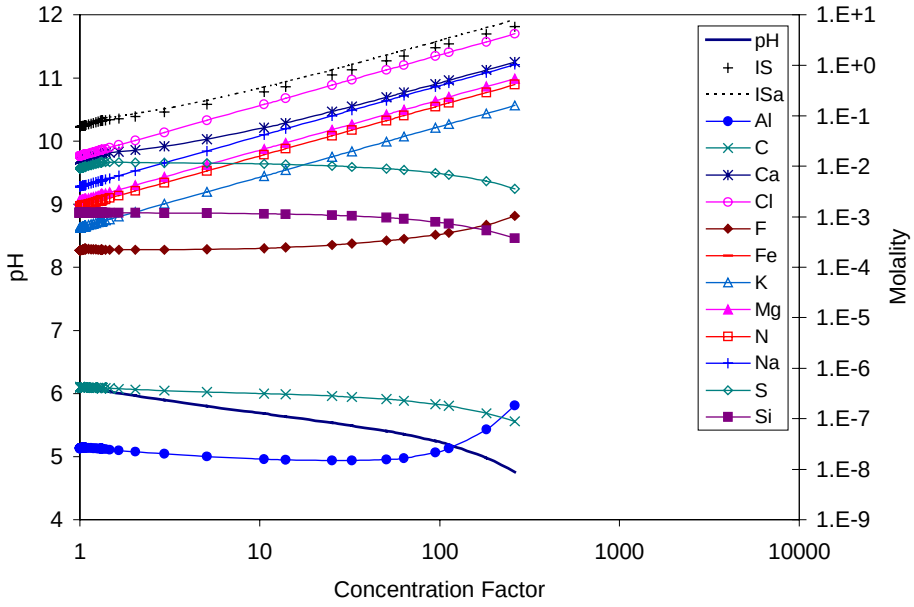

DTN: MO0111MWDVAR12.021

Figure 57. Aqueous Evaporative Evolution for the High Temperature and High Carbon Dioxide Partial Pressure Case for Seepage Wicking into the Invert in the Tptpll Lithology (HHi), Period 3

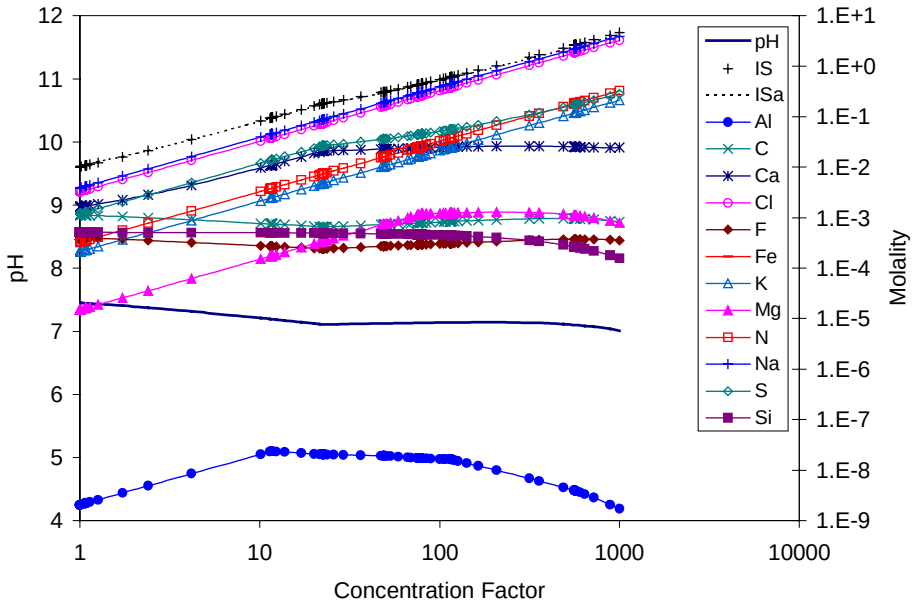

DTN: MO0111MWDVAR12.021

Figure 58. Aqueous Evaporative Evolution for the High Temperature and High Carbon Dioxide Partial Pressure Case for Seepage Wicking into the Invert in the Tptpll Lithology (HHi), Period 4

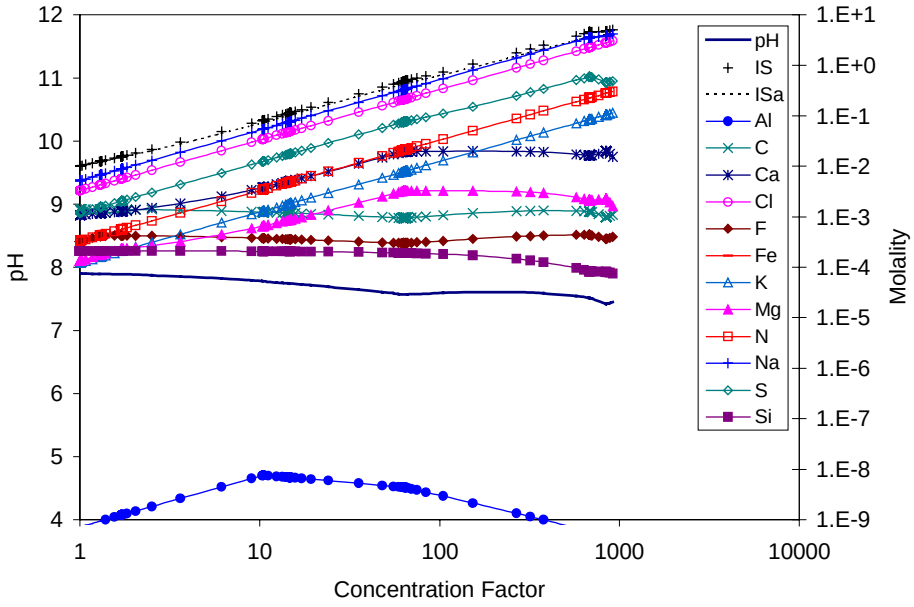

DTN: MO0111MWDVAR12.021

Figure 59. Aqueous Evaporative Evolution for the High Temperature and High Carbon Dioxide Partial Pressure Case for Seepage Wicking into the Invert in the Tptpll Lithology (HHi), Period 5

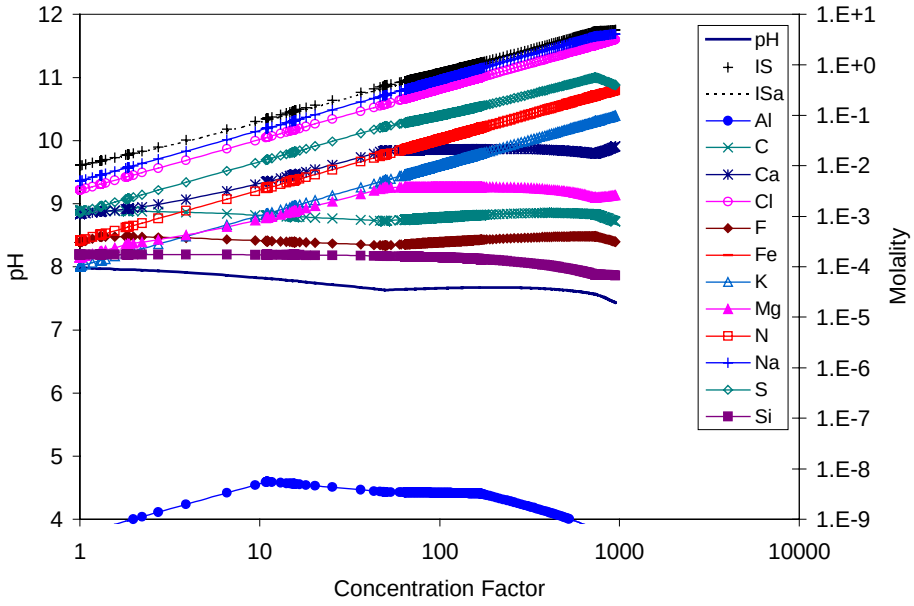

DTN: MO0111MWDVAR12.021

Figure 60. Aqueous Evaporative Evolution for the High Temperature and High Carbon Dioxide Partial Pressure Case for Seepage Wicking into the Invert in the Tptpll Lithology (HHi), Period 6

6.2.1.3 Low Temperature, Low CO_2 Partial Pressure (Case LLi)

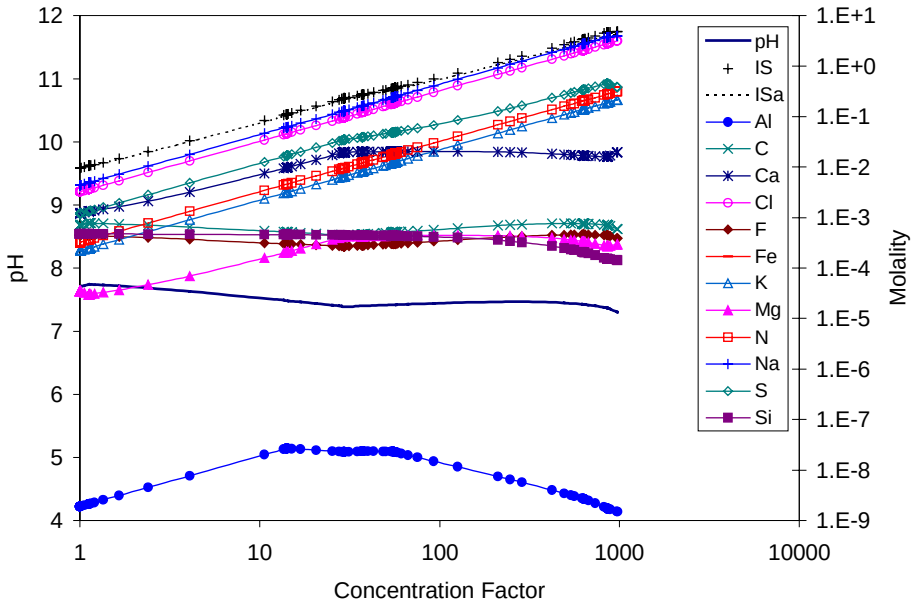

DTN: MO0111MWDVAR12.021

Figure 61. Aqueous Evaporative Evolution for the Low Temperature and Low Carbon Dioxide Partial Pressure Case for Seepage Wicking into the Invert in the Tptpll Lithology (LLi), Period 1

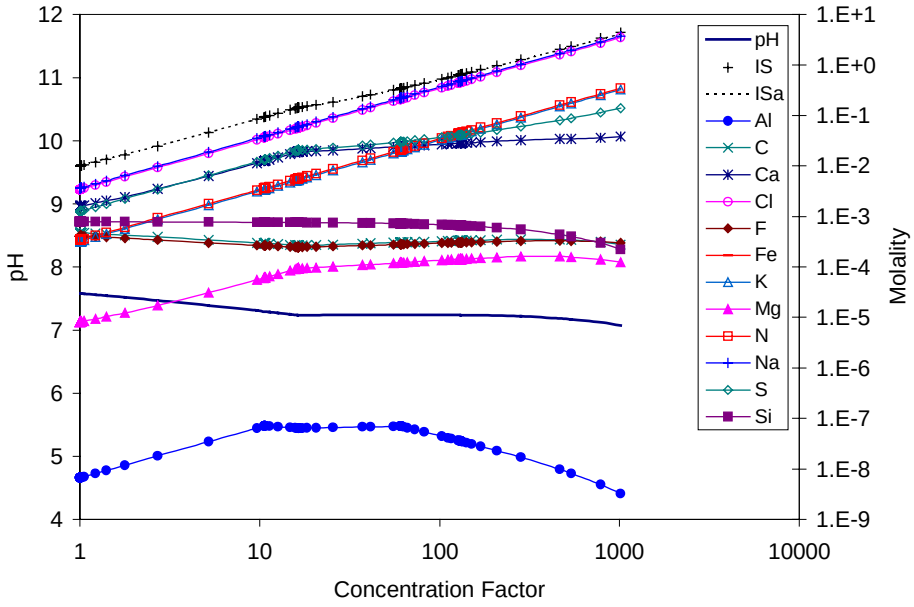

DTN: MO0111MWDVAR12.021

Figure 62. Aqueous Evaporative Evolution for the Low Temperature and Low Carbon Dioxide Partial Pressure Case for Seepage Wicking into the Invert in the Tptpll Lithology (LLi), Period 2

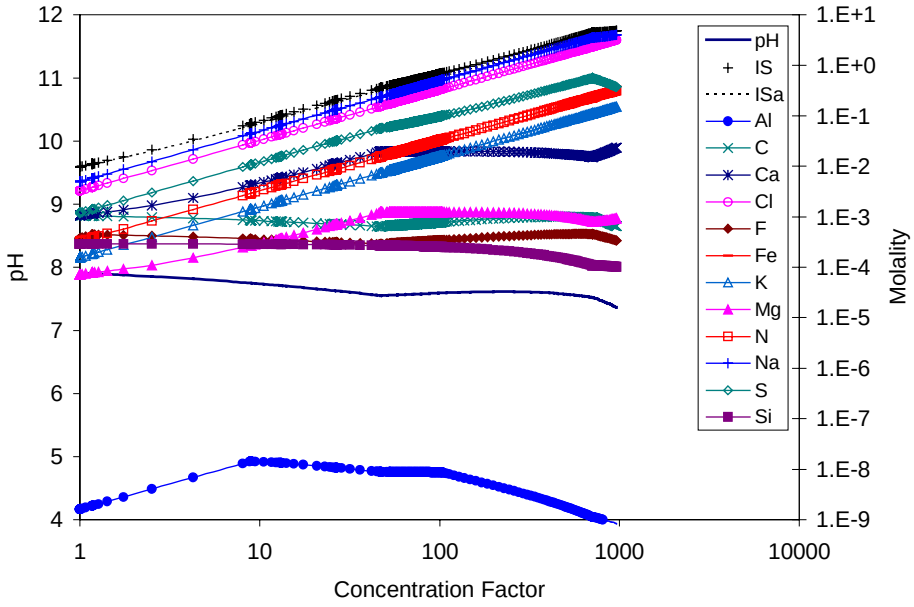

DTN: MO0111MWDVAR12.021

Figure 63. Aqueous Evaporative Evolution for the Low Temperature and Low Carbon Dioxide Partial Pressure Case for Seepage Wicking into the Invert in the Tptpll Lithology (LLi), Period 3

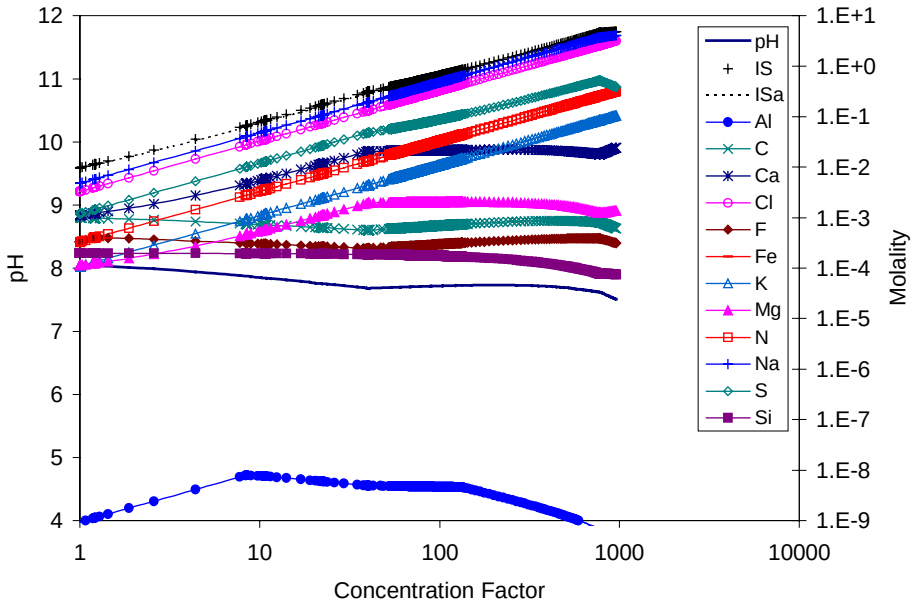

DTN: MO0111MWDVAR12.021

Figure 64. Aqueous Evaporative Evolution for the Low Temperature and Low Carbon Dioxide Partial Pressure Case for Seepage Wicking into the Invert in the Tptpll Lithology (LLi), Period 4

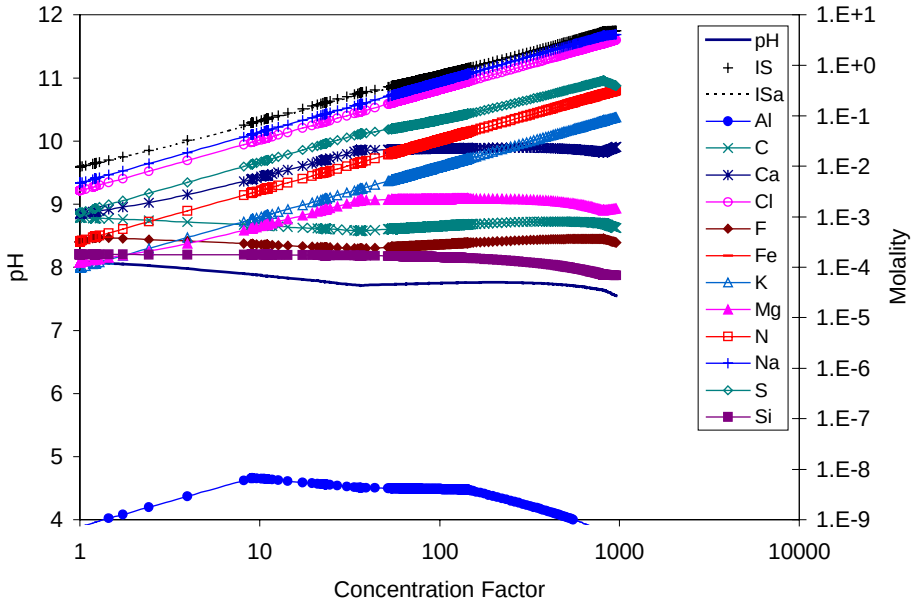

DTN: MO0111MWDVAR12.021

Figure 65. Aqueous Evaporative Evolution for the Low Temperature and Low Carbon Dioxide Partial Pressure Case for Seepage Wicking into the Invert in the Tptpll Lithology (LLi), Period 5

6.2.1.4 Low Temperature, High CO_2 Partial Pressure (Case LHi)

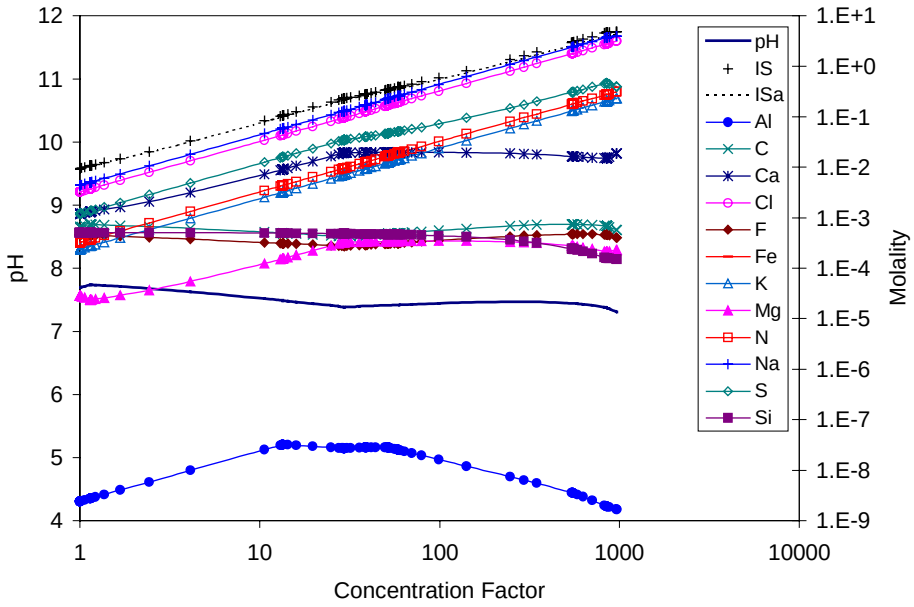

DTN: MO0111MWDVAR12.021

Figure 66. Aqueous Evaporative Evolution for the Low Temperature and High Carbon Dioxide Partial Pressure Case for Seepage Wicking into the Invert in the Tptpll Lithology (LHi), Period 1

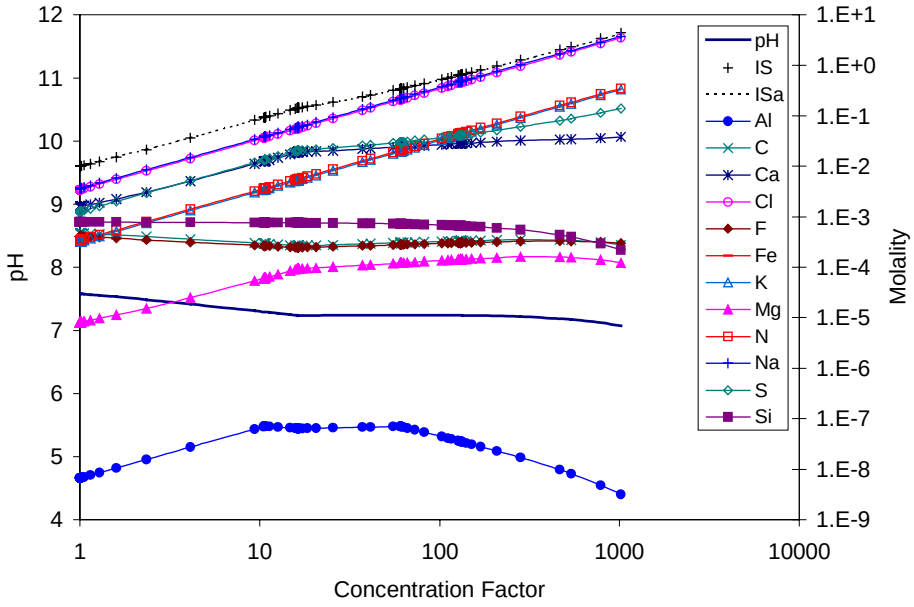

DTN: MO0111MWDVAR12.021

Figure 67. Aqueous Evaporative Evolution for the Low Temperature and High Carbon Dioxide Partial Pressure Case for Seepage Wicking into the Invert in the Tptpll Lithology (LHi), Period 2

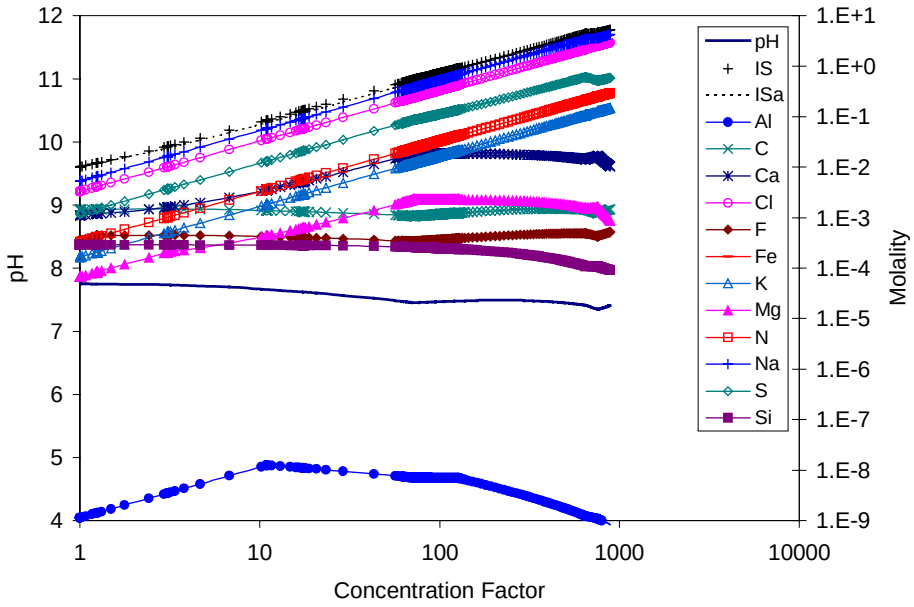

DTN: MO0111MWDVAR12.021

Figure 68. Aqueous Evaporative Evolution for the Low Temperature and High Carbon Dioxide Partial Pressure Case for Seepage Wicking into the Invert in the Tptpll Lithology (LHi), Period 3

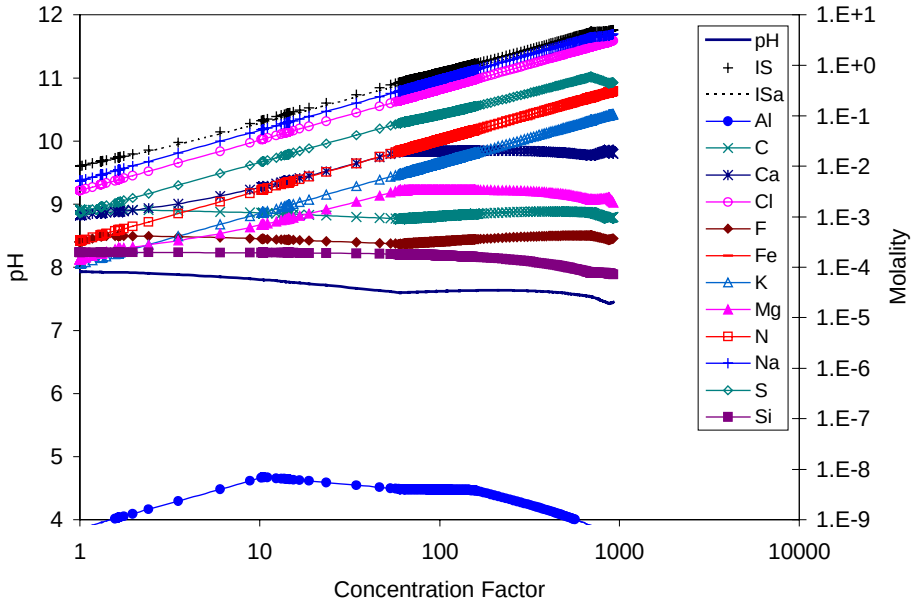

DTN: MO0111MWDVAR12.021

Figure 69. Aqueous Evaporative Evolution for the Low Temperature and High Carbon Dioxide Partial Pressure Case for Seepage Wicking into the Invert in the Tptpll Lithology (LHi), Period 4

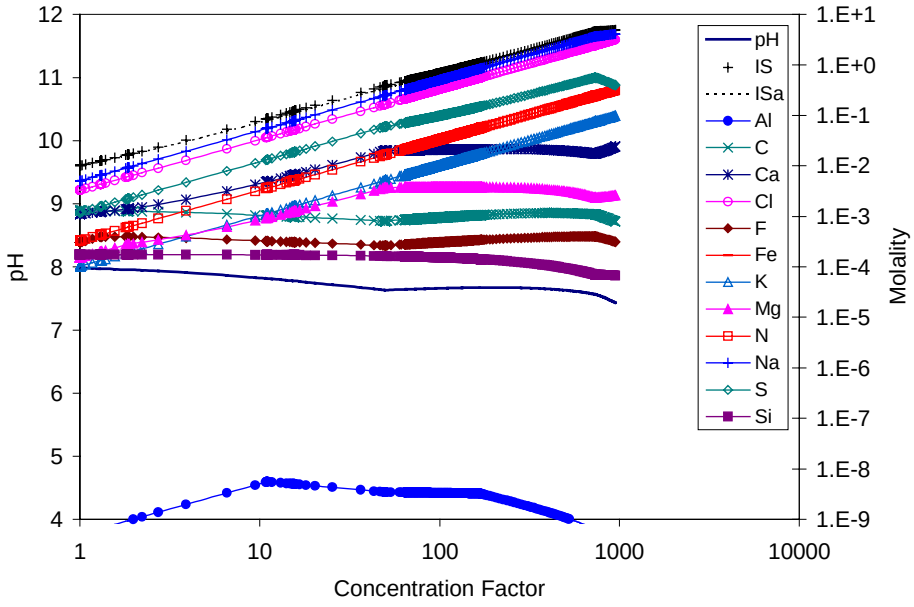

DTN: MO0111MWDVAR12.021

Figure 70. Aqueous Evaporative Evolution for the Low Temperature and High Carbon Dioxide Partial Pressure Case for Seepage Wicking into the Invert in the Tptpll Lithology (LHi), Period 5

6.2.2 Initial Water Composition (UZ-14 Perched Water)

6.2.2.1 High Temperature, High CO_2 Partial Pressure (Case HHip)

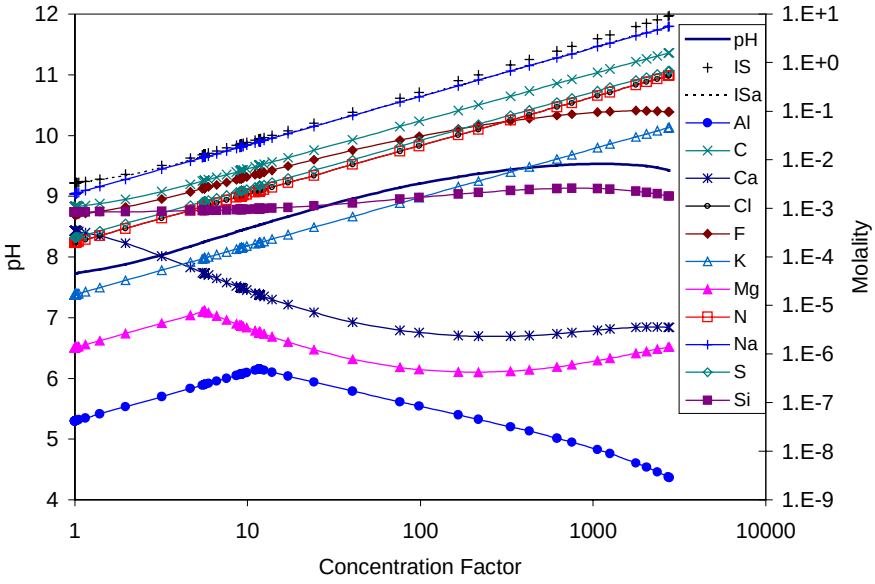

DTN: MO0112MWDTHC12.024

Figure 71. Aqueous Evaporative Evolution for the High Temperature and High Carbon Dioxide Partial Pressure Case for Seepage Wicking into the Invert in the Tptpll Lithology, Initialized Using Water Composition of UZ-14 Perched Water (HHip), Period 1

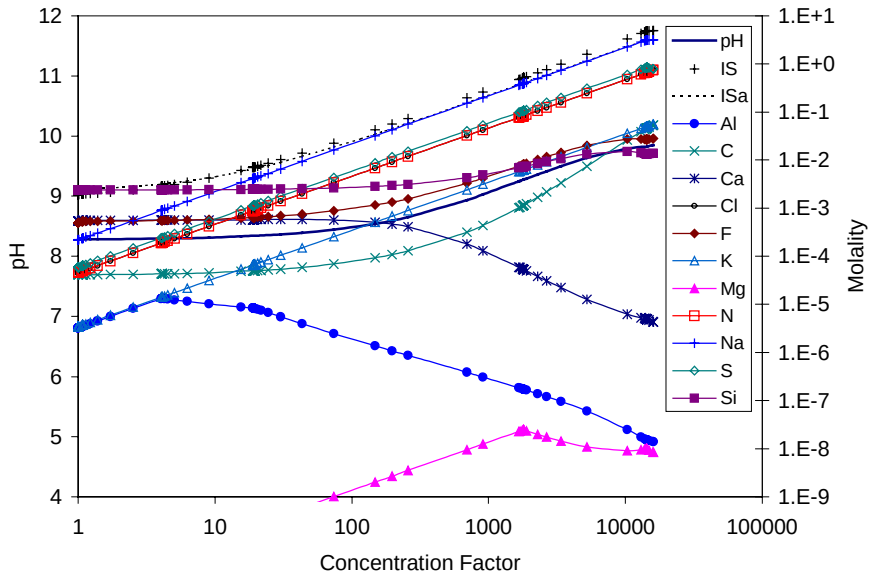

DTN: MO0112MWDTHC12.024

Figure 72. Aqueous Evaporative Evolution for the High Temperature and High Carbon Dioxide Partial Pressure Case for Seepage Wicking into the Invert in the Tptpll Lithology, Initialized Using Water Composition of UZ-14 Perched Water (HHip), Period 2

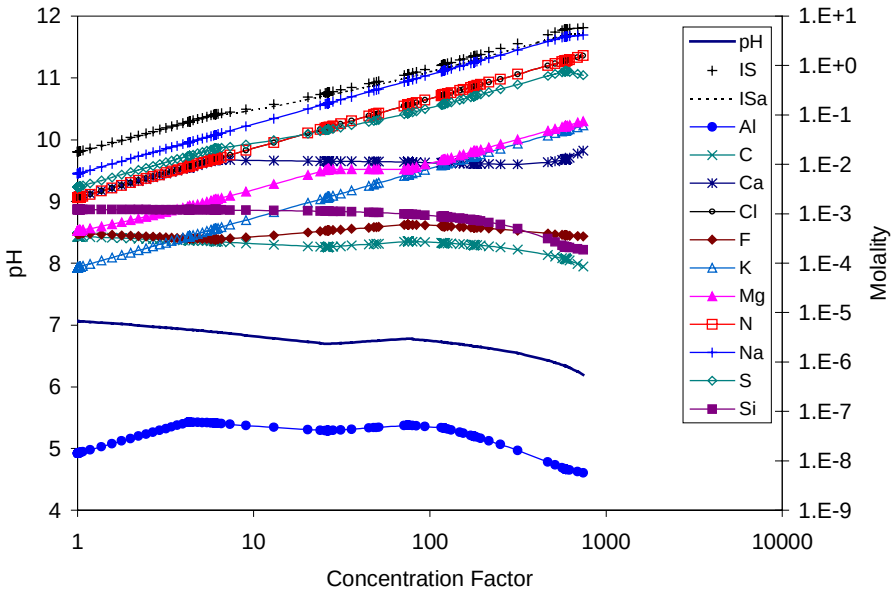

DTN: MO0112MWDTHC12.024

Figure 73. Aqueous Evaporative Evolution for the High Temperature and High Carbon Dioxide Partial Pressure Case for Seepage Wicking into the Invert in the Tptpll Lithology, Initialized Using Water Composition of UZ-14 Perched Water (HHip), Period 3

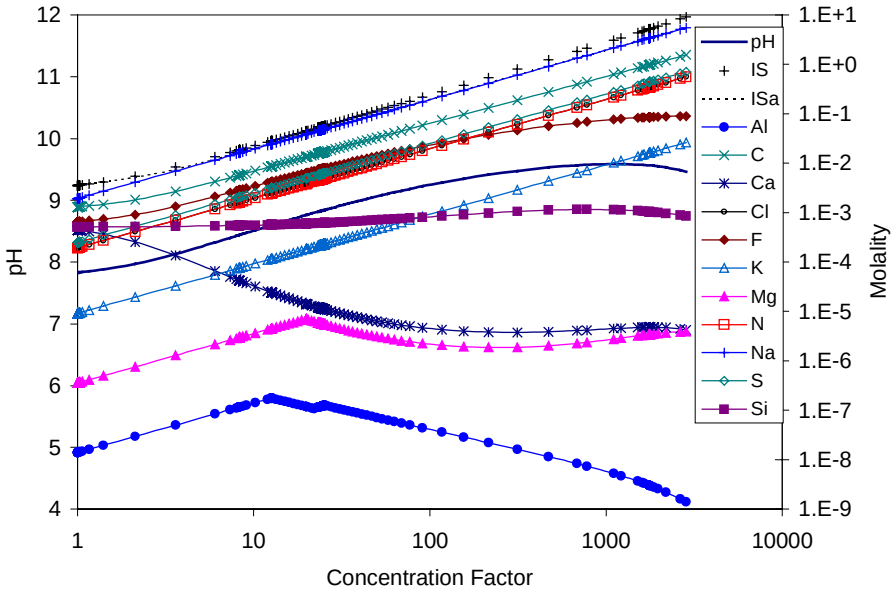

DTN: MO0112MWDTHC12.024

Figure 74. Aqueous Evaporative Evolution for the High Temperature and High Carbon Dioxide Partial Pressure Case for Seepage Wicking into the Invert in the Tptpll Lithology, Initialized Using Water Composition of UZ-14 Perched Water (HHip), Period 4

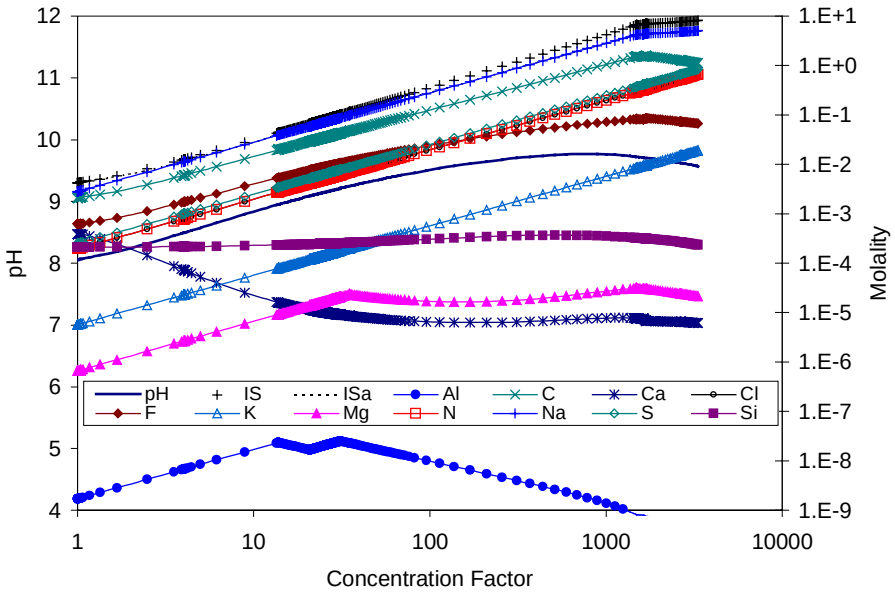

DTN: MO0112MWDTHC12.024

Figure 75. Aqueous Evaporative Evolution for the High Temperature and High Carbon Dioxide Partial Pressure Case for Seepage Wicking into the Invert in the Tptpll Lithology, Initialized Using Water Composition of UZ-14 Perched Water (HHip), Period 5

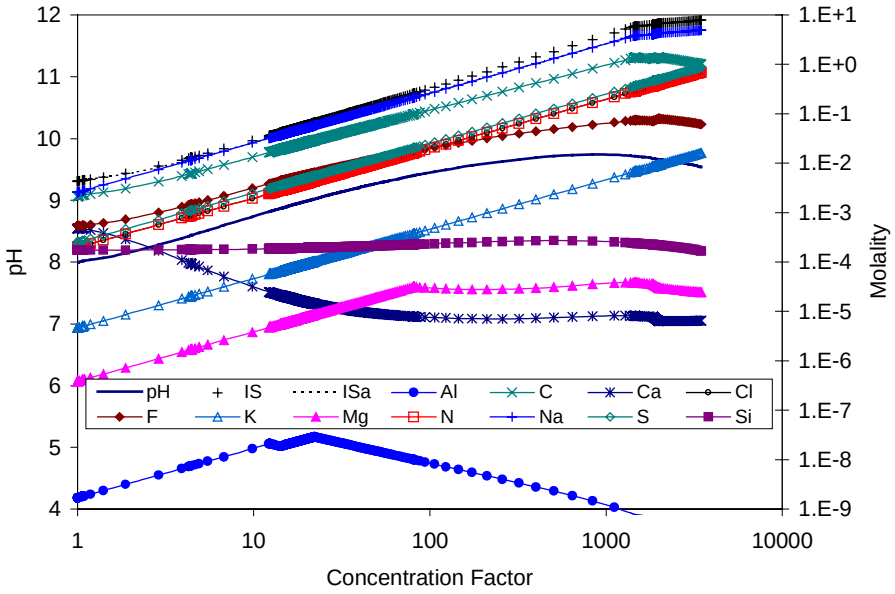

DTN: MO0112MWDTHC12.024

Figure 76. Aqueous Evaporative Evolution for the High Temperature and High Carbon Dioxide Partial Pressure Case for Seepage Wicking into the Invert in the Tptpll Lithology, Initialized Using Water Composition of UZ-14 Perched Water (HHip), Period 6

6.2.2.2 Low Temperature, High CO_2 Partial Pressure (Case LHip)

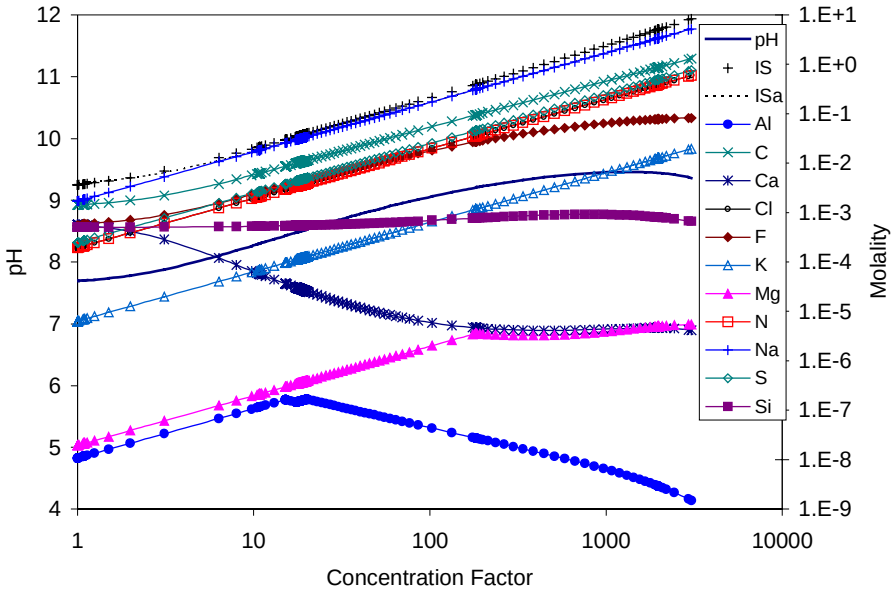

DTN: MO0112MWDTHC12.024

Figure 77. Aqueous Evaporative Evolution for the Low Temperature and High Carbon Dioxide Partial Pressure Case for Seepage Wicking into the Invert in the Tptpll Lithology, Initialized Using Water Composition of UZ-14 Perched Water (LHip), Period 1

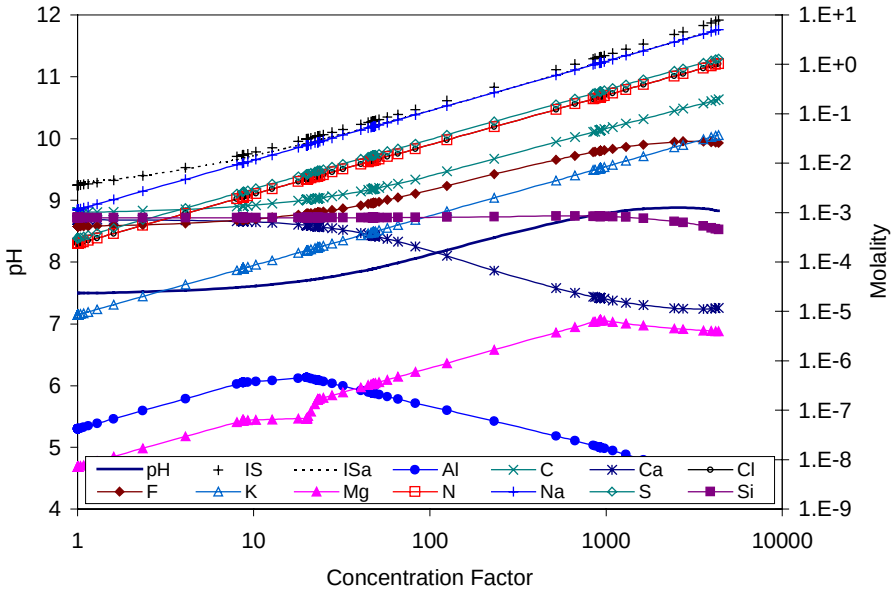

DTN: MO0112MWDTHC12.024

Figure 78. Aqueous Evaporative Evolution for the Low Temperature and High Carbon Dioxide Partial Pressure Case for Seepage Wicking into the Invert in the Tptpll Lithology, Initialized Using Water Composition of UZ-14 Perched Water (LHip), Period 2

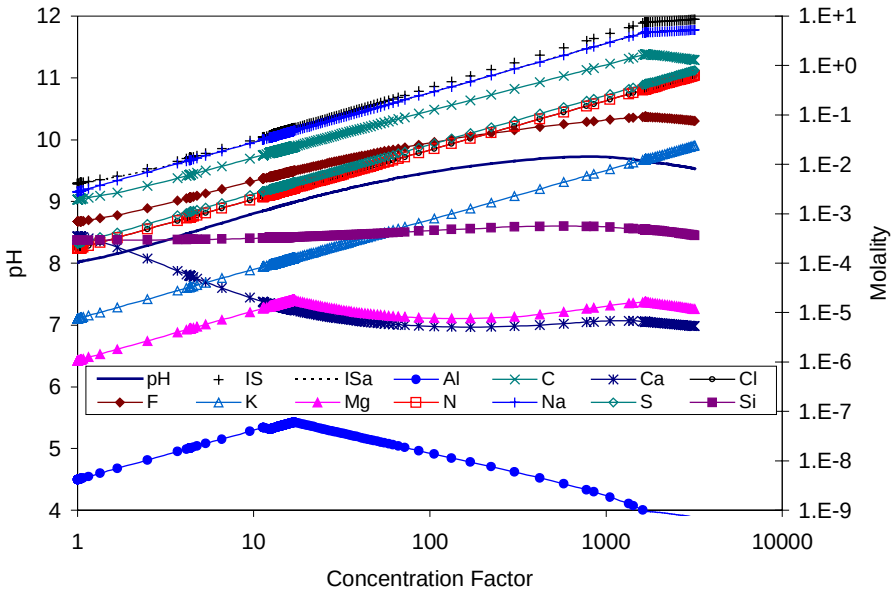

DTN: MO0112MWDTHC12.024

Figure 79. Aqueous Evaporative Evolution for the Low Temperature and High Carbon Dioxide Partial Pressure Case for Seepage Wicking into the Invert in the Tptpll Lithology, Initialized Using Water Composition of UZ-14 Perched Water (LHip), Period 3

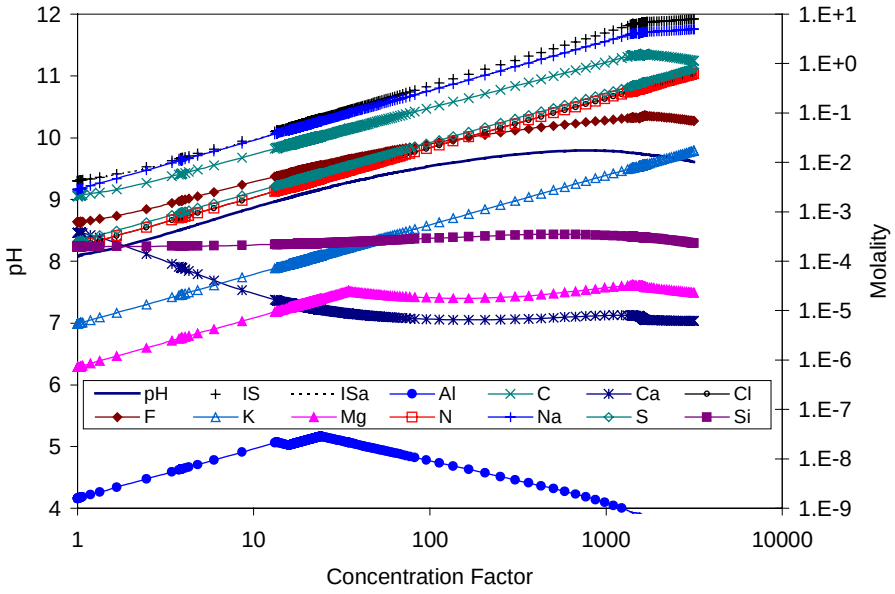

DTN: MO0112MWDTHC12.024

Figure 80. Aqueous Evaporative Evolution for the Low Temperature and High Carbon Dioxide Partial Pressure Case for Seepage Wicking into the Invert in the Tptpll Lithology, Initialized Using Water Composition of UZ-14 Perched Water (LHip), Period 4

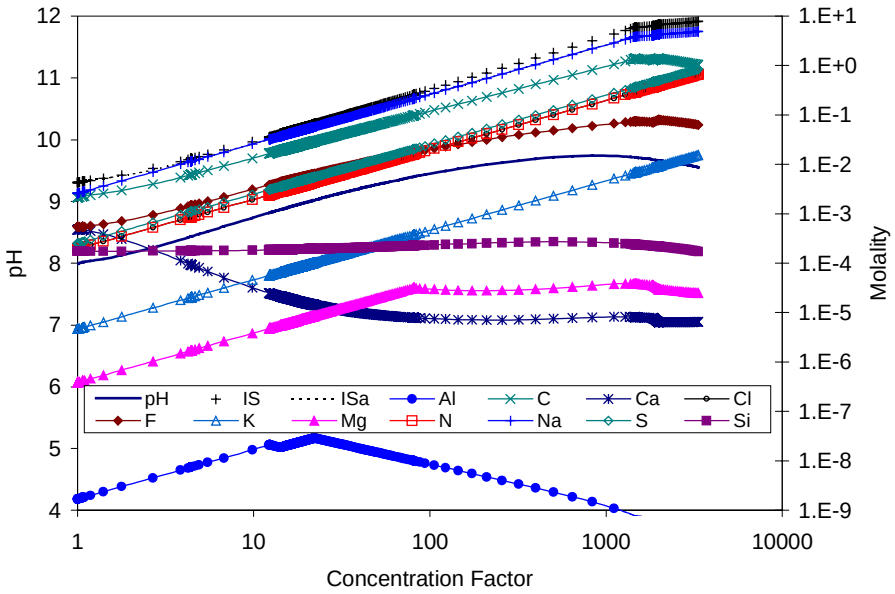

DTN: MO0112MWDTHC12.024

Figure 81. Aqueous Evaporative Evolution for the Low Temperature and High Carbon Dioxide Partial Pressure Case for Seepage Wicking into the Invert in the Tptpll Lithology, Initialized Using Water Composition of UZ-14 Perched Water (LHip), Period 5

6.3 SUMMARY OF HIGH RELATIVE HUMIDITY SALTS MODEL RESULTS

Comparison of Figures 1 through 81 provide insight into the effects of various parameters on model outputs. The following subsections summarize the effects observed as they pertain to the evaporation calculations.

6.3.1 Effects of Lithology (Tptpmn vs. Tptpll)

The effects of lithology can be evaluated by comparing the Bmc and Bmi case results for the Tptpmn (Figures 1 through 24) with the Blc and Bli case results for the Tptpll (Figures 25 through 48). For the most part, there is little difference in the evaporation of these waters. However, several of the comparisons suggest that the pH might be lower in the Tptpll (e.g., Figure 1 vs. Figure 25 and Figure 17 vs. Figure 41). This appears to be especially true for evaporation in the invert, where the pH for the Tptpmn can rise to about 10 while the pH falls below 6 for the Tptpll (Figure 15 vs. Figure 39).

The lower pH values in the Tptpll appear to correlate fairly strongly with lower Na:Cl molar ratios in the Tptpll. That is, for those cases in which the pH is considerably lower in the Tptpll, the Na:Cl molar ratio is also considerably lower. This observation may be important because lower Na:Cl molar ratios enhance the probability of developing a chloride brine instead of a nitrate brine (BSC 2001f, Section 6.1.3).

6.3.2 Effects of Seepage Location (Crown vs. Invert)

The effects of seepage location can be evaluated by comparing the Bmc and Blc case results (Figures 1 through 12 and 25 through 36) with the Bmi and Bli case results (Figures 13 through 24 and 37 through 48), respectively. For the Tptpmn lithology, the pH is generally lower in the crown than the invert for the early periods. This is especially apparent in the boiling period of the Tptpmn (Figure 3 versus Figures 15).

A relationship between pH and seepage location is not clear for the Tptpll results. While the last two periods show almost no differences, the pH differences in the earlier time periods are mixed. Period 1 shows pH values about one unit lower in the crown than the invert while period 3 shows the opposite results. For the other four periods, the pH differences between seepage locations are small in comparison.

Lower Na:Cl molar ratios are observed in the invert than in the crown in the early periods of Tptpll cases and in period 3 of the Tptpmn cases. These results reflect the ratios observed in the incoming seepage composition abstractions and not the effects of further evaporation.

6.3.3 Effects of Thermal Operating Mode (High vs. Low)

Comparison of results in Figures 49 through 60 with the results in Figures 61 through 70 suggest that seepage waters from the higher temperature operating mode have a greater probability of producing lower pH values during the first several thousand years. They also suggest that the higher temperature operating mode has a higher probability of having a Na:Cl molar ratio that falls below one. Ratios falling below one do not occur in the lower temperature operating mode abstractions. Such low ratios enhance the probability of developing a chloride brine instead of a nitrate brine (BSC 2001f, Section 6.1.3).

It is possible, however, that the observed differences in the high and low temperature operating mode abstractions are an artifact of the discretization schemes. That is, it is possible that the discretizations in DTN: MO0110SPAEBS13.038 might not have captured potentially low Na:Cl molar ratios in the lower temperature operating mode because the lower temperature operating mode abstraction was not as highly discretized around the boiling and cool down periods as the higher temperature operating mode abstraction. Reanalysis of the source data for DTN: MO0110SPAEBS13.038 would clarify this issue.

6.3.4 Effects of Carbon Dioxide Fugacity (High vs. Low)

The effects of the carbon dioxide fugacity values used to bound the THC model can be evaluated by comparing the results of the HLi and LLi cases (Figures 49 through 54 and 61 through 65) with the results of the HHi and LHi cases (Figures 55 through 60 and 66 through 70). The pH tends to be slightly lower in the higher carbon dioxide fugacity cases. Other than these small differences, the results appear to be fairly insensitive to the range of bounding carbon dioxide fugacity values used in the simulations.

6.3.5 Effects of Starting Water Composition (Pore Water vs. Perched Water)

The effects of the starting water composition used to initialize the THC model can be evaluated by comparing the results of the HHi and LHi cases (Figures 55 through 60 and 66 through 70) with the results of the HHip and LHip cases (Figures 71 through 81). Initializing the water composition using UZ-14 perched water as in the HHip and LHip cases causes considerable changes in predicted seepage water compositions and how they evolve upon further evaporation. Instead of the pH tending to remain in the neutral range or fall into the acid range, the pH of the waters in the HHip and LHip cases tends to increase upon further evaporation, sometimes to values in the 9 to 10 range. These waters tend to be dominated by Na and CO_3 and have Na:Cl molar ratios that exceed at least three. Also, because of the increased NO_3:Cl molar ratio as explained in Section 3.1, the seepage waters from cases HHip and LHip have a considerably greater probability of developing into sodium nitrate brines (BSC 2001f, Section 6.1.3).

6.4 SUMMARY OF LOW RELATIVE HUMIDITY SALTS MODEL RESULTS

The LRH model results for this calculation are documented in DTN: MO0111MWDSEE12.022. They include cases HHi and LHi, which are extended to cases HHc, HLi, HLc, LHc, LLi, and LLc according to Assumption 3.4.1 (Section 3.4).

Figure 82 shows the predicted chloride and ionic strength molalities as a function of relative humidity (*RH*) for the preclosure period of the LHi case. The results are similar for each of the other periods and cases simulated.

As shown in Sections 6.1 and 6.2, the results of the high relative humidity model show that during early time periods when the temperature is elevated, the Na:Cl molar ratio can occasionally fall below one. This is important because this enhances the probability of a chloride brine developing due to predicted chemical divides (BSC 2001f, Section 6.1.3). This possibility is not captured in the low relative humidity model. Future development of the low relative humidity model will focus on predicting and incorporating the possibility of generating a chloride brine. Other important limitations of the model and uncertainties in the results are discussed in Section 6.8.

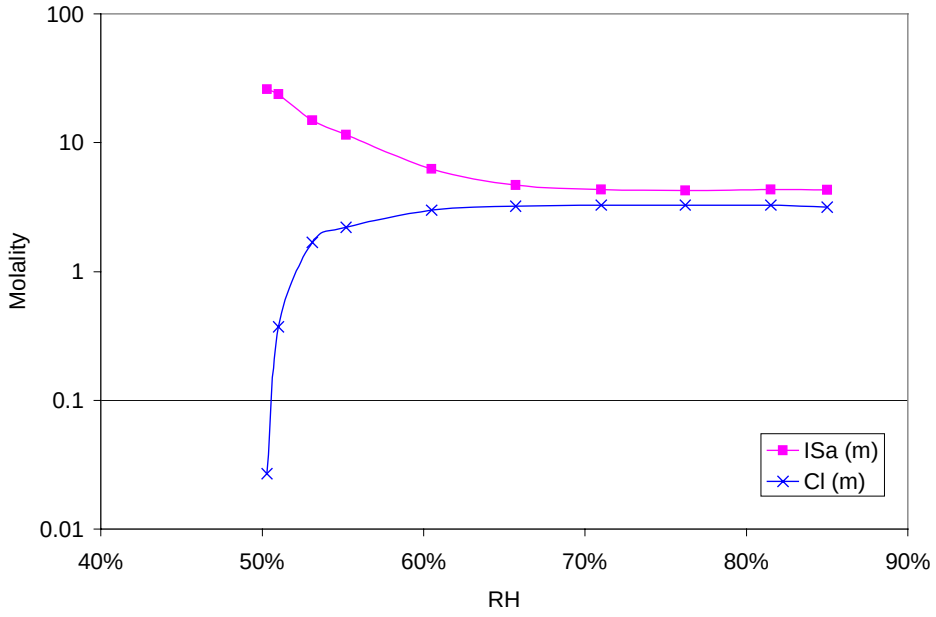

DTN: MO0111MWDSEE12.022

Figure 82. Low Relative Humidity Salts Model Predictions of Ionic Strength and Chloride Concentration for the Low Temperature and High Carbon Dioxide Partial Pressure Case for Seepage Wicking into the Invert in the Tptpll Lithology (LHi), Period 1

6.5 LOOKUP TABLES

The HRH and LRH model results are summarized in a set of lookup tables for the HLi, HHi, LLi, LHi, HLc, HHc, LLc, and LHc cases. These tables are documented in DTN: MO0111SPAPSM12.023. Though the tables are only qualified for pH, *ISa*, and Cl technical product output, they also include predictions for true ionic strength, total concentrations of CO_3, F, K, NO_3, Na, SO_4, Al, Ca, Fe(III), Mg, and Si, and individual species concentrations of HCO_3-, CO_3^{2-}, OH^-, H^+, $H_2SiO_4^{2-}$, $H_3SiO_4^-$, and $MgOH^+$.

Figure 83 and Table 6 show values for selected model output parameters from the lookup table for the preclosure period of the LLi case. As explained in Sections 4.1.3 and 6.4.2 of the Precipitates/Salts model AMR (BSC 2001b), R^{es} is the ratio of the evaporation flux (Q^e) to seepage flux (Q^s). At steady state, R^{es} is related to the concentration factor by the following equation

$$\frac{C}{C_o} = \frac{1}{1 - R^{es}} \qquad \text{(Eq. 2)}$$

where the concentration factor (C/C_o) is the ratio of the steady state nitrate concentration in the cell divided by the nitrate concentration in the incoming seepage. Thus, when (1 - R^{es}) is equal to 0.001, 0.01, 0.1, 1.0 and 10 at steady state, then C/C_o is equal to 1000, 100, 10, 1.0, and 0.1, respectively. A concentration factor of 0.1 implies a ten-fold dilution.

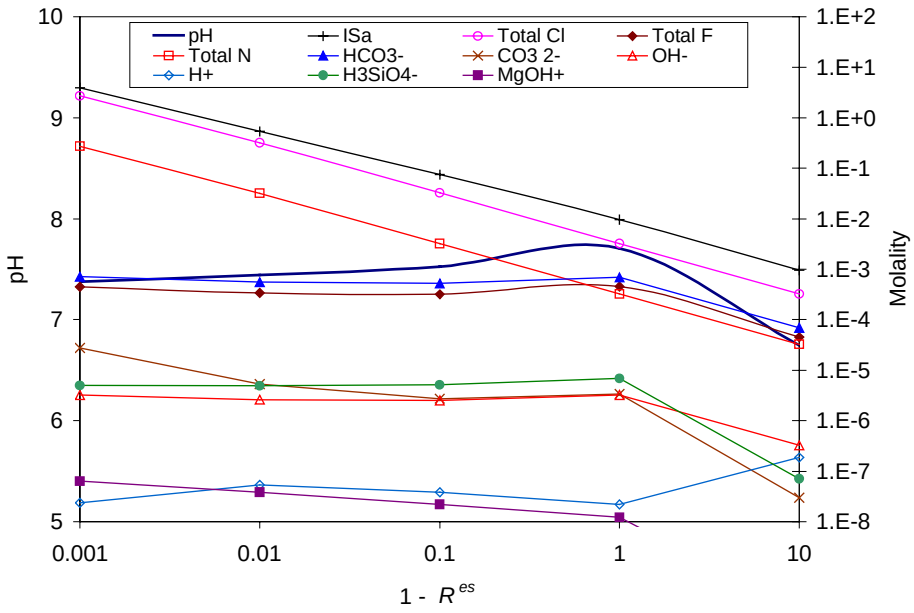

DTN: MO0111SPAPSM12.023

Figure 83. Steady State Predictions of pH and Selected Aqueous Components and Species vs. (1 – R^{es}) for the Low Temperature and Low Carbon Dioxide Partial Pressure Case for Seepage Wicking into the Invert in the Tptpll Lithology (LLi), Period 1

Table 6. Example Precipitates/Salts Model Lookup Table for Selected Outputs

Input Parameters[a]		Precipitates/Salts Model Output for: Invert Low Temperature Low CO_2 Preclosure Period (0-300 yr)											
		Qualified Output			Preliminary Unqualified Output								
RH **(%)**	Q^e/Q^s	**pH**	***ISa*** **(molal)**	**Total Cl (molal)**	**Total F (molal)**	**Total N (molal)**	HCO_3^- **(molal)**	CO_3^{2-} **(molal)**	OH^- **(molal)**	H^+ **(molal)**	$H_2SiO_4^{2-}$ **(molal)**	$H_3SiO_4^-$ **(molal)**	$MgOH^+$ **(molal)**
< 50.3	NA[b]	NA	NA	NA	NA	NA	NA	NA	NA	NA	NA	NA	NA
50.3	NA	7.30	2.61E+01	2.70E-02	NA	NA	NA	NA	NA	NA	NA	NA	NA
51.0	NA	7.30	2.38E+01	3.72E-01	NA	NA	NA	NA	NA	NA	NA	NA	NA
53.1	NA	7.30	1.49E+01	1.69E+00	NA	NA	NA	NA	NA	NA	NA	NA	NA
55.2	NA	7.30	1.15E+01	2.20E+00	NA	NA	NA	NA	NA	NA	NA	NA	NA
60.5	NA	7.30	6.26E+00	2.99E+00	NA	NA	NA	NA	NA	NA	NA	NA	NA
65.7	NA	7.30	4.68E+00	3.22E+00	NA	NA	NA	NA	NA	NA	NA	NA	NA
71.0	NA	7.30	4.32E+00	3.28E+00	NA	NA	NA	NA	NA	NA	NA	NA	NA
76.2	NA	7.30	4.24E+00	3.29E+00	NA	NA	NA	NA	NA	NA	NA	NA	NA
81.5	NA	7.30	4.33E+00	3.27E+00	NA	NA	NA	NA	NA	NA	NA	NA	NA
85.0	NA	7.30	4.29E+00	3.17E+00	3.87E-04	3.17E-01	5.88E-04	2.17E-05	2.84E-06	2.24E-08	1.85E-10	4.18E-06	7.38E-08
> 85	-9.00	6.75	9.62E-04	3.25E-04	4.54E-05	3.25E-05	6.99E-05	2.99E-08	3.28E-07	1.87E-07	1.85E-14	7.04E-08	1.74E-10
> 85	0.00	7.71	9.63E-03	3.25E-03	4.54E-04	3.25E-04	6.88E-04	3.38E-06	3.24E-06	2.18E-08	2.06E-11	6.84E-06	1.22E-08
> 85	0.90	7.53	7.46E-02	3.24E-02	3.18E-04	3.24E-03	5.23E-04	2.74E-06	2.51E-06	3.81E-08	1.64E-11	5.11E-06	2.20E-08
> 85	0.99	7.44	5.34E-01	3.18E-01	3.42E-04	3.18E-02	5.58E-04	5.33E-06	2.61E-06	5.40E-08	3.35E-11	4.87E-06	3.83E-08
> 85	0.999	7.38	3.92E+00	2.72E+00	4.47E-04	2.72E-01	7.10E-04	2.75E-05	3.24E-06	2.37E-08	2.25E-10	5.02E-06	6.37E-08
> 85	> 0.999	7.30	4.29E+00	3.17E+00	3.87E-04	3.17E-01	5.88E-04	2.17E-05	2.84E-06	2.24E-08	1.85E-10	4.18E-06	7.38E-08

DTN: MO0111SPAPSM12.023 (developed from MO0111MWDVAR12.021 [files: LLI1C900.6O, LLI1E000.6O, LLI1E900.6O, LLI1E990.6O, and LLI1E999.6O] and MO0111MWDSEE12.022 [file: LHI1.MCD])

NOTE: [a] Q^e/Q^s is the evaporative flux divided by the seepage flux.
[b] Not applicable to model (dry conditions at relative humidity less than 50.3 percent).

6.6 SENSITIVITY OF MINERAL SUPPRESSIONS

To evaluate the sensitivity of three minerals permitted to precipitate in the HLi, HHi, LLi, LHi, HLc, HHc, LLc, and LHc cases, the HHi cases were rerun with these minerals suppressed. The three minerals were talc, chrysotile, and magnesite. These minerals were not suppressed in the original calculations performed for SSPA and documented in DTN: MO0111MWDVAR12.021 and Section 6.2.1 above. As a result, talc precipitated in many of the simulations. Chrysotile and magnesite never did. The only other difference in how the HHi cases were rerun was that the PT5v2 database was used instead of the PT5v1 database. These two databases differ only by the presence of nesquehonite in the PT5v2 database.

The aqueous evaporative evolution of the HHi waters as rerun using the PT5v2 database and the additional mineral suppressions are presented in Figure 84 through Figure 89. Compared to the results presented in Figures 55 through 60, they show only minor differences. The pH tends to be higher, though less than about one pH unit, during periods 2 and 3 when the three minerals are suppressed. The chloride and ionic strength approximations are approximately unchanged. These results indicate that Assumption 3.3.1 is justified for the qualified outputs.

The entire set of EQ3/6 input and output files for the rerun HHi case is included in DTN: MO0112MWDTHC12.024.

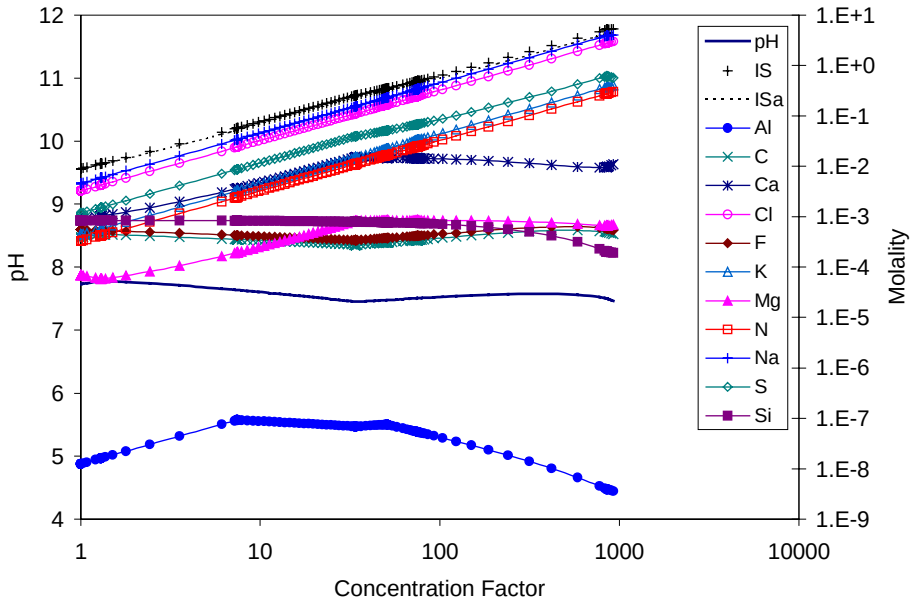

DTN: MO0112MWDTHC12.024

Figure 84. Aqueous Evaporative Evolution for the HHi Case Using the PT5v2 Thermodynamic Database and the Full List of Mineral Suppressions, Period 1

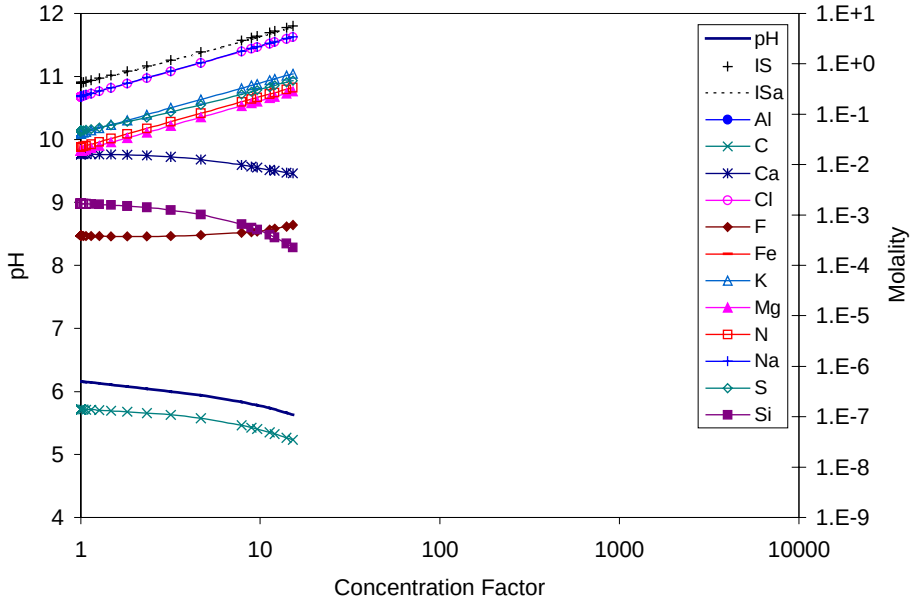

DTN: MO0112MWDTHC12.024

Figure 85. Aqueous Evaporative Evolution for the HHi Case Using the PT5v2 Thermodynamic Database and the Full List of Mineral Suppressions, Period 2

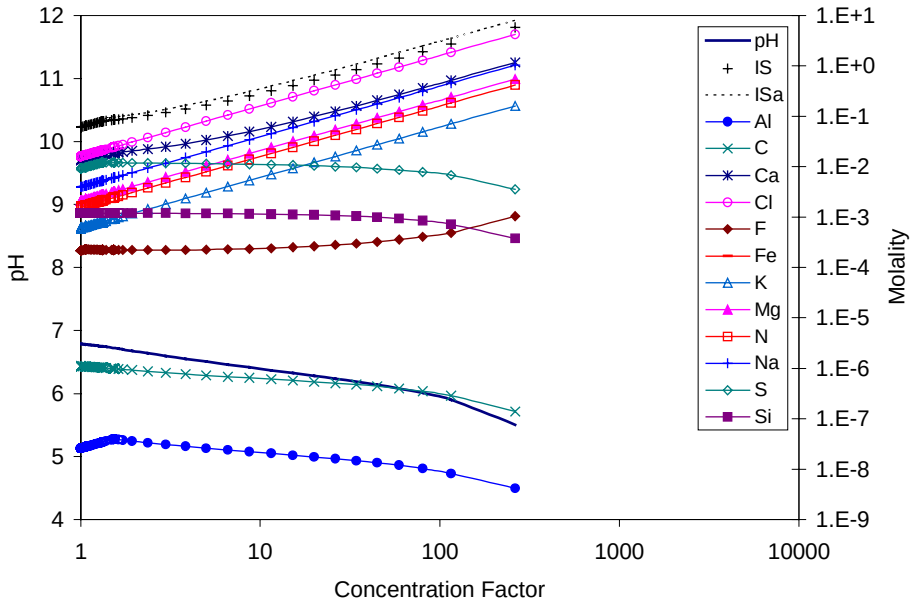

DTN: MO0112MWDTHC12.024

Figure 86. Aqueous Evaporative Evolution for the HHi Case Using the PT5v2 Thermodynamic Database and the Full List of Mineral Suppressions, Period 3

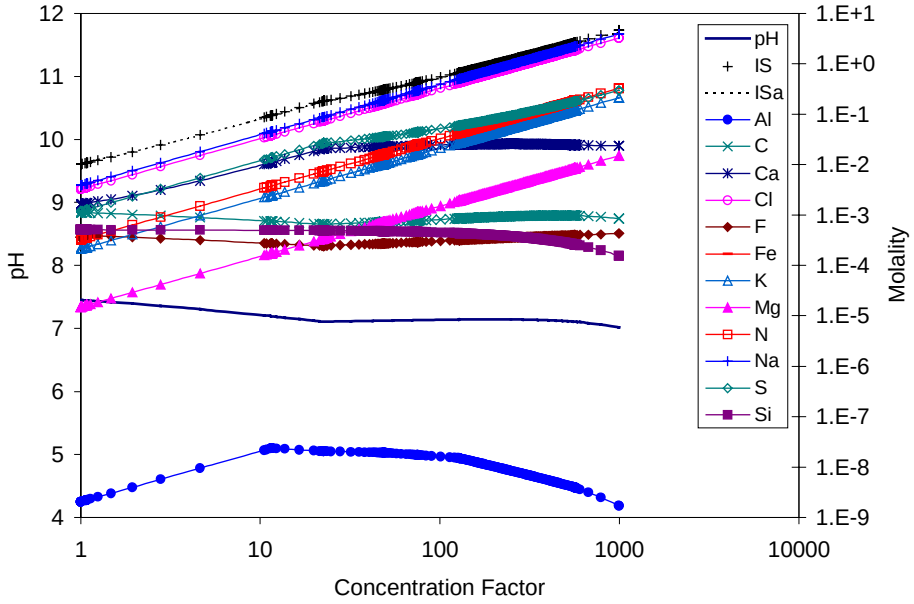

DTN: MO0112MWDTHC12.024

Figure 87. Aqueous Evaporative Evolution for the HHi Case Using the PT5v2 Thermodynamic Database and the Full List of Mineral Suppressions, Period 4

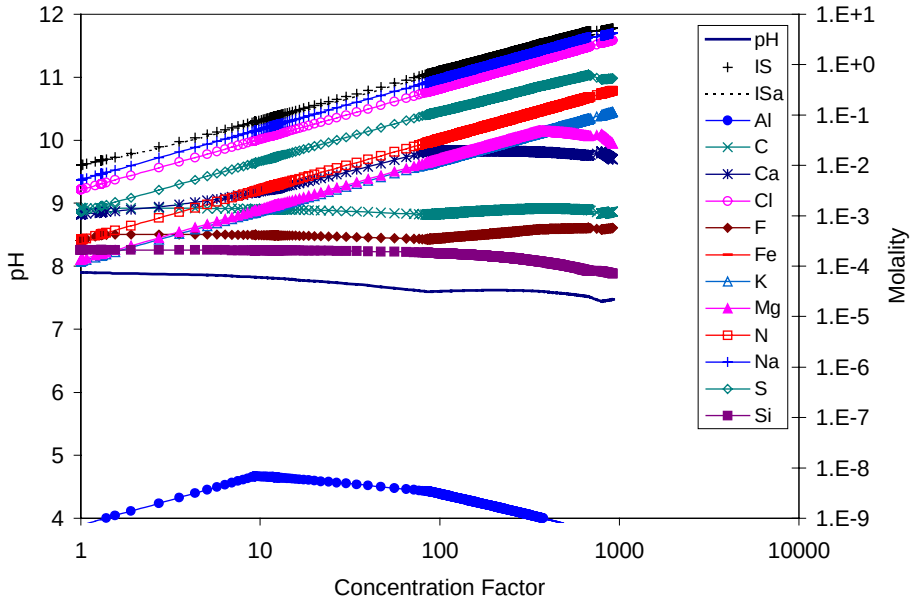

DTN: MO0112MWDTHC12.024

Figure 88. Aqueous Evaporative Evolution for the HHi Case Using the PT5v2 Thermodynamic Database and the Full List of Mineral Suppressions, Period 5

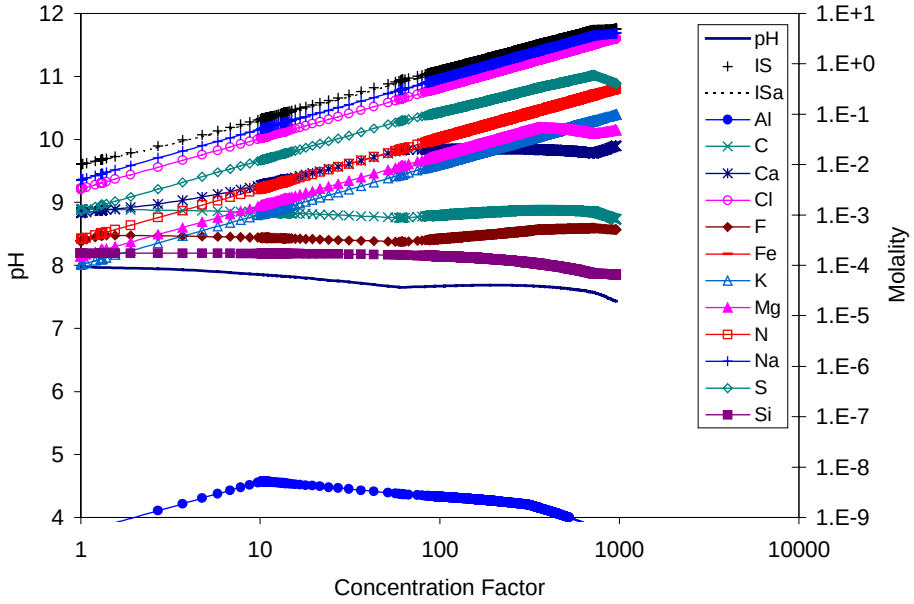

DTN: MO0112MWDTHC12.024

Figure 89. Aqueous Evaporative Evolution for the HHi Case Using the PT5v2 Thermodynamic Database and the Full List of Mineral Suppressions, Period 6

6.7 EVAPORATION CALCULATIONS FOR SEEPAGE GROUT INTERACTIONS MODEL INPUT

Several additional evaporation calculations were performed to provide the Seepage Grout Interactions Model (BSC 2001d) with waters that had been subjected to evaporation by the Precipitates/Salts Model. These included the Bmc case waters in Table 1 and the UZ-14 perched water and Drift-Scale Heater test water samples listed in Table 2. The two water samples in Table 2 are the same samples used in evaporation calculations documented in *Precipitates/Salts Model Sensitivity Calculations* (BSC 2001f, Figures 13 through 18 and 25 through 30, respectively).

Each of these waters was evaporated using the HRH salts model and PT5v2 Pitzer database to an ionic strength of 0.5 molal. The Seepage Grout Interactions Model uses the B-dot equation to approximate activity coefficients, so further evaporation would have provided model input near or exceeding the ionic strength range of the B-dot equation. The UZ-14 perched water sample and Drift-Scale Heater test water sample were evaporated at three different carbon dioxide fugicities: 10^{-1}, 10^{-3}, and 10^{-6}.

The EQ3/6 input and output files generated for these calculations are documented in two DTNs. The files for the Bmc case are included in DTN: MO0112MWDTHC12.024 (files: MCC1.6O, MCC2.6O, MCC3.6O, MCC4.6O, MCC5.6O, and MCC6.6O). They provide the same results as presented in Section 6.1 above for the Bmc case except that they do not include results at ionic strength in excess of 0.5 molal. The corresponding files for the waters in Table 2 are

documented in DTN: MO0111MWDHRH12.019. Like the Bmc case, they provide the same results presented elsewhere (Section 6.1.1.1) except that they do not include results at ionic strength in excess of 0.5 molal. The evaporation of the perched and Drift-Scale Heater Test water samples to a water activity of 0.85 is documented in *Precipitates/Salts Model Sensitivity Calculations* (BSC 2001f, Sections 6.1.2.3 and 6.1.2.5).

6.8 UNCERTAINTY AND LIMITATIONS

General model uncertainties and limitations are discussed in terms of model validation in Section 7.3 of *In-Drift Precipitates/Salts Analysis* (BSC 2001b). Additional uncertainties and limitations associated with starting water composition, carbon dioxide fugacity, and mineral suppressions are addressed in sensitivity calculations presented in *Precipitates/Salts Model Sensitivity Calculations* (BSC 2001f, Sections 6.1, 6.2, and 6.3). Finally, the results in the current calculation provide insight into the uncertainties and potential effects associated with lithology, seepage location, operating temperature, carbon dioxide bounding conditions, and starting water compositions.

Remaining unquantified uncertainties include uncertainties in the representation of processes that govern the evaporative evolution of seepage under repository conditions. These include the physical model representation (currently assumed to be a simple flow-through mixing cell), steady-state and equilibrium assumptions, chemical activity models, and thermodynamic database constants. For simple evaporation of synthesized J-13 well water and Topopah Spring tuff pore water in a beaker, uncertainties in thermodynamic constants, activity models, and equilibrium assumptions do not prevent reasonably accurate predictions of pH, chloride concentration, and ionic strength (BSC 2001b, Section 6.5). However, the question remains whether the uncertainties observed for these laboratory experiments are representative of the dominant evaporative processes in a repository.

An important uncertainty in the LRH salts model calculations is the sensitivity of the starting water composition on the evaporative chemical evolution of water in the drift. The LRH salts model makes the assumption that nitrate salts will set the lower limit on the relative humidity at which liquid water is stable within the drift. The HRH salts model calculations presented in the current document suggest that this assumption may not be appropriate in some instances because occasionally, the Na:Cl molar ratio falls below one. A ratio less than one tends to cause the water to evaporatively evolve into a chloride brine instead of a nitrate brine (BSC 2001f, Section 6.1.3).

The uncertainty associated with the evolution of such a chloride brine is borne largely in the uncertainty of the starting water composition. Future efforts to quantify the uncertainty of developing a chloride brine must include quantification of the uncertainty of the input starting water composition.

The model results for each water composition evaluated in this calculation are designated as qualified technical product output (TPO). The output DTNs produced or compared in this calculation are listed in Section 7.2.2 and Table 3. The waters listed in Table 1 use data from qualified DTNs as input. Their results are documented in DTN: MO0112MWDTHC12.024, MO0111MWDVAR12.021, MO0111MWDSEE12.022, and MO0111SPAPSM12.023. The

waters in Table 2 (perched water and Drift-Scale Heater Test water) do not use data from qualified DTNs. Instead, they are qualified for use in sensitivity calculations using assumptions and corroborative data. The results for these two waters are documented in DTN: MO0111MWDHRH12.019. Currently, the Precipitates/Salts model is validated for predicting pH, chloride concentration, and ionic strength.

Results of EQ6 evaporation runs sometimes provide final gas summaries with fugacities that seem unusual for nitrogen and oxygen gas when compared to partial pressures of these gases (~0.7 and ~0.2) at the drift altitude. This happens in evaporation calculations when the fugacities of oxygen and nitrogen are not constrained by the user. However, in the EQ6 runs documented in this calculation, these fugacities have no significant effect on the output of dissolved or precipitated species. The fugacity of oxygen remains high, ensuring that oxidizing conditions prevail (consistent with Assumption 5.2.2 (BSC 2001b)), and nitrogen gas does not oxidize, ensuring that total nitrate is conserved in the EQ6 calculations.

7. REFERENCES

7.1 DOCUMENTS

BSC (Bechtel SAIC Company) 2001a. *Technical Work Plan For Engineered Barrier System Department Modeling and Testing FY 02 Work Activities*. TWP-MGR-MD-000015 Rev 01. Las Vegas, Nevada: Bechtel SAIC Company. URN-0993

BSC 2001b. *In-Drift Precipitates/Salts Analysis.* ANL-EBS-MD-000045 REV 00 ICN 03. Las Vegas, Nevada: Bechtel SAIC Company. URN-0957

BSC 2001c. *EBS Incoming Water and Gas Composition Abstraction Calculations for Different Drift Temperature Environments.* CAL-EBS-PA-000013 REV 00. Las Vegas, Nevada: Bechtel SAIC Company. ACC: MOL20011214.0126

BSC 2001d. *Seepage Grout Interactions Model Calculations.* CAL-EBS-PA-000014 REV 00. Las Vegas, Nevada: Bechtel SAIC Company. URN-0967

BSC 2001e. *FY 01 Supplemental Science and Performance Analyses, Volume 1: Scientific Bases and Analyses.* TDR-MGR-MD-000007 REV 00 ICN 01. Las Vegas, Nevada: Bechtel SAIC Company. ACC: MOL.20010801.0404; MOL.20010712.0062; MOL.20010815.0001.

BSC 2001f. *Precipitates/Salts Model Sensitivity Calculations.* CAL-EBS-PA-000010 REV 00. Las Vegas, Nevada: Bechtel SAIC Company. URN-0955

CRWMS M&O (Civilian Radioactive Waste Management Services Management and Operations) 1998b. "Near-Field Geochemical Environment." Chapter 4 of *Total System Performance Assessment-Viability Assessment (TSPA-VA) Analyses Technical Basis Document.* B00000000-01717-4301-00004 REV 01. Las Vegas, Nevada: CRWMS M&O. ACC: MOL.19981008.0004.

CRWMS M&O 1999a. *Addendum to: EQ6 Computer Program for Theoretical Manual, Users Guide, & Related Documentation.* Software Change Request LSCR198. Las Vegas, Nevada: CRWMS M&O. ACC: MOL.19990305.0112.

CRWMS M&O 2000. *Analysis of Geochemical Data for the Unsaturated Zone.* ANL-NBS-HS-000017 REV 00. Las Vegas, Nevada: CRWMS M&O. ACC: MOL.20000725.0453.

CRWMS M&O 2001. *Precipitates/Salts Model Results for THC Abstraction.* CAL-EBS-PA-000008 REV 00 ICN 01. Las Vegas, Nevada: CRWMS M&O. ACC: MOL.20010125.0231.

Mariner, P. 2001. "Informal Calculation Regarding Precipitates/Salts Model Sensitivity Analyses in Support of SSPA Volume 1." Memorandum from P. Mariner (BSC) to B. MacKinnon, May 30, 2001, PROJ.05/01.075, with enclosure. ACC: MOL.20010531.0029.

Wolery, T.J. 1992a. *EQ3/6, A Software Package for Geochemical Modeling of Aqueous Systems: Package Overview and Installation Guide (Version 7.0).* UCRL-MA-110662 PT I. Livermore, California: Lawrence Livermore National Laboratory. TIC: 205087.

Wolery, T.J. 1992b. *EQ3NR, A Computer Program for Geochemical Aqueous Speciation-Solubility Calculations: Theoretical Manual, User's Guide, and Related Documentation (Version 7.0).* UCRL-MA-110662 PT III. Livermore, California: Lawrence Livermore National Laboratory. ACC: MOL.19980717.0626.

Wolery, T.J. and Daveler, S.A. 1992. *Theoretical Manual, User's Guide, and Related Documentation, Version 7.0.* Volume IV of *EQ6, A Computer Program for Reaction Path Modeling of Aqueous Geochemical Systems.* UCRL-MA-110662. Draft 1.1. Livermore, California: Lawrence Livermore National Laboratory. TIC: 238011.

7.2 DATA, LISTED BY TRACKING NUMBER

7.2.1 Input Data

LL990702804244.100. Borehole and Pore Water Data. Submittal date: 07/13/1999.

MO0110SPAEBS13.038. EBS Incoming Water and Gas Composition Abstraction Calculation Results. Submittal date: 10/16/2001. URN-0968

MO0110SPAPT245.017. PT5 Pitzer Database for EQ3/6, Version 2. Submittal date: 10/04/2001. URN-0994

MO0110SPAPT545.016. PT5 Database for EQ3/6. Submittal date: 10/10/2001. URN-0997

7.2.2 Developed Data

MO0111MWDHRH12.019. High Relative Humidity Salts Model Predictions For Cement Leachate Model. Submittal date: 11/01/2001.

MO0111MWDSEE12.022. Low Relative Humidity Salts Model Mathcad Files for THC REV 01 Seepage. Submittal date: 11/01/2001.

MO0111MWDVAR12.021. High Relative Humidity Salts Model Input/Output Files for Various Thermal Operating Modes. Submittal date: 11/01/2001.

MO0111SPAPSM12.023. Precipitates/Salts Model Lookup Tables for SSPA. Submittal date: 11/06/2001.

MO0112MWDTHC12.024. High Relative Humidity Salts Model Predictions for THC REV 01 Using PT5v2 Thermodynamic Database. Submittal date: 11/28/2001.

7.3 CODES, STANDARDS, REGULATIONS, PROCEDURES, AND SOFTWARE

AP-3.12Q, Revision 0, ICN 4. *Calculations.* Washington, D.C.: U.S. Department of Energy, Office of Civilian Radioactive Waste Management. ACC: MOL.20010404.0008.

AP-SI.1Q, Rev. 3, ICN 2, ECN 1. *Software Management*. Washington, D.C.: U.S. Department of Energy, Office of Civilian Radioactive Waste Management. ACC: MOL.20011030.0598.

CRWMS M&O 1998a. *Software Code: EQ3/6.* V7.2b. LLNL: UCRL-MA-110662.

CRWMS M&O 1999b. *Software Code: EQ6, Version 7.2bLV.* V7.2bLV. 10075-7.2bLV-00.